NPS ARCHIVE
1962.06
RODGERS, B.

THE COLLEGE OF AERONAUTICS
CRANFIELD

THESIS

TITLE: AN INVESTIGATION OF PRESSURE FLUCTUATIONS AROUND A CIRCULAR CYLINDER

B. RODGERS & F. D. SMITH

Thesis
R666

DATE: JUNE 1962

DUDLEY KNOX LIBRARY
NAVAL POSTGRADUATE SCHOOL
MONTEREY CA 93943-5101

18 July 1962

From: LT Frederick D. Smith, Jr., USN, The College of Aeronautics, Cranfield, Bletchley, Bucks., England

To: Superintendent, U.S. Naval Postgraduate School, Monterey, California

Subj: Thesis, forwarding of

Ref: (a) U.S. Naval Postgraduate School Inst 5000.2A (Ch 1)

Encl: (1) College of Aeronautics Thesis, "An Investigation of Pressure Fluctuations Around a Circular Cylinder," by B. Rodgers and F. D. Smith

1. Encl (1) is forwarded pursuant to the instructions contained in Ref (a).

2. This thesis was prepared as part of the two year course of instruction at the College of Aeronautics, Cranfield, England, leading to a Diploma of the College (D.C.Ae.). A requirement was set by the Department of Aerodynamics that each student produce a satisfactory thesis based on theoretical studies and that students working in small groups produce joint theses based on experimental research. Encl (1) satisfies the latter requirement. The thesis satisfying the former requirement is forwarded with a separate letter.

3. In this thesis primary emphasis is placed on frequency analysis of pressure fluctions measured around a circular cylinder. Other measurements were made to correlate this work with previous experiments involving circular cylinders in a moving fluid stream.

Very respectfully,

THE COLLEGE OF AERONAUTICS

DEPARTMENT OF AERODYNAMICS

AN INVESTIGATION OF PRESSURE FLUCTUATIONS AROUND A CIRCULAR CYLINDER

BY

BARRY RODGERS
//
and

FREDERICK D. SMITH, JR.
Lieutenant, U.S. Navy.

Cranfield,

England.

June 1962.

DUDLEY KNOX LIBRARY
NAVAL POSTGRADUATE SCHOOL
MONTEREY CA 93943-5101

SUMMARY

For many years the periodic nature of the flow around bluff bodies has interested investigators. This investigation was conducted to increase the knowledge of pressure distributions and pressure fluctuations on the surface of a circular cylinder.

Measurements were made of the root mean square values of the pressure fluctuations around the cylinder, and frequency analyses of the fluctuating pressures were performed. A condenser microphone fitted with a 2 m.m. probe was mounted in each cylinder to serve as the pressure transducer, and a narrow band (4 c/s) wave analyser was used for the frequency analyses.

Comparison of the mean pressure measurements and the measurements of fluctuations at the Strouhal frequency and its second harmonic compare favourably with previous experiments.

Acoustic signals were found in pairs at frequencies separated by the second harmonic of the Strouhal frequency. The centre frequency of these pairs was constant over a range of Reynolds number from 0.4×10^5 to 3.2×10^5 using three different diameter cylinders. These measurements fail to support the only existing theory regarding acoustic signals associated with flow around a circular cylinder.

Acknowledgments

The authors wish to express their gratitude for the encouragement and advice of Messrs. G.M. Lilley and T.H. Hodgson while conducting these investigations.

LIST OF CONTENTS

NOTATION

c		speed of sound
f	=	$\frac{3c}{2\pi D}$, characteristic acoustic frequency of the cylinder
f_1	=	$\frac{c}{\pi D}$, lowest natural frequency of the cylinder
f'	=	$f\ (1 - \frac{Uo-Us}{c})$, Doppler shifted characteristic frequency
n		fundamental frequency of vortex shedding
p		total head pressure
p_o		static pressure
$\overline{p_f^2}$		mean square of the pressure fluctuations
C_p	=	$\frac{p-p_o}{\frac{1}{2}\rho V^2}$, mean pressure coefficient
C_{p_f}		$\frac{\sqrt{\overline{p_f^2}}}{\frac{1}{2}\rho V^2}$, fluctuating pressure coefficient
C_{p_ω}		coefficient of the pressure fluctuation at frequency ω.
D		diameter of cylinder
R_e	=	$\frac{DV}{\nu}$, Reynolds number
S_t	=	$\frac{nD}{v}$, Strouhal number
$(Uo-Us)$		wake velocity
v		wind tunnel working section velocity

θ	cylinder angle measured clockwise from its leading edge
ν	kinematic viscosity
ρ	density of air
$\phi(\omega)$	$\frac{(C_{p_\omega})^2}{4(c/s)}$ power spectral density
ω	frequency

1. INTRODUCTION

For many years the flow round and in the wake of a bluff body has been a subject of interest to a large number of both theoretical and experimental investigators. One of the investigators was V. Strouhal who observed the periodic character of the wake of a circular cylinder as early as 1878.

Since then, the significance of this phenomenon has been realised. The failure of the Tacoma Narrows Bridge is generally attributed to the vortex shedding exciting the fundamental frequency of the structure. Other examples of engineering significance include smokestacks, submarine periscopes, oil pipe lines and television aerials which often encounter vibrational problems. A more familiar example is, of course, the "singing" of telephone wires in a wind.

More recent problems of aerodynamic interest are the airflow round missiles when standing on their launching pads and the cross flow around cylindrical airframes due to their incidence. For this reason a study of the flow past bluff obstacles, in particular circular cylinders, was initiated in 1955 at the Institute of Aerophysics, University of Toronto as part of a research programme in aerodynamic noise.

Since Strouhal's original paper a large number of notes and reports have been published but, to date, no theory has

been advanced which fully explains the phenomena.

However, in 1949, R.A. Shaw advanced the idea that the frequency with which vortices are shed into the wake of a cylinder is associated with acoustic pulses originating at the point of separation. This theory has not been generally accepted because most workers are sceptical of the significance of the high natural frequencies of the acoustic signals postulated to cause the vortex shedding.

The object of this investigation was to obtain experimental data for comparison with R.A. Shaw's theory. Measurements of the mean pressures and overall intensities of the pressure fluctuations were also made to correlate this work with earlier investigations.

2. REVIEW OF PREVIOUS WORK

2.1 Mean Pressure Distributions Round a Circular Cylinder

One of the earlier investigators of the mean flow round a circular cylinder was Relf, who measured the variation of drag coefficient with Reynolds number of small diameter wires at The National Physical Laboratory in 1914 for Reynolds numbers up to 10^4.

In 1921, measurements were taken in the Göttingen wind tunnel showing the decrease of drag coefficient through the critical Reynolds Number range, and these results were confirmed at The National Physical Laboratory. Later, in 1928, Fage (Ref. 1) studied the transition from laminar to turbulent flow and the separation for the critical Reynolds number range from pressure distributions round an 8.9 inch cylinder. He followed this with work on a 23 inch cylinder (Ref. 2) at still higher Reynolds numbers and showed the gradual increase of drag coefficient above $R_e = 5.8 \times 10^5$. Lindsey (Ref. 3) repeated these tests in 1933 and extended the results to include the effects of compressibility for cylinders up to 0.25 inches diameter. In 1941, Stack (Ref. 4) extended these results even further to include cylinder diameters of up to three inches. In Fig. 13, the variation of drag coefficient with Reynolds number from references 9 and 18 is reproduced. Goldstein, in

Ref. 5, gives a review of the majority of the earlier work on circular cylinders.

More recently, Gowen and Perkins (Ref. 6) used two diametrically opposed orifices to measure pressure distributions for a wide range of Reynolds numbers and Mach numbers and thus obtained the variation of drag coefficient with Reynolds number incorporating compressibility effects. They also measured the drag coefficient from transonic free flight trials. Delany and Sorenson (Ref. 7) extended Lindsey's results to include a wide range of cylinder shapes and higher Reynolds numbers, whilst Roshko (Ref. 8) investigated the effect of putting various interference elements in the wake of a cylinder. In November, 1960, Roshko (Ref. 9) performed tests on large diameter circular cylinders for Reynolds numbers up to 10^7 and verified that the drag coefficient increases for supercritical Reynolds numbers.

2.2 Pressure Fluctuations at the Surface of a Circular Cylinder.

2.2.1. Pressure Fluctuations at the Strouhal Frequency.

The first observation of the periodicity in the wake of a bluff body appears to have been made by Strouhal in 1878, but he did not measure the precise nature of this phenomenon. Mallock, in 1907 (Ref. 10), was the first person to describe the

flow fully. In 1921, Relf and Ower (Ref. 11) performed experiments to show that the note emitted by a circular wire in a wind had the same frequency as the Strouhal frequency, whilst Relf and Simmons (Ref. 12), in 1924, obtained the experimental variation of the Strouhal number with Reynolds number where the Strouhal number is defined as

$$S_t = \frac{nD}{V} \qquad 2.1$$

and where n = Frequency of shedding vortex pairs

D = Diameter of cylinder

and V = Air speed.

They showed that, through the critical Reynolds number range, the Strouhal number increased as the drag coefficient decreased. In Ref. 5, Goldstein gives an excellent review of both experimental and theoretical work accomplished up to 1938.

More recently, Delany and Sorenson (Ref. 7) measured Strouhal frequencies for high Reynolds numbers using a pressure sensitive cell mounted in the tip of a probe. Measurements of the fluctuating pressures on the surface of a circular cylinder have been performed by McGregor at the University of Toronto (Ref. 13) and by Gerrard at the University of Manchester (Ref. 14). Both experiments, which were conducted independently, were

concerned with measurement of the pressure fluctuations due to the fundamental vortex shedding frequency (Strouhal frequency) and its second harmonic. From these measurements estimates were made of the fluctuating lift and drag. McGregor tested a cylinder of one and one-eighth inch diameter in which a condenser microphone was mounted to serve as a transducer for the fluctuating pressure measurements. The microphone was mounted internally in a cavity designed as a Helmholz resonator. These tests were performed at Reynolds numbers ranging from 3.5×10^4 to 10^5.

Gerrard used a cylinder of one inch diameter with a condenser microphone for a pressure transducer. This microphone was mounted in such a way that its diaphragm formed part of the surface of the cylinder. Since this diaphragm was one quarter of an inch in diameter, it spanned an arc of the surface of 28.6°.

Both experimenters used one-third octave filters for their frequency analyses.

Fung (Ref. 15) has made direct force measurements of the fluctuating lift and drag on a cylinder in flows at supercritical Reynolds numbers, but these measurements did not include any pressure fluctuation data.

Keefe (Ref. 16) has made similar direct measurements of

the fluctuating lift and drag forces, but at Reynolds numbers ranging from 5×10^3 to 10^5. He also made acoustic measurements of radiated sound using a one-third octave filter, but no measurements were made of fluctuating pressures on the surface of the cylinder.

2.2.2 High Frequency Pressure Fluctuations.

In 1949, R.A. Shaw postulated an acoustic theory for the flow around a body immersed in a moving fluid. (Ref. 17). The theory assumes that natural frequencies for the flow are defined on the basis of the times which are required for travel and return of a pressure pulse travelling around the profile between centres of disturbance. Shaw argues further that the disturbances will be mutually excited and maintained at these frequencies.

In another paper Shaw applied the acoustic theory to the case of a circular cylinder (Ref. 18). For this case, he suggests that the lowest possible natural frequency is defined by the speed of sound and the full circumference of the cylinder. Thus the lowest natural frequency is

$$f_1 = \frac{c}{\pi D} \qquad 2.2$$

where c is the speed of sound and D is the diameter of the cylinder. But Shaw assumes that the vortices, which are shed from the surface of the cylinder, originate at points 120 degrees around either side from the forward stagnation point, so that the expected characteristic acoustic frequency, f, which they define is

$$f = \frac{3C}{2\pi D} \qquad 2.3$$

It is further argued that this frequency is a characteristic of the wake, so that the vortices downstream act as a chain of sources a wave length apart. The cylinder then receives an acoustic signal from the wake with an apparent frequency f', which has a Doppler shift due to the wake velocity. Therefore

$$f' = f\left(1 - \frac{Uo - Us}{c}\right) \qquad 2.4$$

where (Uo - Us) is the wake velocity.

The two acoustic signals would be expected to provide a "beat" frequency. Shaw argues that the peak of each beat is the occasion for a vortex to be shed. Thus the difference between the two postulated acoustic frequencies, f and f', becomes twice the Strouhal frequency.

A preliminary investigation (Ref. 19) of a circular cylinder was conducted by Shaw. The results were not contradictory to the theory, but the investigations were limited to a single cylinder, $5\frac{1}{8}$ inches in diameter, tested over a range of Reynolds number from 1.02×10^5 to 1.14×10^5. All of the principal results were obtained at a wind speed of 40 ft./sec. which corresponds to a Reynolds number of 1.09×10^5.

Another of Shaw's papers (Ref. 20) provides a concise summary of his acoustic theory applied to the circular cylinder.

3. TEST FACILITIES

3.1 Wind Tunnel

All the tests were performed in The College of Aeronautics 8-ft x 6-ft closed return wind tunnel. The air is driven by an eight blade variable pitch propeller on a 500 h.p. D.C. motor giving continuously variable air speed from 10 to 275 ft./sec. in the working section. For any particular air speed, there is a range of motor speeds corresponding to a continuous range of propeller pitch settings. In the working section there is a motor driven turntable, the perimeter of which is marked off in one degree intervals, and facilities are available for mounting the cylinders (Fig. 1).

3.2 The Models

Three circular cylinders were available of 3", 6" and 12" diameter. These were constructed of a soft wood core with an outer layer of hard wood. The outer layer of the 12" cylinder was Black Walnut while for the other two cylinders Mahogany was used. Brass plates to accommodate the microphone probes were fitted into each cylinder. Orifices for the measurement of mean pressures were installed two inches above the microphone fittings in the same plane through the cylinder axes (Fig. 2). Although the degree of surface finish of the cylinders was quite

good, there were small gaps between the brass fittings and the cylinders. However, for the actual tests these were filled with plasticine. To each end of the cylinders was screwed a wood plate which in turn was fitted to the wind tunnel turntable. Narrow, removable panels were fitted to each cylinder on the side opposite the microphone and pressure orifice to enable fitting of the microphone and its electrical connections (Fig. 3).

A ground board was used for a frequency survey of the overall tunnel noise. Similar fittings to those on the cylinders were incorporated for accommodating the microphone 6" aft of the leading edge on the flat portion of the board.

3.3 Equipment for Measuring Mean Pressures

A 2 m.m. total head tube, the end of which was fitted flush with the surface of the cylinder, passed through the centre of the cylinder and was connected to a Prandtl manometer. Although the Prandtl manometer had various sizes of capillary tubing incorporated to provide selection of several degrees of damping, it was necessary to introduce additional damping for measurements at 100 and 200 ft./secs. This damping was introduced by incorporating a ten inch length of $\frac{1}{2}$ m.m. capillary tubing and 250 c.c. reservoir into the pressure line between the cylinder

orifice and the manometer. At higher Reynolds numbers, the Prandtl manometer proved to be too small to read the large negative pressures, and one tube of the bank of standard tunnel manometers was used.

3.4 Equipment for Measuring Fluctuating Pressures

All sound measurements were made using a Brüel and Kjær Type 4133 Condenser Microphone as a pressure transducer with a Brüel and Kjær Type 2107 Frequency Analyzer as a pre-amplifier. Voltages proportional to the root mean square of the pressure fluctuations could be read directly from the Brüel and Kjær Frequency Analyzer. A Marconi Wave Analyzer Type TF.455.D-D/1 with a four cycle per second band width was used for the frequency analyses. For monitoring the wave form of the pressure fluctuations, a Tektronix Type 551 Dual Beam Oscilloscope was used. A Solarton Type C.0546 Oscillator was used to check the accuracy of the frequency setting on the Marconi Wave Analyzer and to calibrate the frequency response of the microphone with probe.

4. EXPERIMENTAL PROCEDURE.

4.1 Calibration of the Microphone.

No suitable means was available for calibration of the microphone locally for pressure response. The manufacturer's acoustic calibration was accepted which was 0.94 millivolts per μb output for frequencies from 0 to 20,000 c/s.

For frequency response of the microphone with probe, a calibration chamber and driver were provided by the manufacturers. The microphone probe was fitted into its conical head and inserted into the side of the calibration chamber. First the microphone was fitted into the face of the chamber opposite the driver and a blank plug screwed into the probe cone. The driver was powered by the Solartron Oscillator, and a constant 100 mW output was maintained for each calibration reading. After measurements were recorded throughout the frequency range, the procedure was repeated with the positions of the microphone and blank plug reversed. Output was read from the Bruel and Kjær Frequency Analyzer taking full spectrum RMS readings. An exploded view of the microphone is shown in Fig. 5.

Since the frequency response of the microphone was level over the range of interest, the calibrated microphone response was the ratio of the response measured when fitted with the probe to the response measured directly from the calibration chamber.

This procedure cancelled the response characteristics of the driver and the calibration chamber. To prevent resonance in the probe and cone, small tufts of wire wool were introduced into the probe, and the calibration repeated until a satisfactory response characteristic was obtained.

All tests were conducted using this microphone with 2 m.m. probes. A straight probe was used in the 6" and 12" cylinders, but a bent probe was necessary to fit the microphone into the 3" cylinder and the ground board. The results of the microphone calibration for these two probes can be found in Figures 6 and 7.

4.2 Tunnel Experiments.

4.2.1 Mean Pressures.

The mean pressures were measured using the total head tube against the static pressure taken from the wall static. These were connected to opposite sides of a Prandtl manometer which had methylated spirits as the working fluid. Pressure measurements were taken at 1°, 2° or 5° intervals around the cylinder depending on the size of pressure fluctuations and the rate of change of pressure at any particular angle from $\theta = 0$ to 360°. θ is the angle of the pressure orifice measured clockwise relative to the upstream direction. The cylinder was rotated in the wind tunnel working section by means of the turntable.

Pressure distributions measured around the 6" cylinder indicated that the pressure orifice was within half a degree of the zero marking on the turntable and within one degree on the three inch cylinder.

Because of the large pressure fluctuations in the critical Reynolds number range, damping was introduced into the pressure line in lieu of that incorporated into the Prandtl manometer. This external damping took the form of a ten inch length of $\frac{1}{2}$ m.m. capillary tubing and a 250 c.c. reservoir placed in the cylinder total head pressure line.

The negative pressures on the 6" cylinder at 200 ft./sec. corresponding to a Reynolds number of 6.4×10^5 were too large to be measured on the Prandtl manometer and one of the tubes of the bank of standard tunnel manometers with methylated spirits as the working fluid was used.

Spot checks on each run were taken on different occasions, and the results were found to be repeatable. However tests conducted at 100 and 200 ft./sec. during November 1961 and May 1962 were found to disagree, the earlier tests giving negative pressure peaks of less magnitude than the later checks. In the later tests the readings were checked with and without all forms of damping and their repeatability was found to be good. The only conclusion that can be drawn from this is that in the

earlier tests there was a leak in the pressure line from the cylinder.

4.2.2 Root mean Square Fluctuations

Using the microphone as a pressure transducer, voltages proportional to the root mean square of the pressure fluctuations were read directly from the Brüel and Kjær Frequency Analyzer. For these readings the "selective section" was turned off so that the meter read the pressure fluctuations over the whole frequency spectrum. The accuracy of these results is limited because the measurements were taken by eye from a meter whose needle fluctuated as much as half scale through a large range of cylinder angles. Whilst measuring these pressure fluctuations an oscilloscope was used to monitor the wave forms.

Throughout the frequency analyses the root mean square voltages were rechecked and on all occasions the readings were found to be repeatable to within 10%.

4.2.3 Tunnel Noise Investigations.

Pressure fluctuations through the frequency range from 0 to 2000 cycles per second were measured for the ground board and the 6" cylinder ($\theta = 0^{\circ}$ and 60°) at two different speeds.

For the ground board tests, the Brüel and Kjær condenser

microphone with the bent probe was used as the pressure transducer and the Brüel and Kjær Frequency Analyzer served as a pre-amplifier. The actual measurements were made using the Marconi Wave Analyzer. For all tests the electronic equipment was turned on two hours in advance to ensure maximum stability. A block diagram of the microphone instrumentation is shown on Fig. 4. Great care was taken in the setting up of both wave analyzers and the calibrations were checked periodically throughout the tests. A good indication of the positions of the peak amplitudes was obtained from a maximum reading voltmeter connected to the output of the Marconi Wave Analyzer.

Due to the crude frequency scale on the Marconi Wave Analyzer, it was impossible to measure the frequency to within 1 c/s at very low frequencies and 20 c/s at high frequencies. However, where peak amplitudes occured with frequencies above 25 c/s, they were checked by tuning the oscillator to the Marconi Wave Analyzer and reading the frequency from the oscillator which had a much larger scale.

The large fluctuations of the meter needle made accurate assessment of each reading impossible, and the results can only be regarded as being within 20% of their true values.

For the 6" cylinder tests the straight microphone probe

was used, but the other instrumentation was exactly the same.

4.2.4 Fluctuating Pressures at the Strouhal Frequencies.

These were measured at two speeds and various angles around the 6" and 3" cylinder but only at one speed on the 12" cylinder. The same experimental procedure was used as that for the tunnel noise investigations. Again, due to the inadequate frequency scale on the Marconi Wave Analyzer, readings could only be taken at $2\frac{1}{2}$ c/s intervals. For most cases the Strouhal frequency was less than 25 c/s which is the lowest limit of the oscillator, so the true frequencies could not be checked. It was also impossible to measure the Strouhal frequencies with any degree of accuracy below 10 c/s. Nevertheless, readings were found to be repeatable to within 20%.

4.2.5 Fluctuating Pressures at the Acoustic Frequencies.

The method of measuring these was the same as that for the other frequency analyses. Similar difficulties were experienced in reading the amplitudes of the pressures. In the range of interest for the acoustic measurements, the Marconi frequency scale was marked off in 200 c/s intervals. Repeatability was, therefore, not as good as in the other cases because it proved difficult to retune the Marconi at any particular frequency.

However when peak amplitudes were observed their frequency was checked using the oscillator; thus it was possible to repeat the peak readings to a greater accuracy than would otherwise have been experienced.

5. REDUCTION OF RESULTS

5.1 Mean Pressure Measurements

Mean pressure measurements were reduced to standard pressure coefficient form.

$$C_p = \frac{p-p_o}{\frac{1}{2}\rho V^2} \qquad 5.1$$

The difference between cylinder pressure and tunnel static pressure was measured directly by the manometer. These readings were corrected for the manometer error. To compute pressure coefficients, the corrected manometer reading for the upstream position of the cylinder was taken as the dynamic pressure. This was verified in each case to be the correct dynamic pressure by comparison with the dynamic pressure measured by the wind tunnel Betz manometer.

Values of the drag coefficient were obtained by integration of plots of $C_p \cos\theta$ against θ.

5.2 Root Mean Square Measurements of the Pressure Fluctuations.

The measurements of root mean square values of the pressure fluctuations were corrected for the Brüel and Kjær meter scale factor and converted to units of pressure using the microphone calibration factor. Because by far the greatest amount of energy

was contained in the pressure fluctuations at the fundamental shedding frequency and its second harmonic, no corrections to the microphone calibration were needed. The measurements were then converted into pressure coefficient form by

$$C_{pf} = \frac{\sqrt{\overline{p_f^2}}}{\frac{1}{2}\rho V^2} \qquad 5.2$$

where $\overline{p_f^2}$ is the mean square of the fluctuation of the pressure.

No attempt was made to correct for the contribution due to tunnel noise.

5.3 Reduction of Frequency Analysis Measurements

The data recorded from frequency analysis measurements were first corrected for the frequency response of the pressure transducer. This correction was applied by dividing the reading by the response factor for that frequency from the appropriate calibration curve, (see Figures 6 and 7). Corrections for the scale factors of both the Marconi Wave Analyzer and the Brüel and Kjær Frequency Analyzer were applied, and the measurements were converted to pressure coefficients in the same manner as for the measurements of the root mean square values of the full spectrum pressure fluctuations. Pressure coefficients were

converted to power spectral density by

$$\phi(\omega) = \frac{\left(C_{p_\omega}\right)^2}{4(c/s)} \qquad 5.3$$

where C_{p_ω} is the pressure coefficient of the fluctuation at frequency ω cycles per second and the denominator of 4 cycles per second is the band width of the Marconi Wave Analyzer.

No corrections were made to these data for tunnel noise.

6. DISCUSSION OF RESULTS

6.1 Mean Pressure and Root Mean Square Pressure Fluctuation Distributions.

No measurements appear to have been made in the past on root mean square pressure fluctuation distributions except for those by McGregor (Ref. 13) which were estimated from frequency analyses in the Strouhal frequency range. Thus, there is no means by which the measurements made in this series of tests can be correlated with other experiments. Undoubtedly the root mean square of the pressure fluctuations is intimately related to the mean pressure. This becomes more apparent by comparing the mean pressure distributions of Figs. 8 and 9 with the fluctuating pressure distributions of Figs. 14 and 15. Figs. 8 and 14 are for the 3" cylinder at a Reynolds number of 0.8×10^5 and Figs. 9 and 15 are for the 6" cylinder at the same Reynolds number.

The mean pressure distributions compare favourably with those obtained by Fage (Ref. 1), Falkner (Ref. 5) and Roshko (Ref. 9) at similar Reynolds numbers. They are characteristic of the flows with a laminar separation and a turbulent transition at some point behind the cylinder. It is interesting to note that the root mean square of the pressure fluctuation rises from a minimum value at the leading edge of the cylinder to a maximum

at the point of separation. The separation is characterised by a mean pressure recovery followed by a region of almost constant pressure. There is then a reduction in the pressure fluctuations which can be associated with the dead region behind the point of separation. A second peak in pressure fluctuations occurs between $\theta = 150^{\circ}$ and 160° indicating that this could be the region of maximum interference between the vortices which are being alternately shed from each side of the cylinder. In Ref. 13, McGregor calculated root mean square pressure fluctuation coefficients at 20° intervals round a $1\frac{1}{8}$" cylinder for a Reynolds number of 1.2×10^5 and found that they fell to a fairly low level at the rear stagnation point. However, the pressure fluctuations measured from this series of tests indicate that this decrease in pressure fluctuations is not so marked as McGregor suggests. Visual observations of the wave forms of the pressure fluctuations were made from the oscilloscope and these were of similar form to those observed by McGregor.

The drag coefficients calculated from these mean pressure distributions are plotted on Fig. 13. This shows that they are within the limits with which they are usually measured.

The pressure distributions for the 6" cylinder at 50 ft./sec., corresponding to a Reynolds number of 1.6×10^6, indicates a

laminar separation (Fig. 10) and are similar in form to those already discussed. Likewise, the distribution of pressure fluctuations around the surface of the cylinder are of the same form as those for the lower Reynolds number (Fig. 15). However, it will be noticed that there is a much larger dip in the pressure fluctuations behind the separation point at $\theta = 125^{\circ}$ corresponding to a slight increase in the mean pressure coefficient. This indicates that the dead zone is much more predominant at this Reynolds number which corresponds to the point at which the drag coefficient starts to decrease (Fig. 13). It was at first thought that the readings taken in this region were rogue points, but repeatability was demonstrated during the frequency analyses. Even through the 1000 to 1400 c/s range, a marked decrease in background noise level was observed.

For both the higher Reynolds numbers considered, the mean pressure distributions indicate that the flow has both laminar to turbulent flow transition and turbulent separation at the surface of the cylinder. The transition appears to take place near $\theta = 60^{\circ}$ on both Figs. 11 and 12, corresponding to Reynolds numbers of 3.2×10^5 and 6.4×10^5 respectively. This is accompanied by a separation bubble which is indicated by a change in slope of the mean pressure curves and a small region of almost constant pressure characteristic of separation bubbles

(Ref. 21 and 22). This early transition does not appear to have been observed by any previous investigators in this field, perhaps because they did not take many pressure readings in this region. The repeatability of these readings was found to be good. Nevertheless, without a detailed investigation of the boundary layer in this region no definite conclusions can be drawn.

The mean pressure distribution for the Reynolds number of 6.4×10^5 is more characteristic of those obtained by earlier investigators, especially one by Flachsbart at a Reynolds number of 6.7×10^5 which is reproduced by Roshko in Ref. 9. However, the pressure recovery is not so complete as that measured by Flachsbart. This has the effect of increasing the drag coefficient to 0.5 compared with a more usual value of 0.3 to 0.35. It should be remembered that, for this case, the peak negative pressure could not be measured on the Prandtl manometer and one of the tubes of the bank of tunnel manometers had to be used. Thus, the accuracy was reduced.

The root mean squares of the pressure fluctuations (Fig. 16) for both these cases are at a much lower level around the cylinder than for the lower Reynolds numbers considered except at the peak readings. It will be noticed that after the flow has separated, become turbulent, and re-attached there is a sudden rise in the

pressure fluctuations. Corresponding to the separation of the turbulent flow, there is a sharp decrease in the pressure fluctuations and then a slight increase where the effect of the turbulent wake is more predominant. From Fig. 13 it can be seen that the Reynolds number 3.2×10^5 lies in the critical range so that any peculiarities in the flow might be expected to show their influence. This would account for the many small peaks on the curve showing the distribution of pressure fluctuations round the cylinder.

6.2 Frequency Analyses.

6.2.1 Frequency Surveys.

Frequency spectrum surveys of the pressure fluctuations present in the wind tunnel were made at working section wind velocities of 25 ft./sec. and 50 ft./sec. using fan speeds of 150 and 210 r.p.m. respectively. To obtain these data, the pressure transducer was fitted into the ground board which spanned the tunnel on the horizontal centerline. This was done to remove the effect of the cylinder on the pressure fluctuations present. The measurements were made over a continuous range of frequencies from 0 to 2000 c/s. The ground board data for 25 ft./sec. wind velocity are shown in Fig. 17 and for 50 ft./sec. in Fig. 20. Figures 18, 19, 21 and 22 are

similar surveys with the microphone fitted in the 6" cylinder and the ground board removed. Figures 18 and 21 show frequency surveys at $\theta = 0^{\circ}$ for wind velocities of 25 ft./sec. and 50 ft./sec. respectively; figures 19 and 22, at $\theta = 60^{\circ}$ for the same respective wind velocities. For the cylinder tests, data were omitted from these figures in the range near the Strouhal frequency to permit the remaining data to be plotted to the same scale as the ground board data. These data have been corrected for microphone response, but they have not been converted to pressure or coefficient form because they are shown in these figures for tunnel noise comparison only. The interesting portions of the cylinder data appear later in fully reduced form.

At both wind velocities peaks appear at 100 c/s intervals for frequencies less than 800 c/s. Smaller intermediate peaks below 500 c/s make it unlikely that acoustic frequencies associated with the cylinder would be distinguishable from the noise unless they were of really great strength, e.g., the Strouhal frequency. It is clear from the 60° cylinder surveys that a pair of signals associated with the presence of the cylinder occurs near 1200 cycles per second.

The frequency spectrum surveys for the 3" and 12" cylinders are included in the data which has been reduced to power spectral

density. The 3" cylinder frequency surveys (Figs. 59 - 62) were conducted at $\theta = 60^{\circ}$ and 90° from 1000 - 2700 c/s for tests at 25 ft./sec. Those at 50 ft./sec. were done from 1000 - 3000 c/s for $\theta = 60^{\circ}$ and 1000 - 2700 c/s for $\theta = 90^{\circ}$ (Figs. 68 - 70). Again pairs of peaks near 1200 c/s appear. The 12" cylinder frequency surveys (Figs. 74 - 76) were conducted at $\theta = 0^{\circ}$, 60° and 90° from 300 - 1400 c/s at 25 ft./sec. only. The peaks at each multiple of 100 c/s are particularly pronounced for the 12" cylinder at 25 ft./sec., for they appear up to and including 900 c/s (Fig. 74). Once more, a pair of signals near 1200 c/s is apparent for $\theta = 60^{\circ}$ and 90° (Figs. 75 and 76).

Frequency analyses were performed at tunnel fan speeds of 150, 210 and 340 r.p.m. for working section wind velocities of 25, 50 and 100 ft./sec. respectively except for the tests performed on the 3" cylinder at 25 ft./sec. These tests were done at a tunnel fan speed of 210 r.p.m. because the primary frequency associated with the eight-bladed propeller coincided with the Strouhal frequency when the tunnel was run at a fan speed of 150 r.p.m. It was not appreciated at the time that this raised the general background level at high frequencies as well as shifting the discrete frequencies due to the fan. Attempts to repeat the data previously obtained with the 6" cylinder in the 1000 - 1400 c/s frequency range brought out this fact. In future

experiments of this type it is recommended that frequency surveys be conducted for a range of fan speeds at each wind velocity to be used in testing. In that way the most favourable fan speed may be selected for the frequency range in which measurements are to be taken. It is suspected at this time that, in general, the lowest feasible fan speed will prove to be the most suitable except where discrete frequencies at the lower end of the spectrum coincide with the frequencies of specific interest, e.g., the case of the Strouhal frequency cited previously.

6.2.2 Strouhal Frequency Measurements.

Measurements in the frequency range near the Strouhal frequency were made at regular intervals around the 6" cylinder for wind velocities of 25 ft./sec. and 50 ft./sec. Figs. 23 - 28 give the data for the tests at 25 ft./sec. in 30° intervals, and Figs. 34 - 45 give the data for the tests at 50 ft./sec. in 15° intervals. Figs. 56 - 58 and Figs. 63 - 67 give data for Strouhal frequency measurements for the 3" cylinder at 25 and 50 ft./sec. respectively. Figs. 72 and 73 show Strouhal frequency measurement for the 12" cylinder at 25 ft./sec.

For all of these tests the Strouhal number was approximately .2 except for the 12" cylinder results. The accuracy with which

the frequency could be measured at these low frequencies prevents a more accurate assessment of the Strouhal number. This is particularly true of the 12" test.

These data show that in this quasi-non-dimensional form, i.e., power spectral density, the Strouhal frequency intensities for any given angle tend to collapse to a common value. Likewise, the values for the second harmonic, where they are distinguishable, collapse to a common value.

Comparison of the values of pressure coefficient of the Strouhal frequency with those obtained by McGregor (Ref. 13) shows excellent agreement, and the values of the second harmonic also compare favourably.

6.2.3 Frequency Analyses in the Acoustic Range.

All of the early tests were performed on the 6" cylinder. Shaw's predicted value for the expected acoustic signal (equation 2.3) was about 1050 c/s. The frequency surveys discussed in paragraph 6.2.1 had failed to detect any pairs of signals near this frequency or even an isolated signal, but a pair of signals near 1200 c/s was detected.

The first group of tests were performed at a wind velocity of 50 ft./sec, (R_e = 1.6 x 10^5). The frequency band from 1000 - 1400 c/s was analysed at 5° intervals around one side of

the cylinder. These data are shown in Figs. 46 - 54. Only representative data have been shown for the extreme back of the cylinder because the background level rose to completely mask the signals being studied.

The first salient feature noted was that the two peaks were separated by 40 c/s, just twice the Strouhal frequency, as would be true of Shaw's predicted frequency. These two signals were consistently detected at 1165 and 1205 c/s as accurately as could be determined. Next, it was concluded that neither signal was consistently larger than the other. The differences in signal strength are attributable to the difficulty of tuning the Marconi Wave Analyzer, for the 4 c/s band width corresponded to approximately 0.1° of arc of the frequency scale in the range from 1000 - 1400 c/s.

It was then noted that the signals rose from an undetectable level at the front of the cylinder. The peak values rose in magnitude to a maximum near the angle of peak suction of the mean pressures, and then remained nearly constant further around the cylinder. This gave a maximum signal to noise ratio at $\theta = 65^{\circ}$. For greater angles the background level rose until the acoustic signals became undetectable at $\theta = 90^{\circ}$ where the background level corresponded with the amplitudes of the peaks.

It was noted in paragraph 6.1 that the R.M.S. value of the pressure fluctuations had a pronounced minimum near $\theta = 125^{\circ}$ for the 6" cylinder at 50 ft./sec. This was verified when performing the frequency analyzer measurements in this range. As a result of the drop in the overall pressure fluctuations, the pair of signals was again detected at $\theta = 120^{\circ}$ and 125°. The peak amplitudes were of the same order as those observed for $\theta = 65^{\circ}$ and the frequencies were unchanged. For angles greater than this the background level again rose to mask these signals.

Tests of the same frequency range for the 6" cylinder at 25 ft./sec. ($R_e = 0.8 \times 10^5$) are shown for 15° intervals in Figures 29 - 33. One of the pair of signals was detected at the front of the cylinder, but the other comments regarding signal strength made for the 50 ft./sec. tests on this cylinder remain valid. At 25 ft./sec. the background level did not mask the peaks until $\theta = 135^{\circ}$, and it did not drop again to permit their re-appearance. The frequencies determined for these signals were 1180 and 1200 c/s. This, again, is twice the Strouhal frequency. The amplitudes of the peaks in power spectral density units are identical within the limits of experimental accuracy for corresponding angles. An extraneous peak of half amplitude appeared for $\theta = 105^{\circ}$ at 1105 c/s. During the 50 ft./sec.

tests it had been thought that the near critical Reynolds number might account for the difference between the measured frequencies and Shaw's predicted values, but these tests at a clearly sub-critical Reynolds number refuted that premise.

Sampling tests were performed on the 3" cylinder and 12" cylinder to explore the effects of cylinder diameter on the observed frequencies. For the 3" cylinder, the predicted frequency was about 2100 c/s, so the frequency range was analyzed from 1000 - 2700 c/s. These data for the 3" cylinder at 25 ft./sec. ($R_e = 0.4 \times 10^5$) are shown in Figs. 59 - 62. A pair of signals occurred at 1170 and 1215 c/s of similar amplitude to the 6" cylinder tests at corresponding angles. Again the frequency separation was by twice the Strouhal frequency. The signal to noise ratio was not so large as had been the case for the 6" cylinder at the same speed. This was due to the fan speed selection discussed in paragraph 6.2.1. No other signals were detected in the frequency range from 1000 - 2700 c/s. The results of the 3" cylinder tests at 50 ft./sec. ($R_e = 0.8 \times 10^5$) are shown in Figures 66 - 70. At $\theta = 60^\circ$, the frequency band analyzed was 1000 - 3000 c/s, and at 90° the band analyzed was 1000 - 2700 c/s. Data for a frequency band of 1000 - 1400 c/s are also shown for $\theta = 30^\circ$, 120° and 180° in Figs. 68, 66, and

67 respectively. The only peak signals found were the pair separated by twice the observed Strouhal frequency at 1155 and 1230 c/s. Peak amplitudes again correspond with the other data at the same angles. For the 12" cylinder, the predicted frequency is 525 c/s. Frequency analyses of tests on the 12" cylinder at 25 ft./sec. (R_e = 1.6 x 10^5) are shown for θ = 0°, 60°, and 90° in Figures 74 - 76. At each of these angles, measurements were taken for frequencies ranging from 300 - 1400 c/s. Single peaks occur at 500 c/s for each of these, but nothing appears between 500 and 600 c/s. It is felt that these peaks at 500 c/s are associated with the peaks which occurred in all tests at integral multiples of 100 c/s. At θ = 60° and 90° a pair of signals occur near 1200 c/s. At 60° the frequencies were 1195 and 1210 c/s, and at 90° the frequencies were 1185 and 1200 c/s. The separation between peaks was twice the measured Strouhal frequency, but the slight apparent drift in the frequencies is not accounted for. Peak amplitudes were similar to those at comparable angles in other tests. Measurements were made between 1000 and 1400 c/s on the 12" cylinder at θ = 90° with the tunnel wind velocity as low as possible (Fig. 71). This was approximately 10 ft./sec. with a fan speed of 110 r.p.m. Small peaks appeared at 1085, 1105, and 1120 c/s. These are possibly related to the extraneous peak which appeared at 1105 c/s for one of the 6" cylinder tests. One large peak appeared at 1205 c/s. Since

the Strouhal frequency would only be 2 c/s at this speed for the usual Strouhal number of .2, a difference of twice the Strouhal frequency would not have been detectable with a 4 c/s band width filter. This last peak was slightly higher than was typical of other values at $\theta = 90^{\circ}$ by a factor of about 2 to 3; but this is not surprising if the wave analyzer were, in fact, measuring a pair of signals within its band width rather than an isolated signal.

Shaw found that the acoustic signals disappeared when he forced transition with fixed wires. While mean pressure measurements were being rechecked at 100 ft./sec., which is in the critical Reynolds number range, checks of the 1000 - 1400 c/s range were done at $\theta = 30^{\circ}$ and $\theta = 60^{\circ}$ (Fig. 55). The pair of signals still appeared clearly at comparable magnitudes separated by twice the measured Strouhal frequency. The measured frequencies were 1145 and 1230 c/s.

The theory proposed by Shaw implied that the second signal of the pair of acoustic signals would have its frequency fixed by the cylinder geometry while the other signal would be at a lower frequency by twice the value of the Strouhal frequency. The acoustic signals measured in this report did not shift frequency with either signal holding a fixed value, but rather both signals shifted about a mean. The mean value of the

frequency pairs is very nearly 1190 c/s for all pairs detected irrespective of cylinder size or tunnel wind velocity. This might tend to suggest that the basic frequency of 1190 c/s is a wind tunnel phenomenon, or one associated with the wind tunnel versus cylinder relation, in which the 1190 c/s signal "beats" with the Strouhal signal causing a modulation of the original signal into a pair of signals, one raised and one lowered by the Strouhal frequency. Curiously, in Shaw's experiments (Ref. 19) the principal pair of signals which he recorded are also centered about 1190 c/s; however, his tests were conducted in a 9' x 7' wind tunnel. Therefore, the likelihood of the wind tunnel, or wind tunnel cylinder relation, providing the source of the acoustic signal is placed in some doubt. Tests with circular discs attached to the cylinder normal to the axis in varying locations, or with some other means of drastically altering the geometry of the cylinder surroundings might help to clarify this point.

7. CONCLUSIONS AND RECOMMENDATIONS

1. In similar future investigations, it is recommended that full spectrum frequency surveys of wind tunnel noise be conducted at various tunnel fan speeds for each working section wind velocity to be used.

2. The studies of the mean pressure distribution indicate the likelihood of a small separation bubble near $\theta = 60^{\circ}$ for the tests at the critical Reynolds number of 3.2×10^5 and the super-critical Reynolds number of 6.4×10^5.

3. The maximum intensity of the pressure fluctuations was found to be associated with the positions of peak suction of the mean pressures. A second large maximum in the curves of pressure coefficients of the fluctuating pressures occurred near $\theta = 160^{\circ}$ for all tests.

4. Intensities of pressure fluctuations at the Strouhal frequency increased from a minimum at the front of the cylinder to a maximum at the sides. A constant level was then maintained until near the 180° position where a rapid drop occurred. These results agreed quantitatively with the measurements made by McGregor (Ref. 13).

5. Intensities of the pressure fluctuations at the second harmonic of the Strouhal frequency increased from a minimum at the front of the cylinder to a maximum at the back where the harmonic

was the dominant frequency of the whole spectrum. Measured values again agreed with McGregor's results.

6. A pair of acoustic signals, whose frequencies differed by the second harmonic of the Strouhal frequency, was detected on each of the three cylinders tested at all wind velocities for which frequency analyses were performed.

7. The centre frequency of the acoustic signal pairs was essentially constant for all cylinders at 1190 c/s regardless of wind velocity. Measurements of these acoustic frequencies made by Shaw (Ref. 19) also show a centre frequency of 1190 c/s.

8. The intensities of these acoustic signals increased from a minimum at the front of the cylinder to a maximum near the point of peak negative mean pressure. Aft of this point the intensities remained constant until the signals were lost in the increasing background noise.

9. The power spectral density values of the acoustic frequencies were of the same order for corresponding angles on all cylinders at all wind velocities.

10. The acoustic signals were detectable for flow in the critical Reynolds number range at $R_e = 3.2 \times 10^5$. No measurements were made at $R_e = 6.4 \times 10^5$.

11. Further tests are recommended in which the geometry of the surroundings of the cylinder differs significantly, or can

be varied, from the geometry of these tests to determine the effect on the frequencies of the acoustic signals.

REFERENCES

1. Fage, A. The Airflow Around a Circular Cylinder in the Region where the Boundary Layer Separates from the Surface. R. and M. No. 1179, August 1925.

2. Fage, A. The Drag of Circular Cylinders and Spheres at High Values of Reynolds Number. R. and M. No. 1370, May 1930.

3. Lindsey, W.F. Drag of Cylinders of Simple Shapes. N.A.C.A. Report 619 (1938).

4. Stack, J. Compressibility Effects in Aeronautical Engineering. N.A.C.A., A.C.R. (1941).

5. Goldstein, S. Fluid Dynamics VOL. 2. Oxford University Press (1938).

6. Gowen, F.E. and Perkins, E.W. Drag of Circular Cylinders for a Wide Range of Reynolds Numbers and Mach Numbers. N.A.C.A. T.N. 2960 (1953).

7. Delany, N.K. and Sorensen, N.E. Low Speed Drag of Circular Cylinders of Various Shapes. N.A.C.A. T.N. 3038. (June 1953).

8. Roshko, A. On the Drag and Shedding Frequency of Two-dimensional Bluff Bodies. N.A.C.A. T.N. 3169. (July 1954).

9. Roshko, A. Experiments on the Flow past a Circular Cylinder at very high Reynolds Number. Journal of Fluid Mechanics, VOL. 10, Part 3. (1961).

10. Mallock, A. On the Resistance of Air Proc. Royal Society, LONDON A.79 (262-273) 1907.

11. Relf, E.F. and Ower, E. The Singing of Circular and Stream-line Wires. R. and M. No. 825 (March 1921).

12. Relf, E.F. and Simmons, L.F.G. The Frequency of the Eddies Generated by the Motion of Circular Cylinders Through a Fluid. R. and M. No. 917. (June 1924).

13. McGregor, D.M. An Experimental Investigation of the Oscillating Pressure on a Circular Cylinder in a Fluid Stream. University of Toronto, Institute of Aerophysics. UTIA Technical Note No. 14, 1957.

14. Gerrard, J.H. Measurements of the Fluctuating Pressure on the Surface of a Circular Cylinder. Part I. Cylinder of 1" Diameter, A.R.C. 19,844, 1958.

15. Fung, V.C. Fluctuating Lift and Drag Acting on a Cylinder in a Flow at Supercritical Reynolds Numbers. Journal of the Aerospace Sciences. 1960, Vol. 27, No. 11, pp 801 - 814.

16. Keefe, R.T. An Investigation of the Fluctuating Forces Acting on a Stationary Cylinder in a Subsonic Stream and of the Associated Sound Field. University of Toronto, Institute of Aerophysics, UTIA Report No. 76. September, 1961.

17. Shaw, R.A. A Theory of Acoustic Frequency and Resonance as Controlling Factors in Aerodynamics. A.R.C. 12,376. 30th May, 1949.

18. Shaw, R.A. The Solution of the Problem of a Cylinder Shedding a Periodic Wake. A.R.C. 12,696. 7th November, 1949.

19. Shaw, R.A. A Preliminary Investigation of the Acoustic Theory of Airflow. Low Speed Wind Tunnel Tests on an Aerofoil and a Cylinder. A.R.C. 13,795. 21st February, 1951.

20. Shaw, R.A. An Explanation of Vortex Shedding in the Basis of Pulses Travelling at the Speed of Sound. A.R.C. 18,455. 1st May, 1956.

21. Burrows, F.M. and Newman, B.G. The Application of Suction to a Two-dimensional Laminar Separation Bubble. The Aerophysics Department of Mississippi State University. Research Report 27 (1959).

22. Thwaites, B. Incompressible Aerodynamics, Oxford University Press, 1960, pp. 102 - 106.

6" Cylinder in 8'x6' Wind Tunnel

Fig. 1

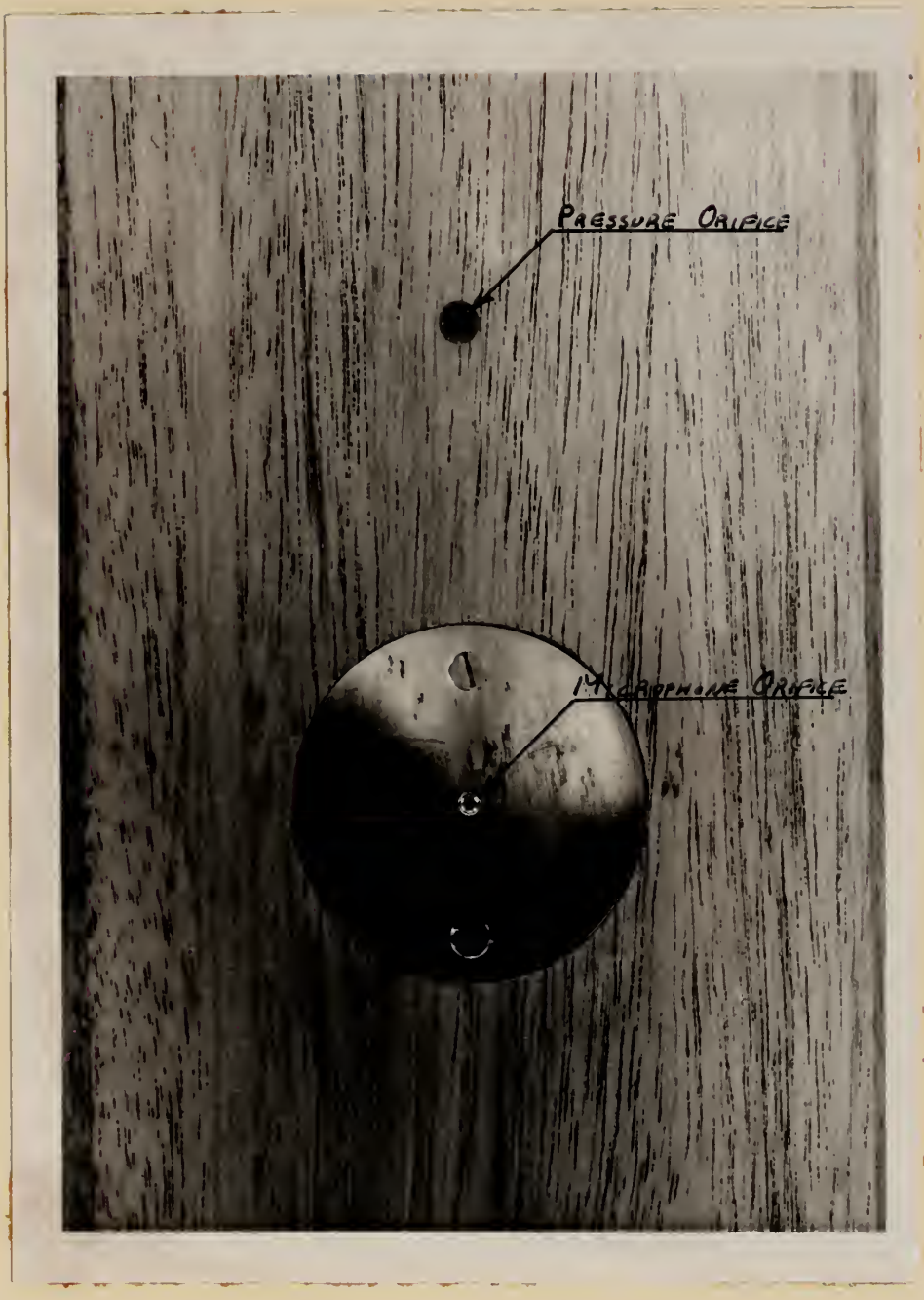

6" CYLINDER DETAIL

FIG. 2

Details of Model Assembly

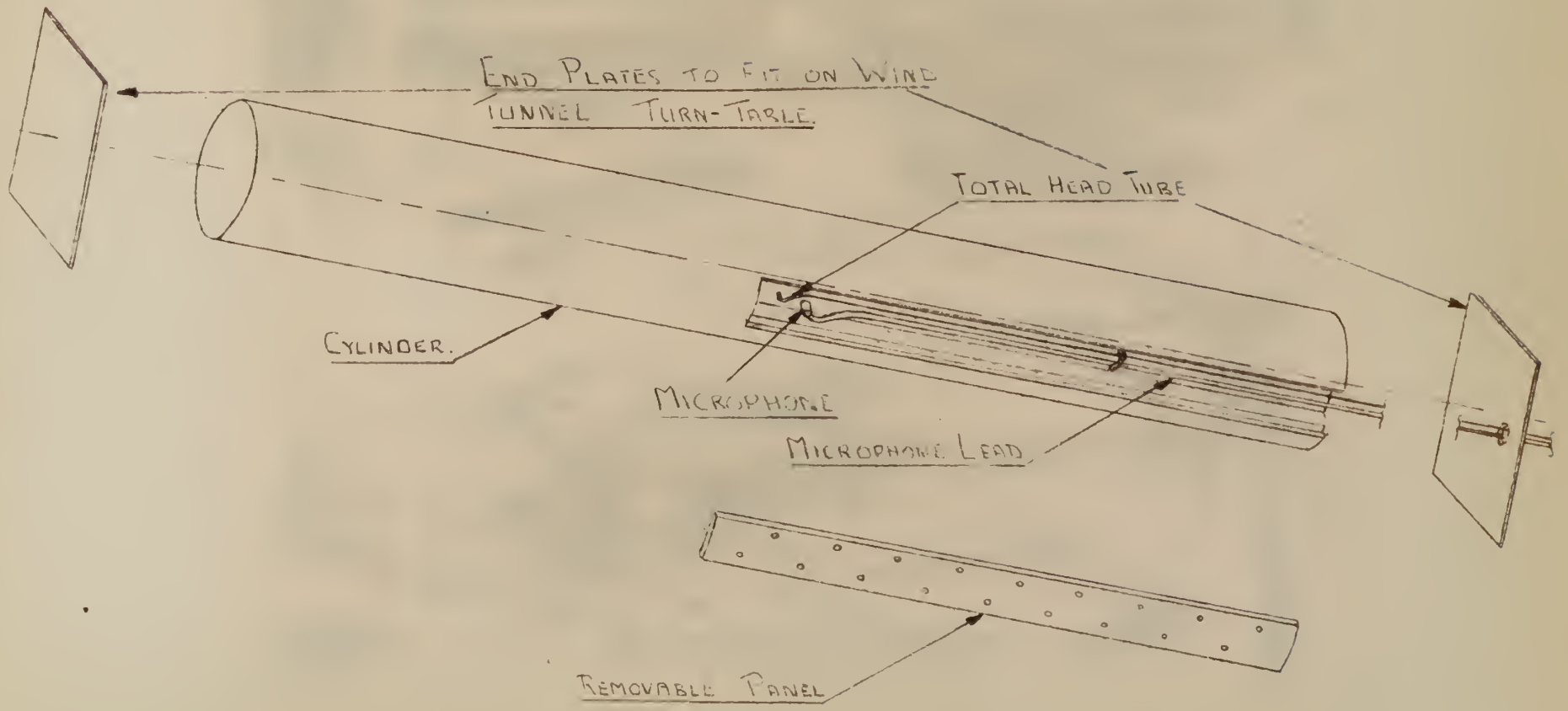

Fig. 3

BLOCK DIAGRAM OF MICROPHONE INSTRUMENTATION

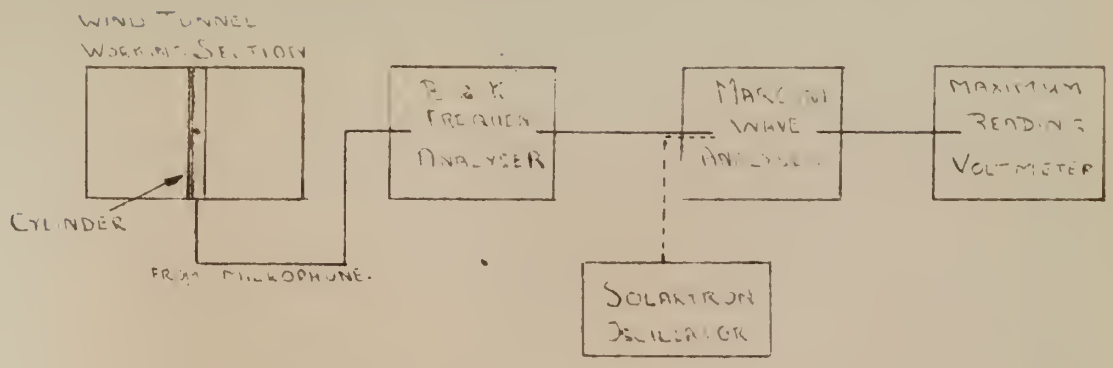

FIG. 4

MICROPHONE

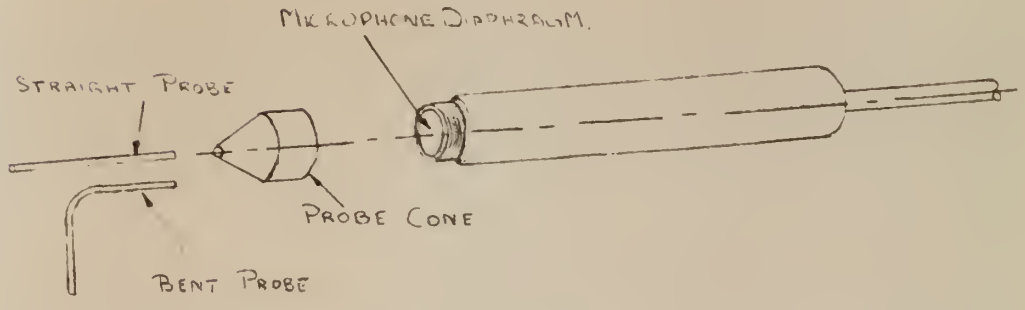

FIG. 5

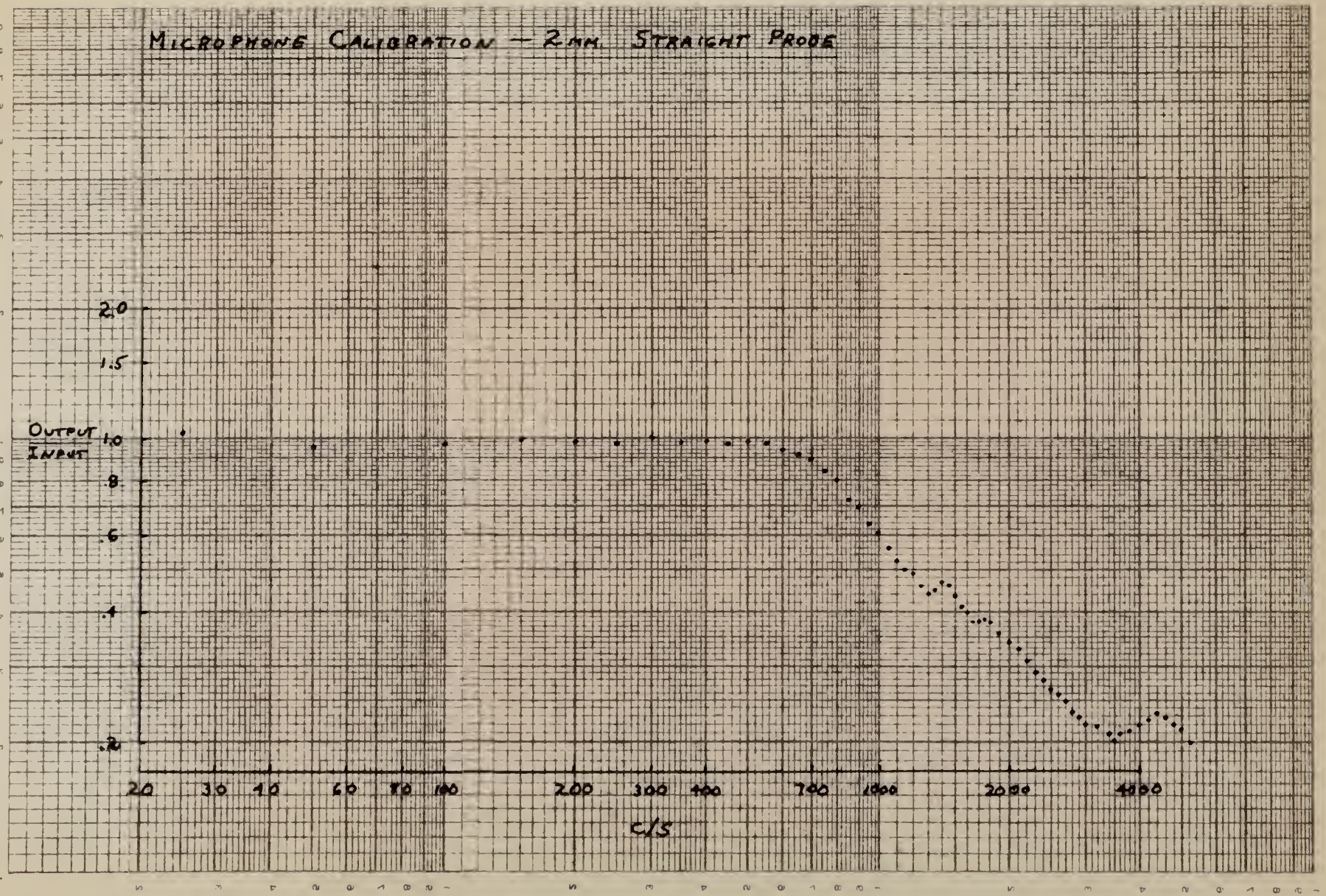
MICROPHONE CALIBRATION — 2 MM. STRAIGHT PROBE
OUTPUT / INPUT
2.0
1.5
1.0
.8
.6
.4
.2
20
30
40
60
80
100
200
300
400
700
1000
2000
4000
C/S

FIG. 6

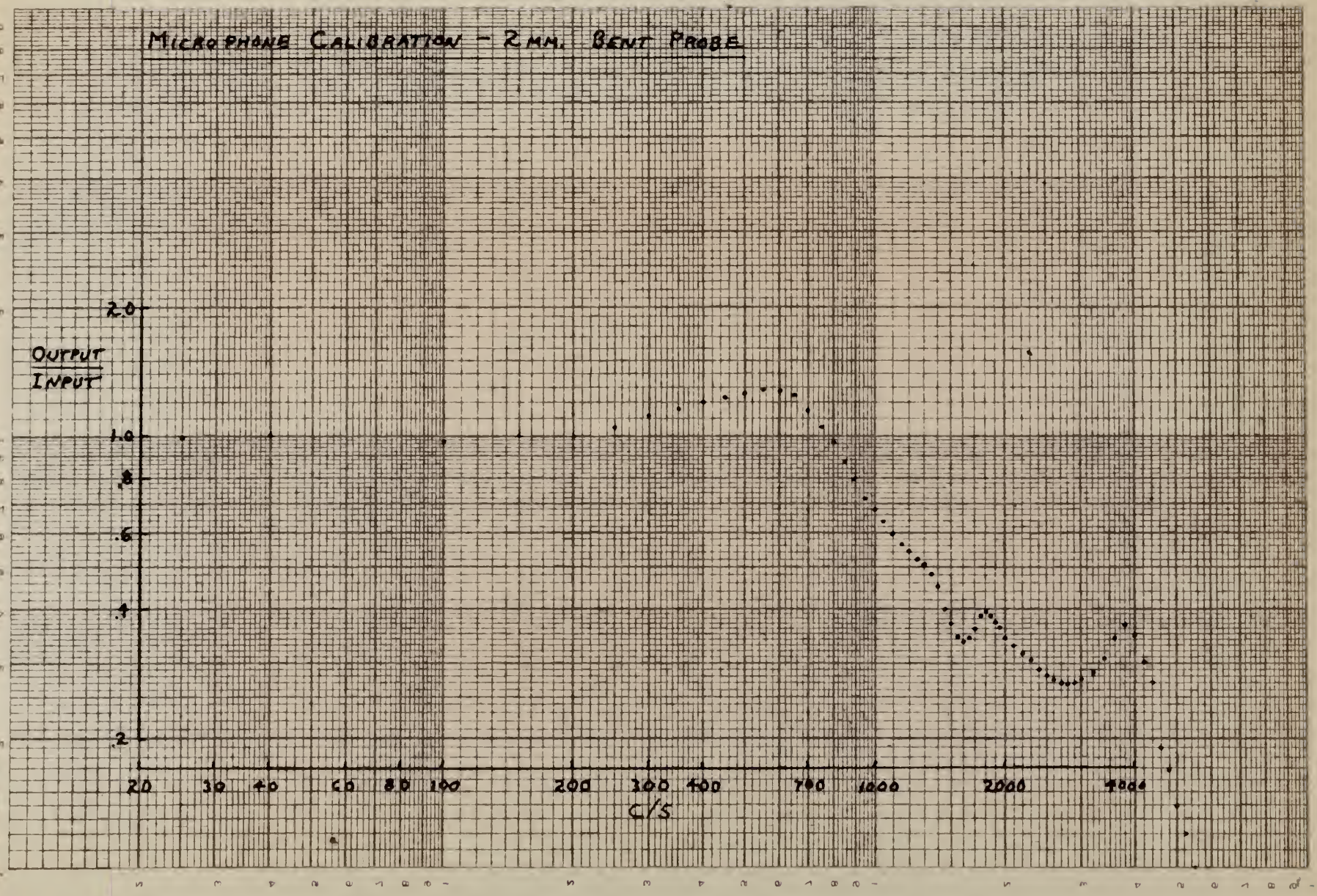
MICROPHONE CALIBRATION - 2 MM. BENT PROBE
OUTPUT / INPUT
2.0
1.0
.8
.6
.4
.2
20
30
40
60
80
100
200
300
400
700
1000
2000
4000
C/S

FIG. 7

K·E 10 X 10 TO THE ½ INCH 359H-12
KEUFFEL & ESSER CO. MADE IN U.S.A.

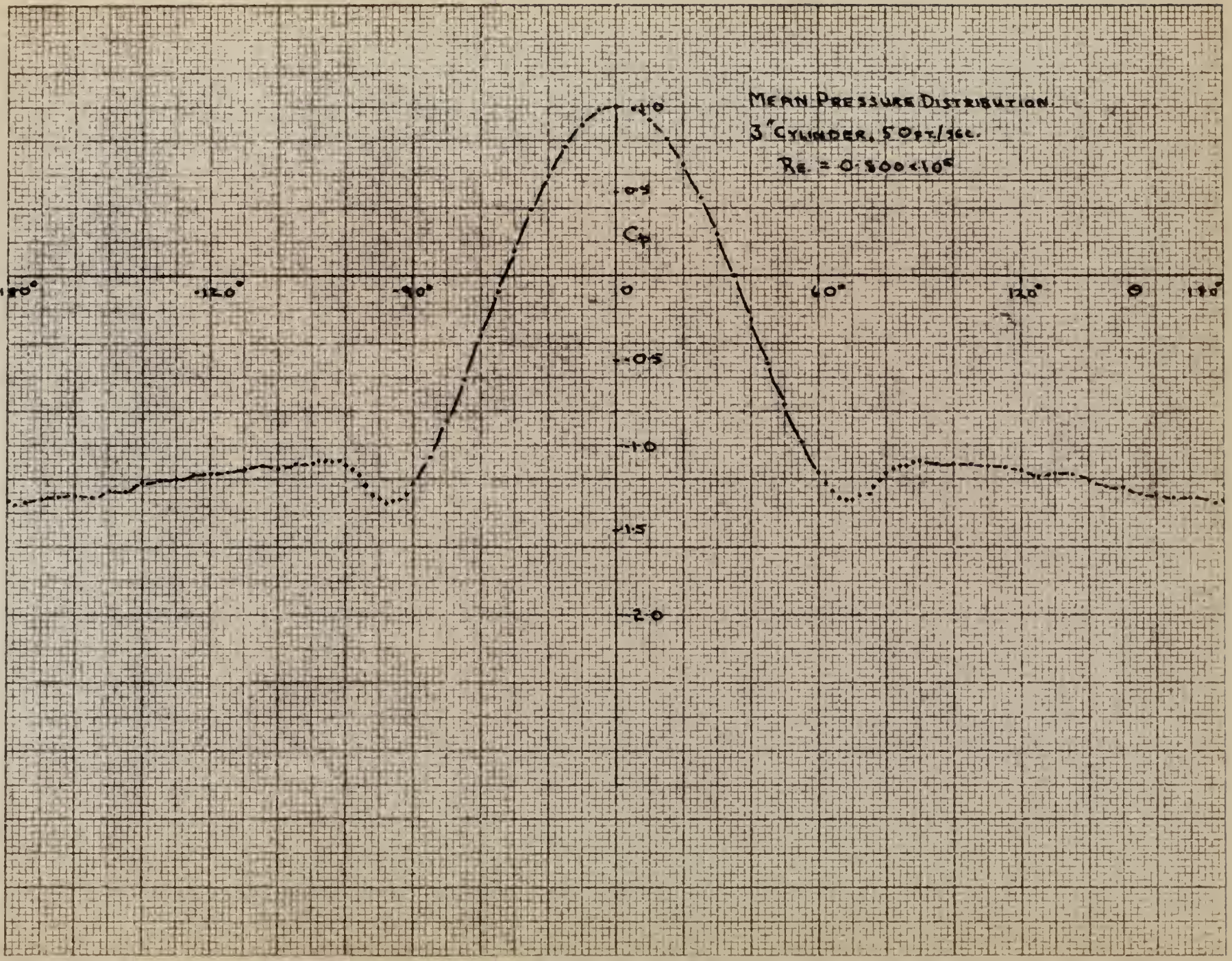

Fig. 8.

K+E 10 X 10 TO THE ½ INCH 359H-12
KEUFFEL & ESSER CO. MADE IN U.S.A.

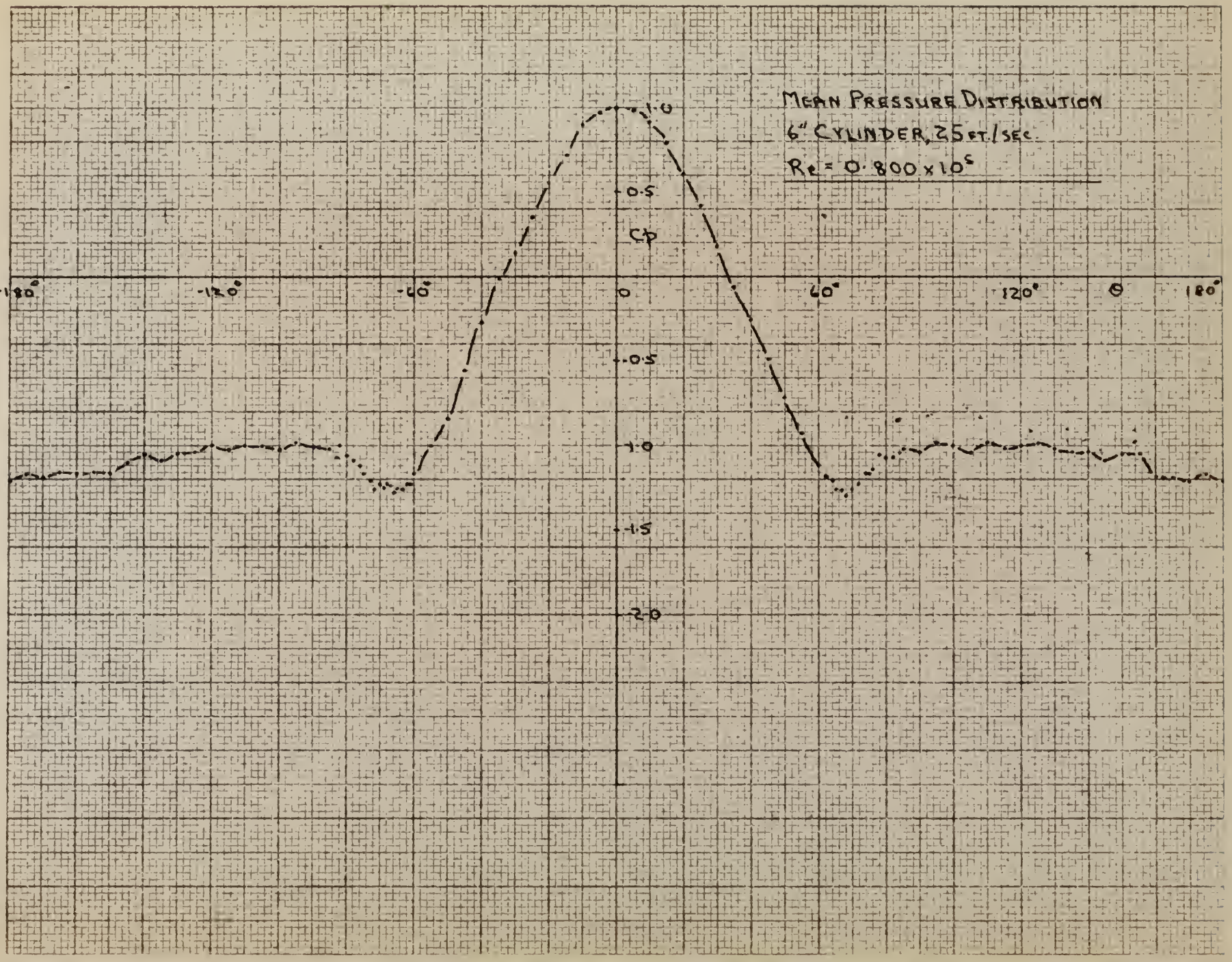

Fig. 9

K&E 10 X 10 TO THE ½ INCH 359H-12
KEUFFEL & ESSER CO. MADE IN U.S.A.

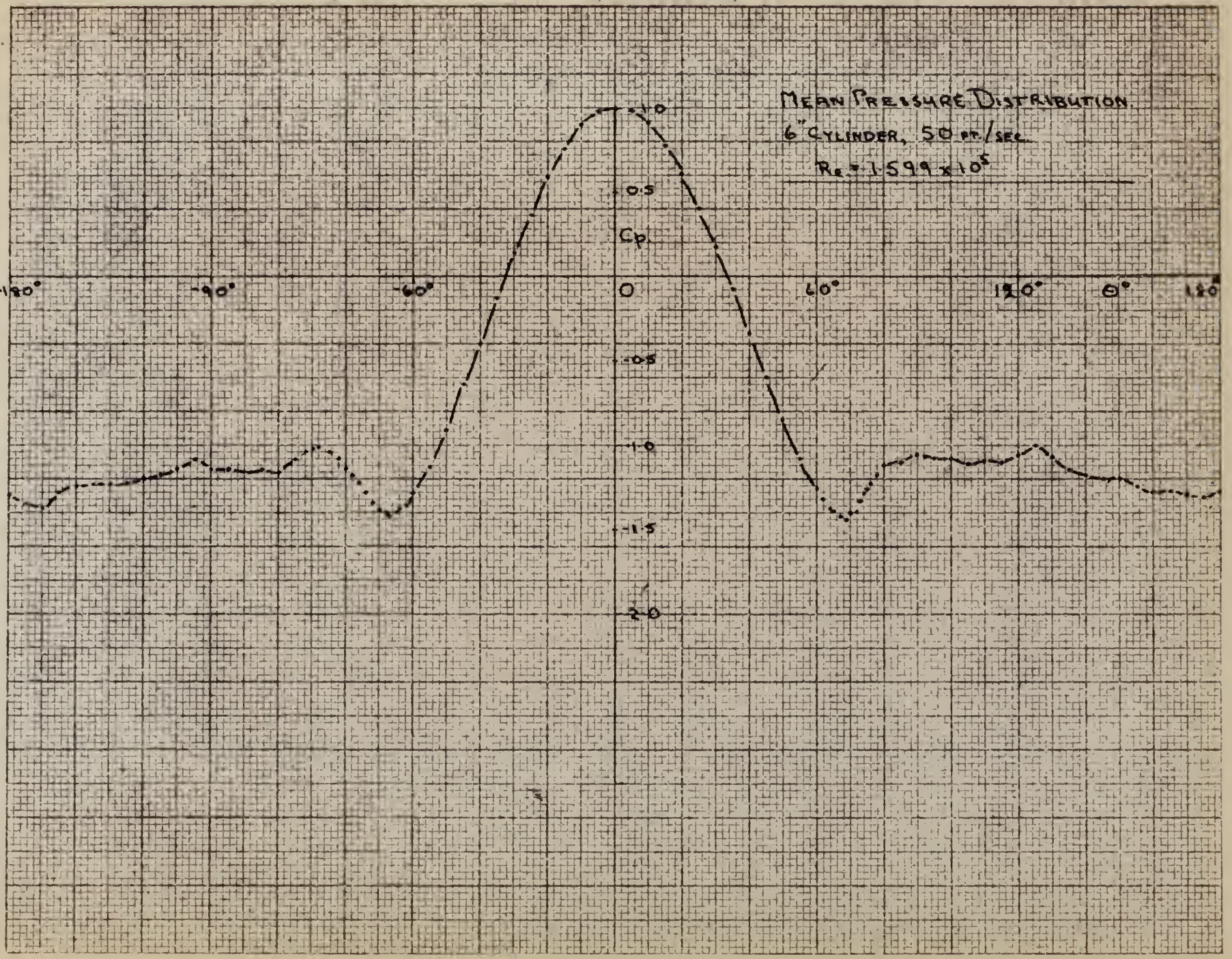

Fig. 10

K·E 10 X 10 TO THE ½ INCH 359H-12
KEUFFEL & ESSER CO. MADE IN U.S.A.

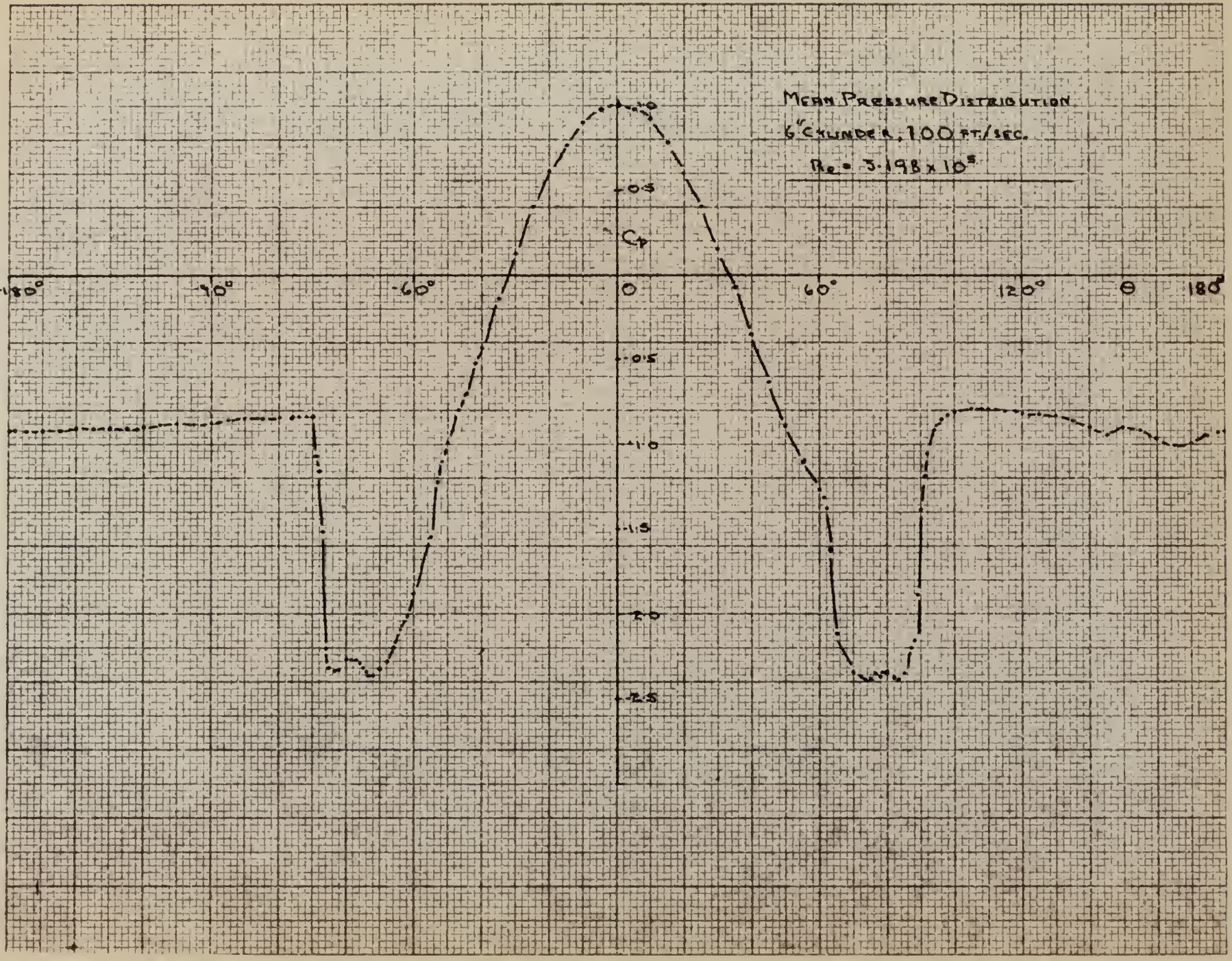

Fig. 11

K&E 10 X 10 TO THE ½ INCH 359H-12
KEUFFEL & ESSER CO. MADE IN U.S.A.

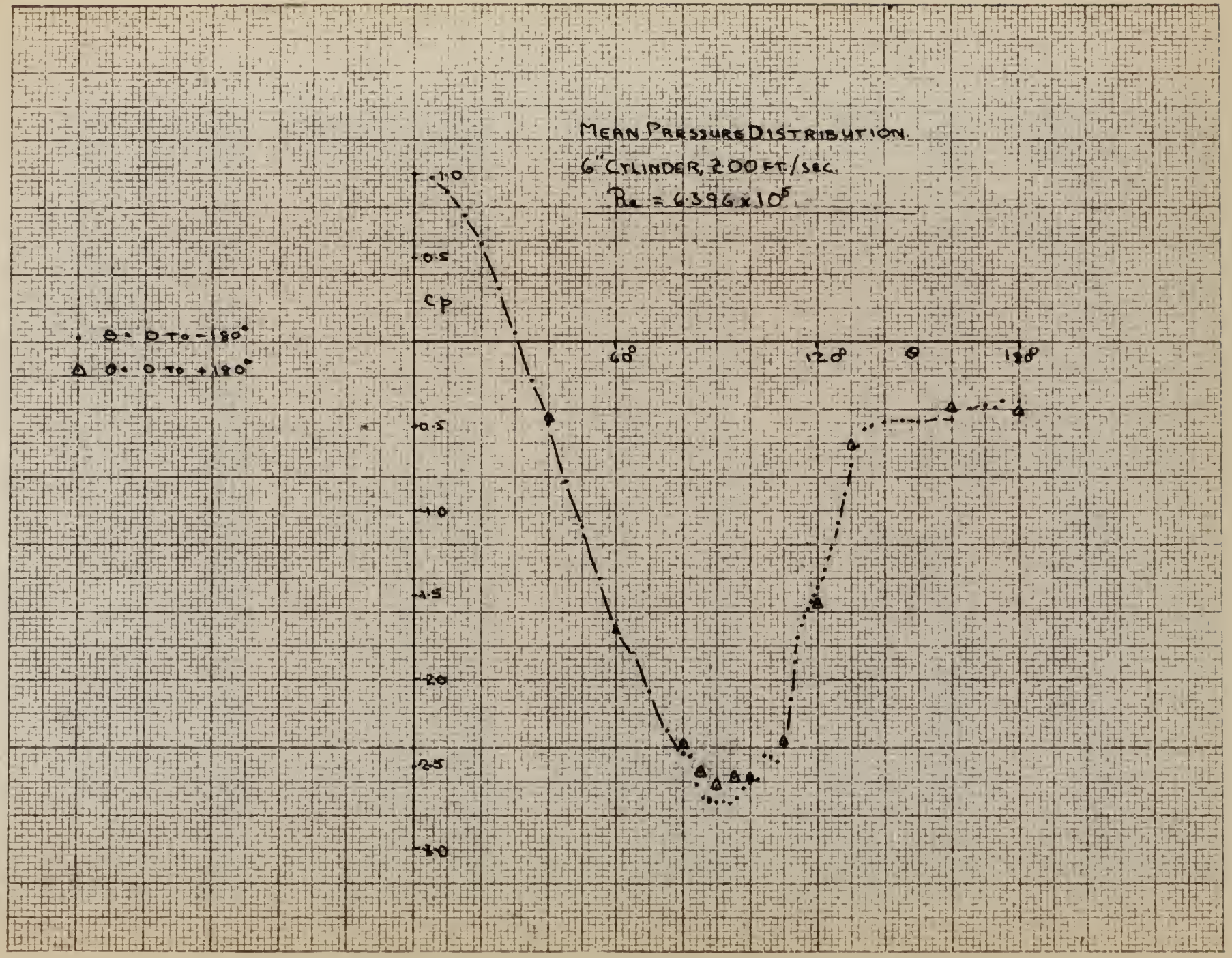

FIG. 12

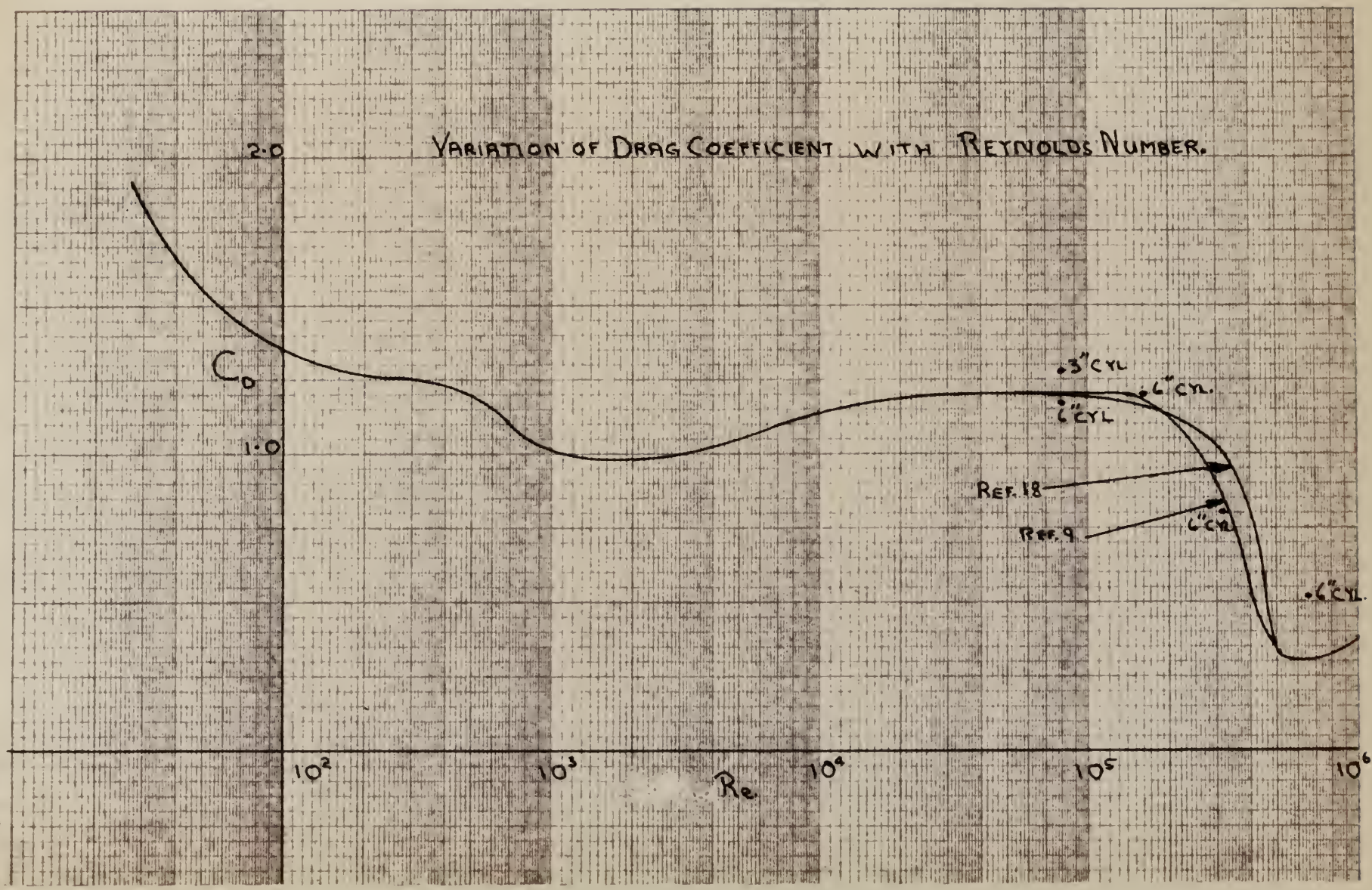
GRAPH SHEET No 5555
VARIATION OF DRAG COEFFICIENT WITH REYNOLDS NUMBER.
2·0
1·0
C_D
.3" CYL
.4" CYL.
.6" CYL
REF. 18
REF. 9
.6" CYL
.6" CYL.
10^2
10^3
Re.
10^4
10^5
10^6

FIG. 13

DISTRIBUTION OF PRESSURE FLUCTUATIONS

3" CYLINDER, 50 FT/SEC, $R_e = 0.8 \times 10^5$

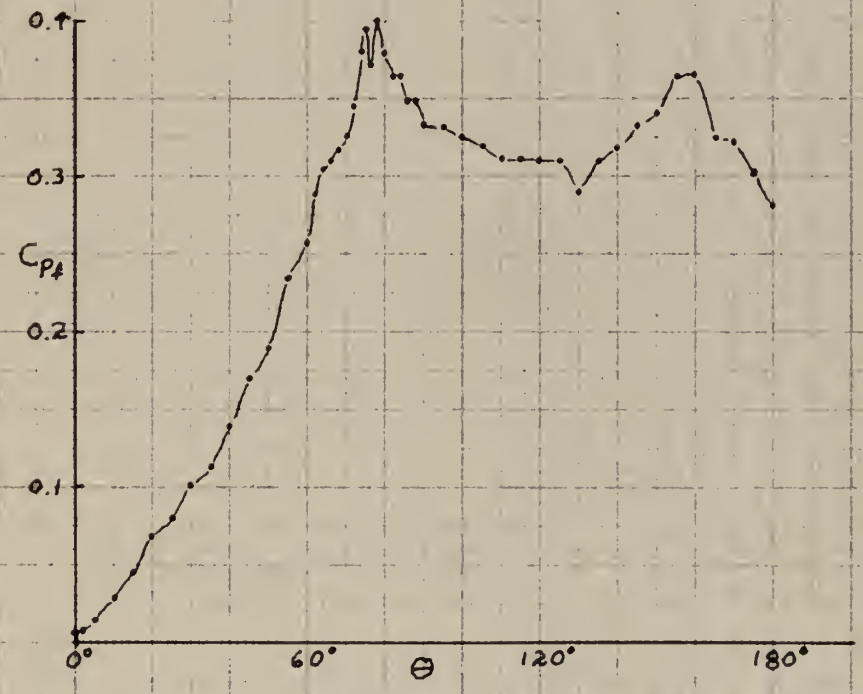

FIG. 14

DISTRIBUTION OF PRESSURE FLUCTUATIONS, 6" CYLINDER

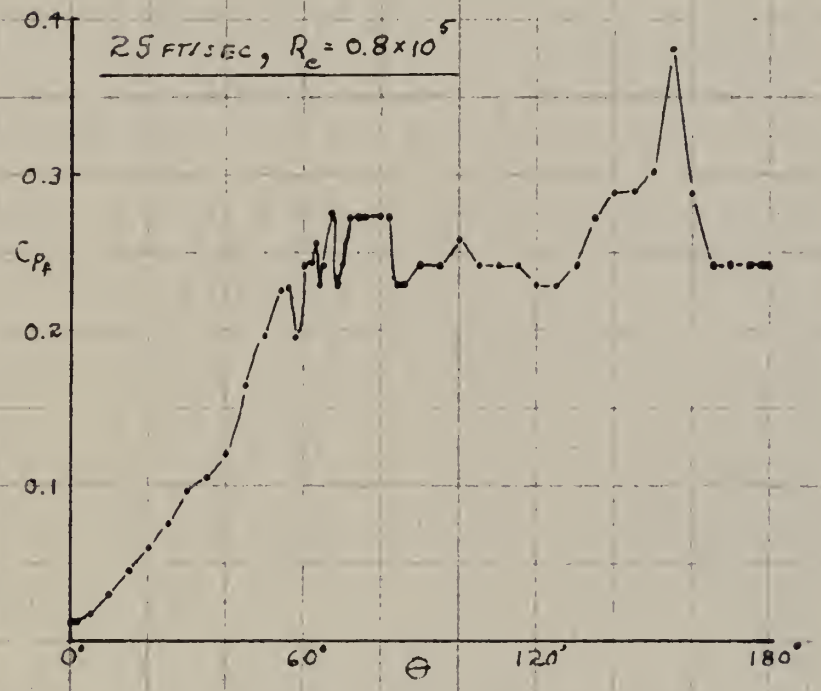

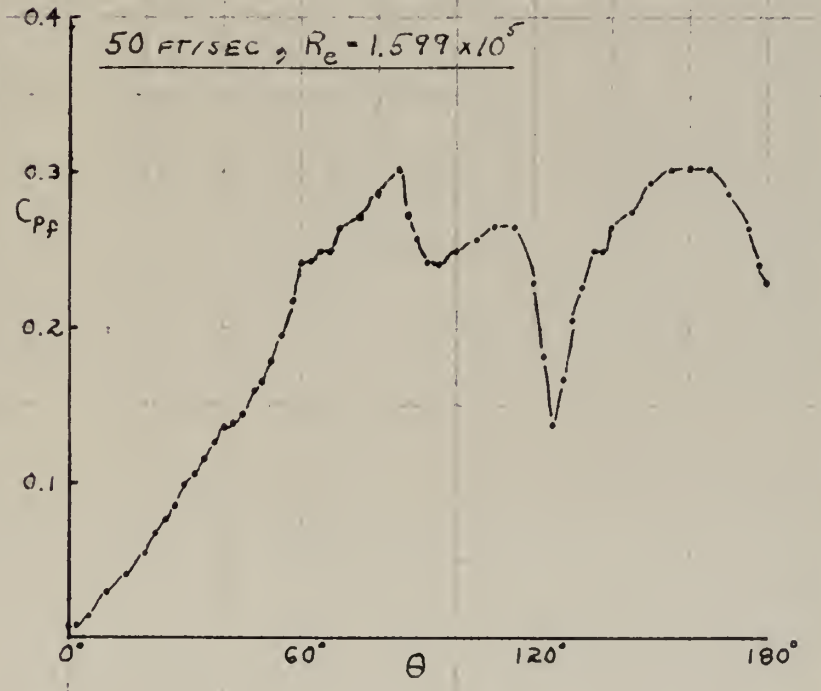

FIG. 15

DISTRIBUTION OF PRESSURE FLUCTUATIONS, 6" CYLINDER

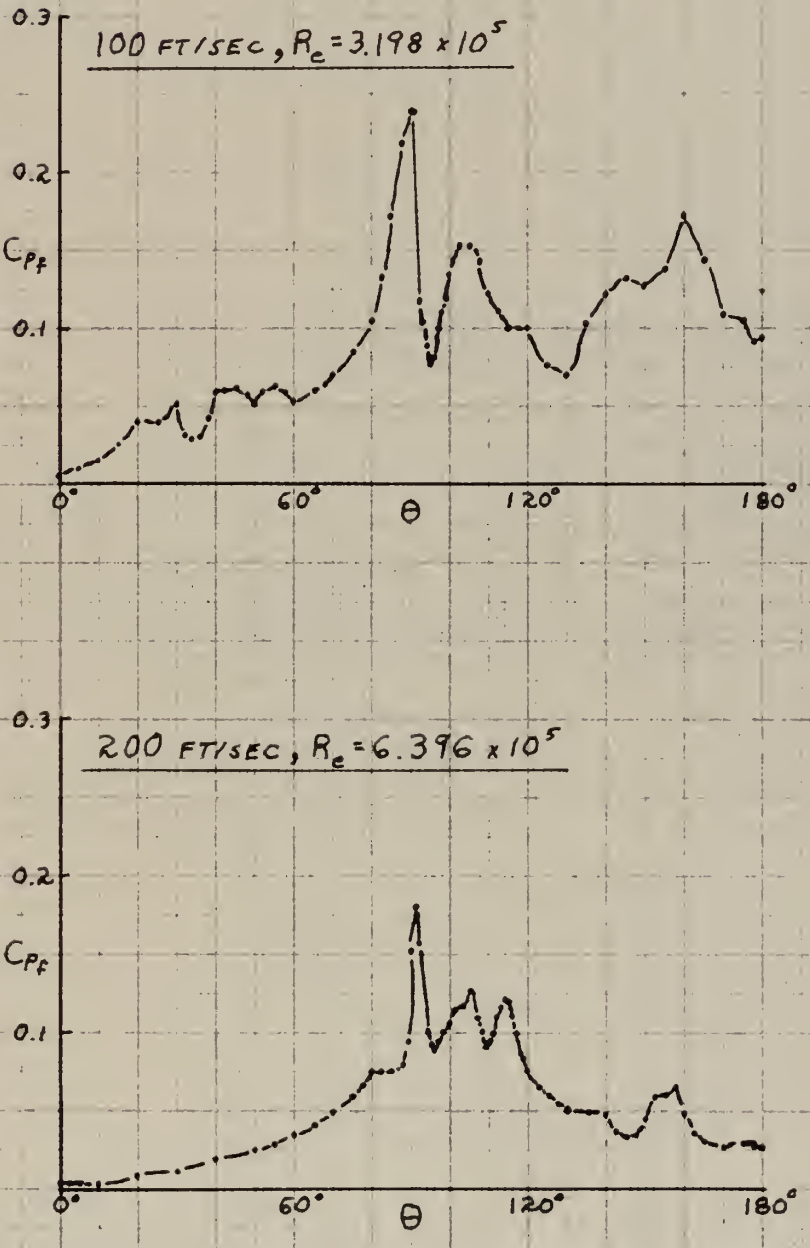

FIG 16

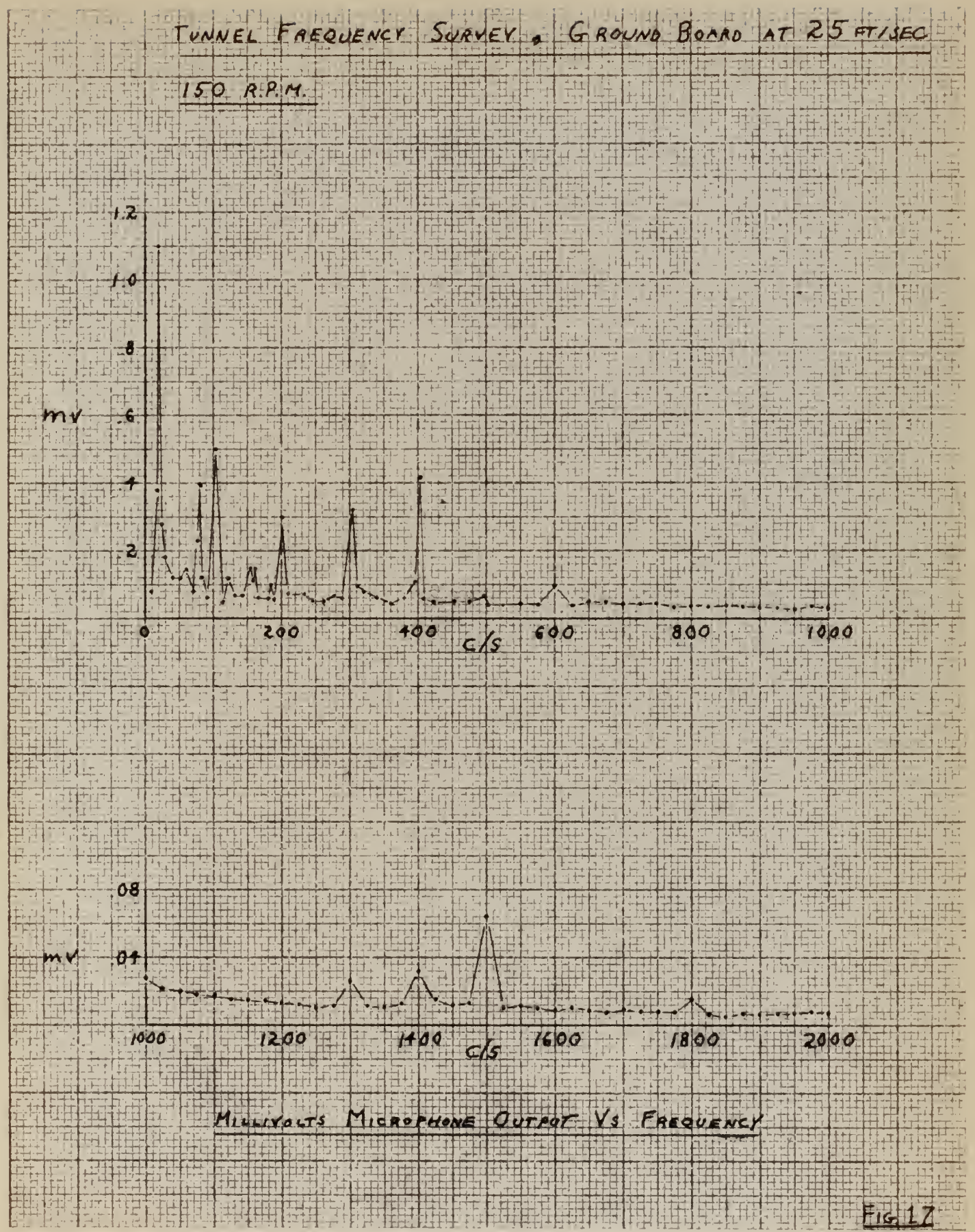

10 X 10 TO THE INCH 359H-12
KEUFFEL & ESSER

FIG 18

10 X 10 TO THE ½ INCH 359H-12
KEUFFEL & ESSER

6" Cylinder, Frequency Survey at 25 Ft./Sec R.P.M. 150

$\theta = 0°$

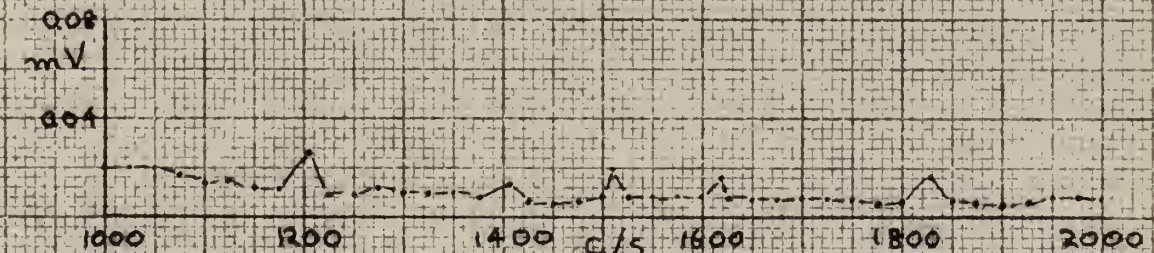

Millivolts Microphone Output Vs Frequency

Fig. 19

10 X 10 TO THE ½ INCH 359H-12
KEUFFEL & ESSER

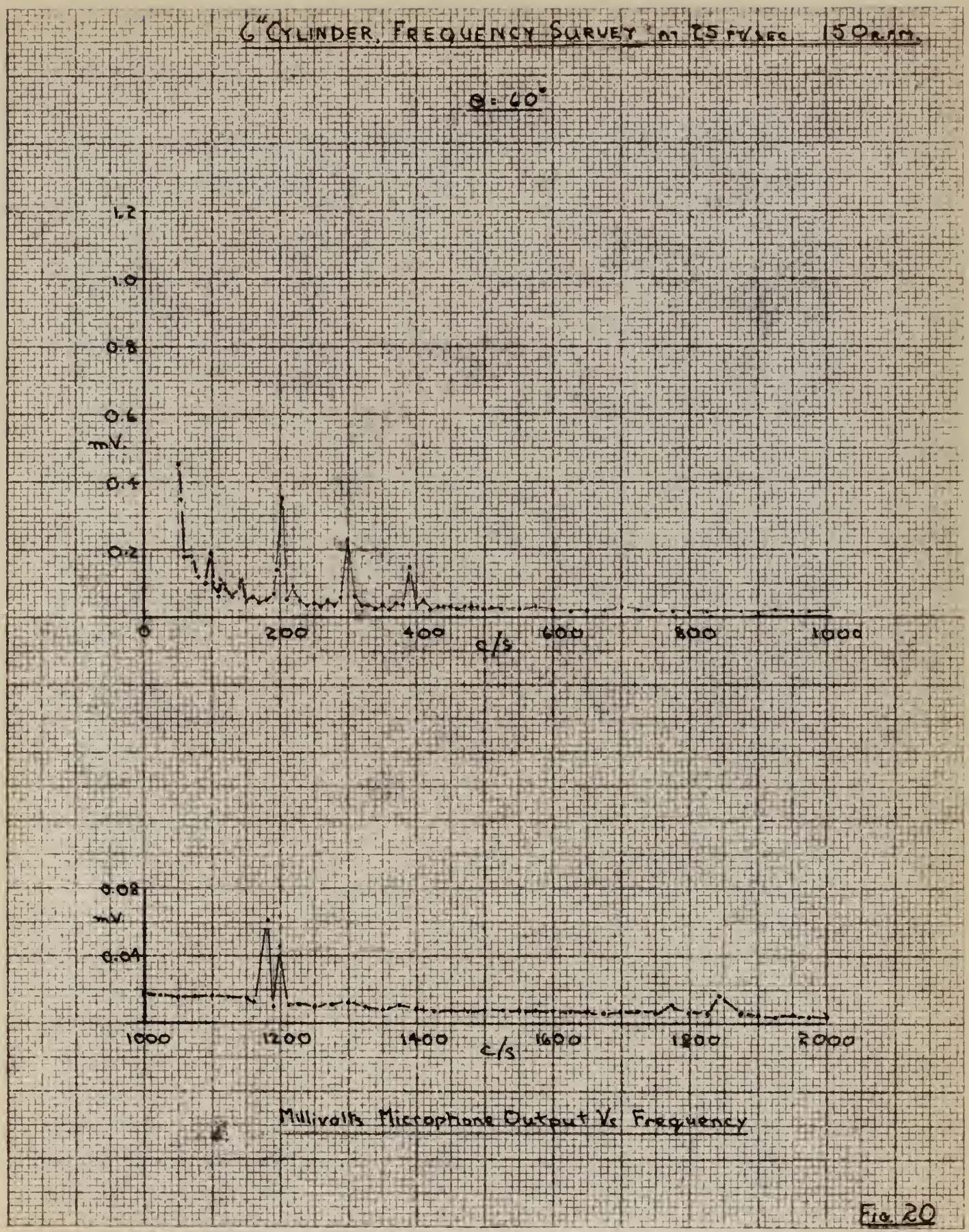
6" CYLINDER. FREQUENCY SURVEY at 25 FT/SEC 150 R.P.M.
θ = 60°
1.2
1.0
0.8
0.6
mV.
0.4
0.2
0
200
400
600
800
1000
c/s
0.08
mV.
0.04
1000
1200
1400
1600
1800
2000
c/s
Millivolts Microphone Output Vs Frequency

FIG. 20

6" Cylinder, Frequency Survey at 50 ft/sec. 210 R.P.M.

θ = 0°

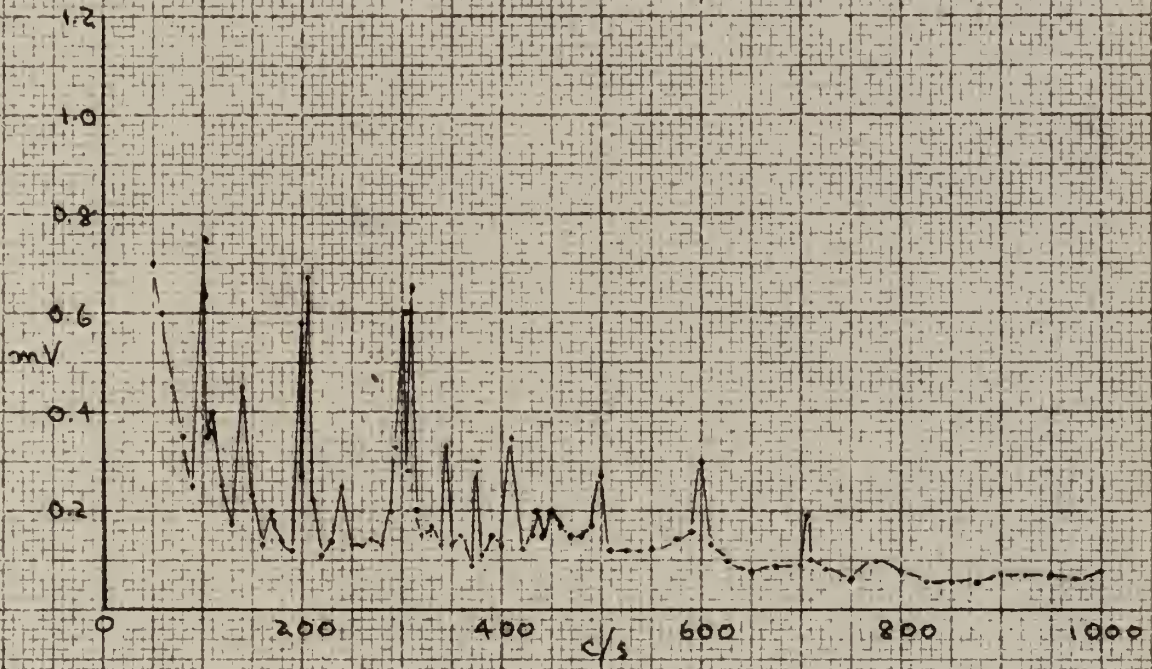

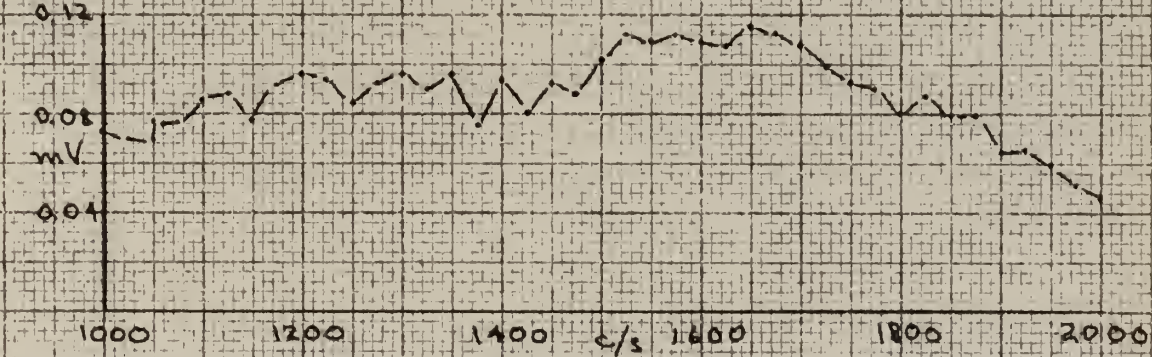

Millivolts Microphone Output Vs Frequency

Fig 21

10 X 10 TO THE ½ INCH 359H-12
KEUFFEL & ESSER MADE IN U.S.A.

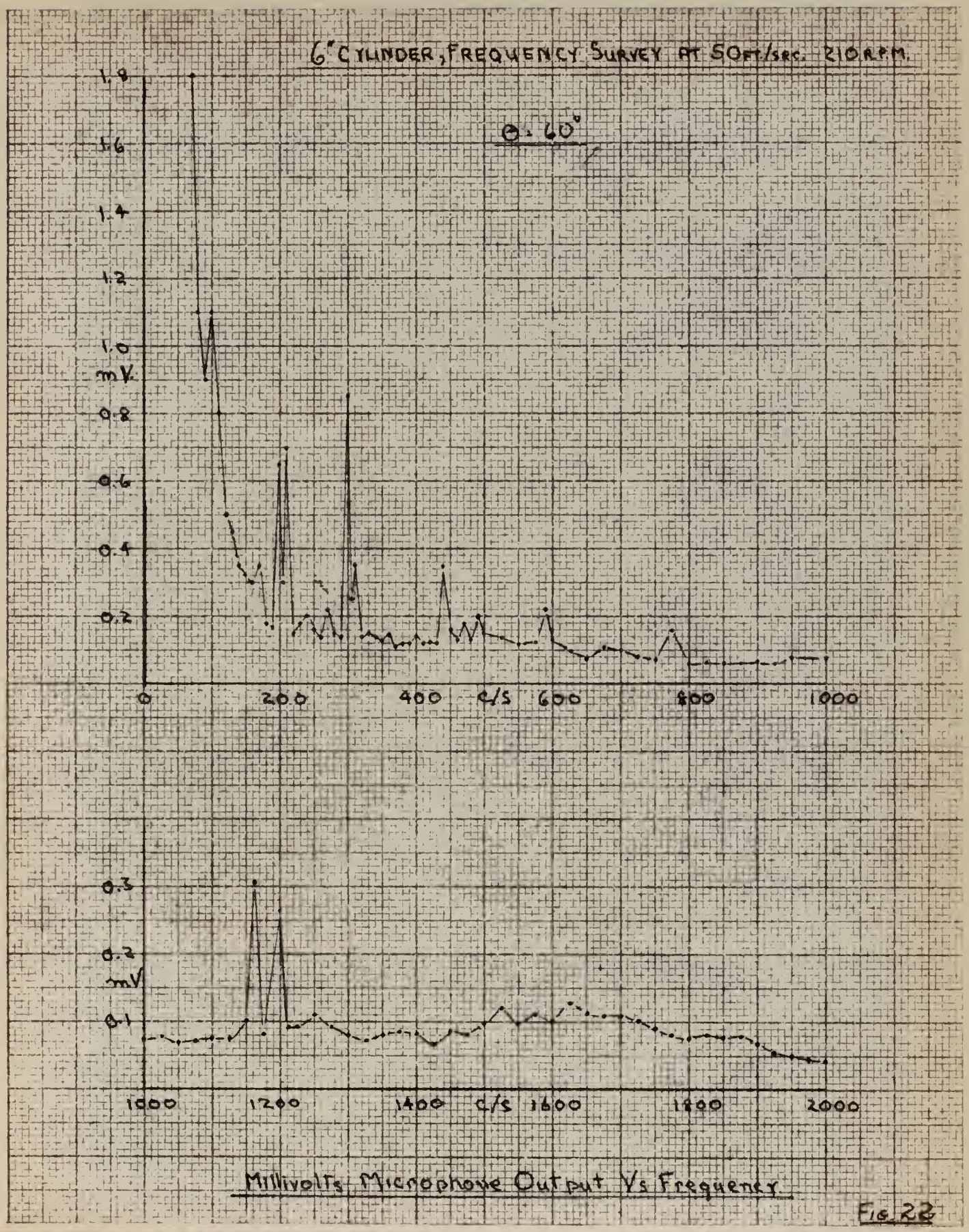

Fig 22

10 X 10 TO THE INCH 359H-12
KEUFFEL & ESSER MADE IN U.S.A.

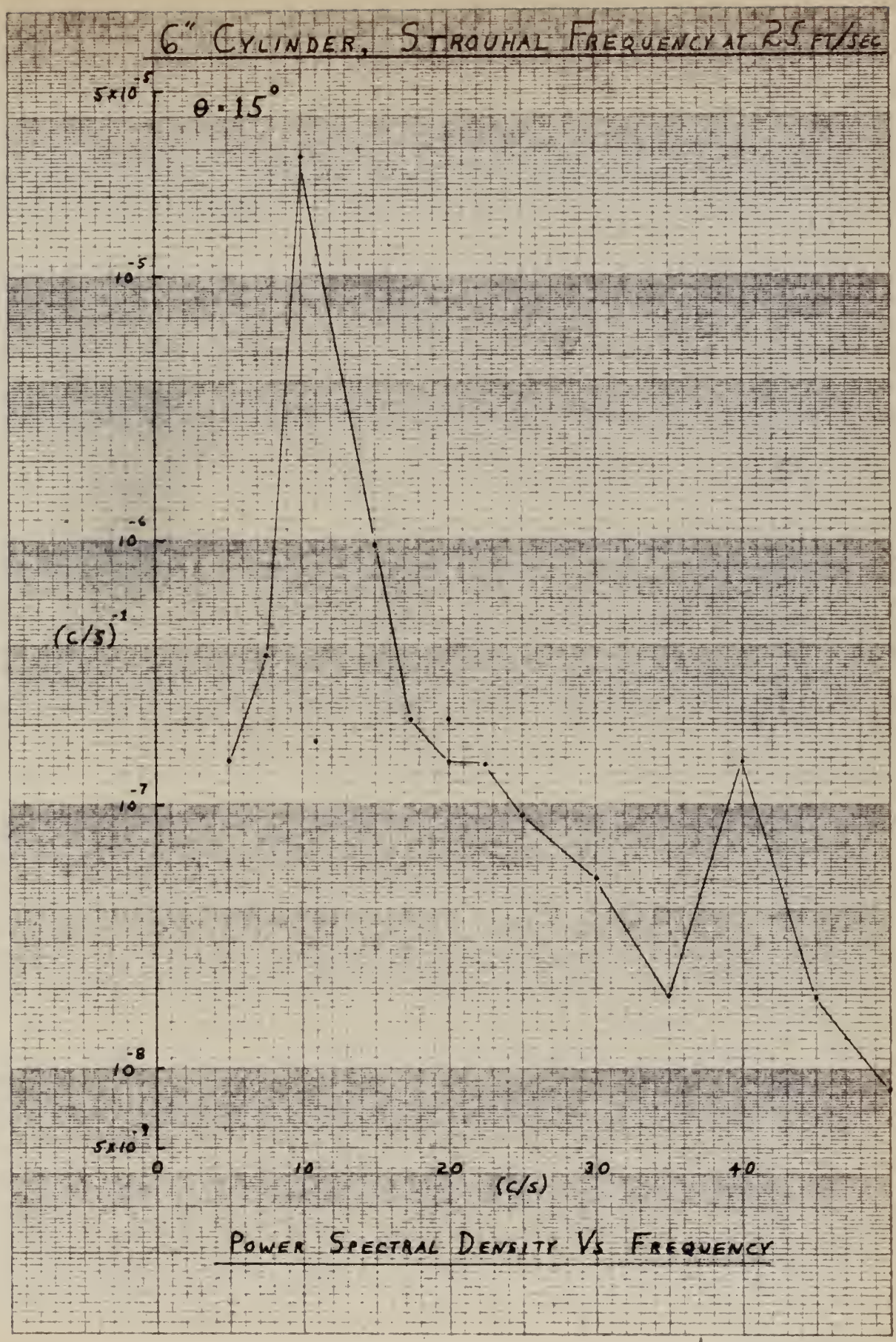
6" CYLINDER, STROUHAL FREQUENCY AT 25 FT/SEC
θ = 15°
5x10⁻⁵
10⁻⁵
10⁻⁶
10⁻⁷
10⁻⁸
5x10⁻⁹
(c/s)⁻¹
0
10
20
30
40
(c/s)
POWER SPECTRAL DENSITY VS FREQUENCY

FIG. 23

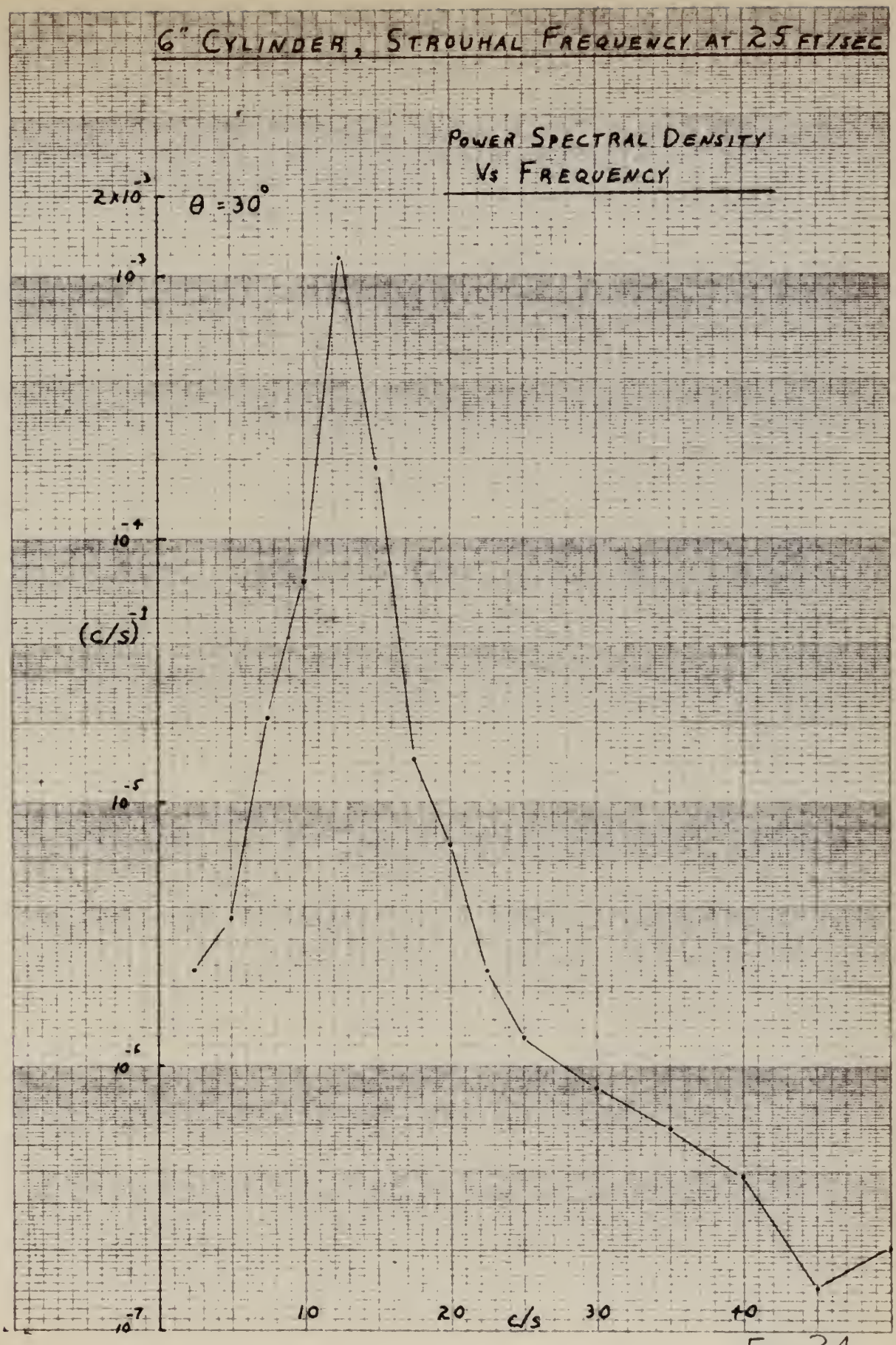
6" CYLINDER, STROUHAL FREQUENCY AT 25 FT/SEC
POWER SPECTRAL DENSITY
VS FREQUENCY
θ = 30°
2x10^-3
10^-3
10^-4
10^-5
10^-6
10^-7
(c/s)^-1
10
20
c/s
30
40

FIG. 24

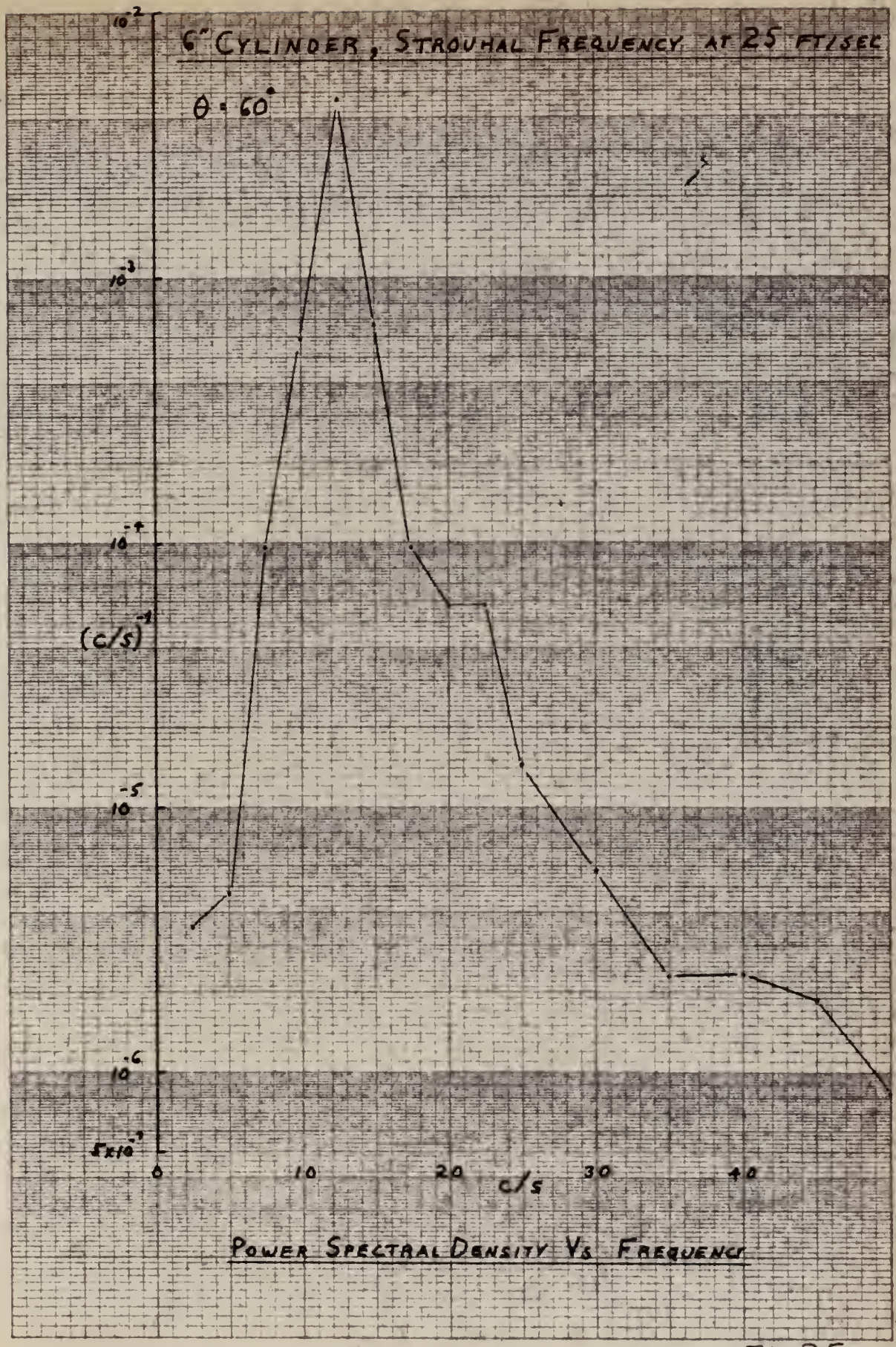

POWER SPECTRAL DENSITY VS FREQUENCY

FIG. 25

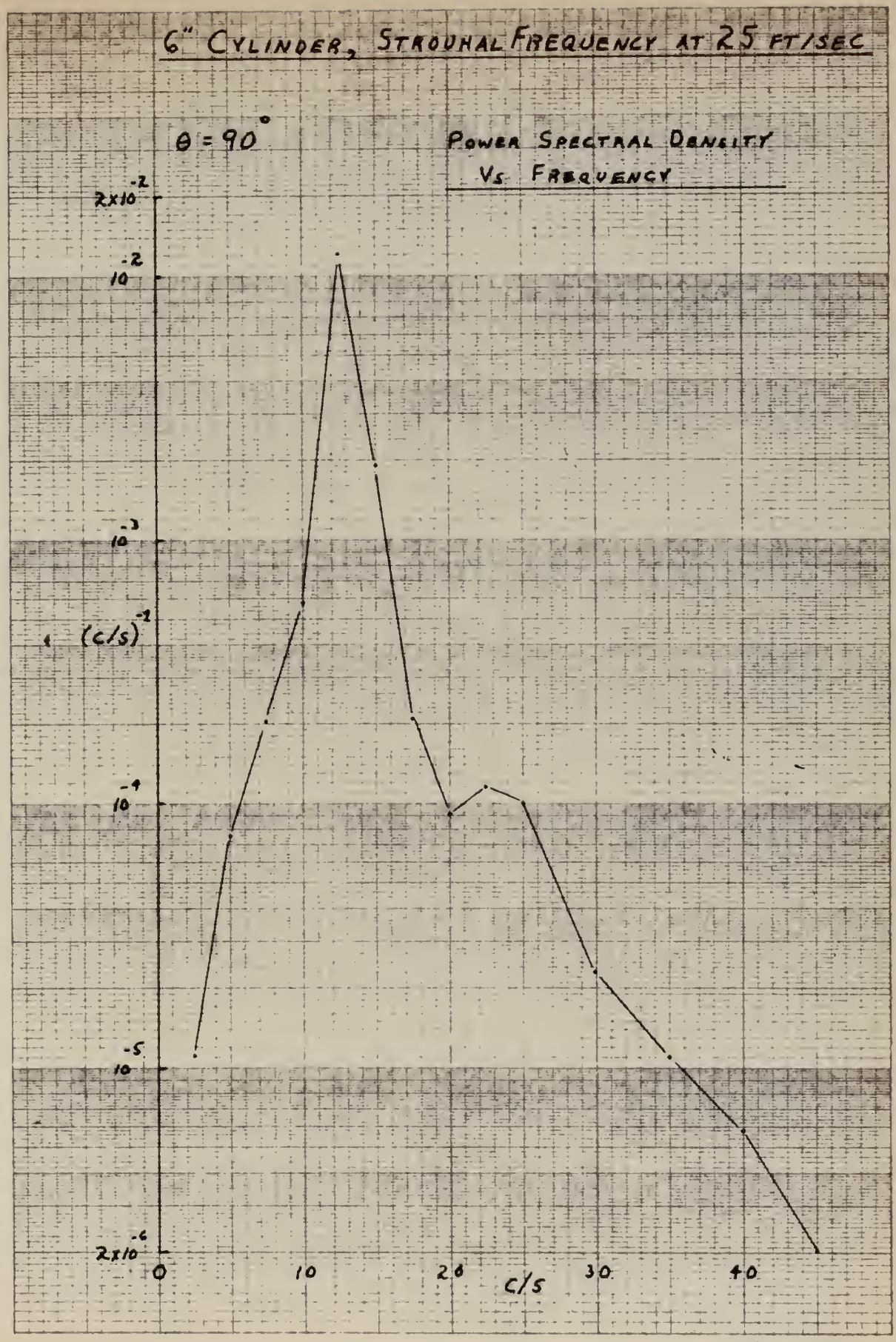
6" CYLINDER, STROUHAL FREQUENCY AT 25 FT/SEC
θ = 90°
POWER SPECTRAL DENSITY
VS FREQUENCY
2x10^-2
10^-2
10^-3
(c/s)^-2
10^-4
10^-5
2x10^-6
0
10
20
30
40
c/s

FIG. 26

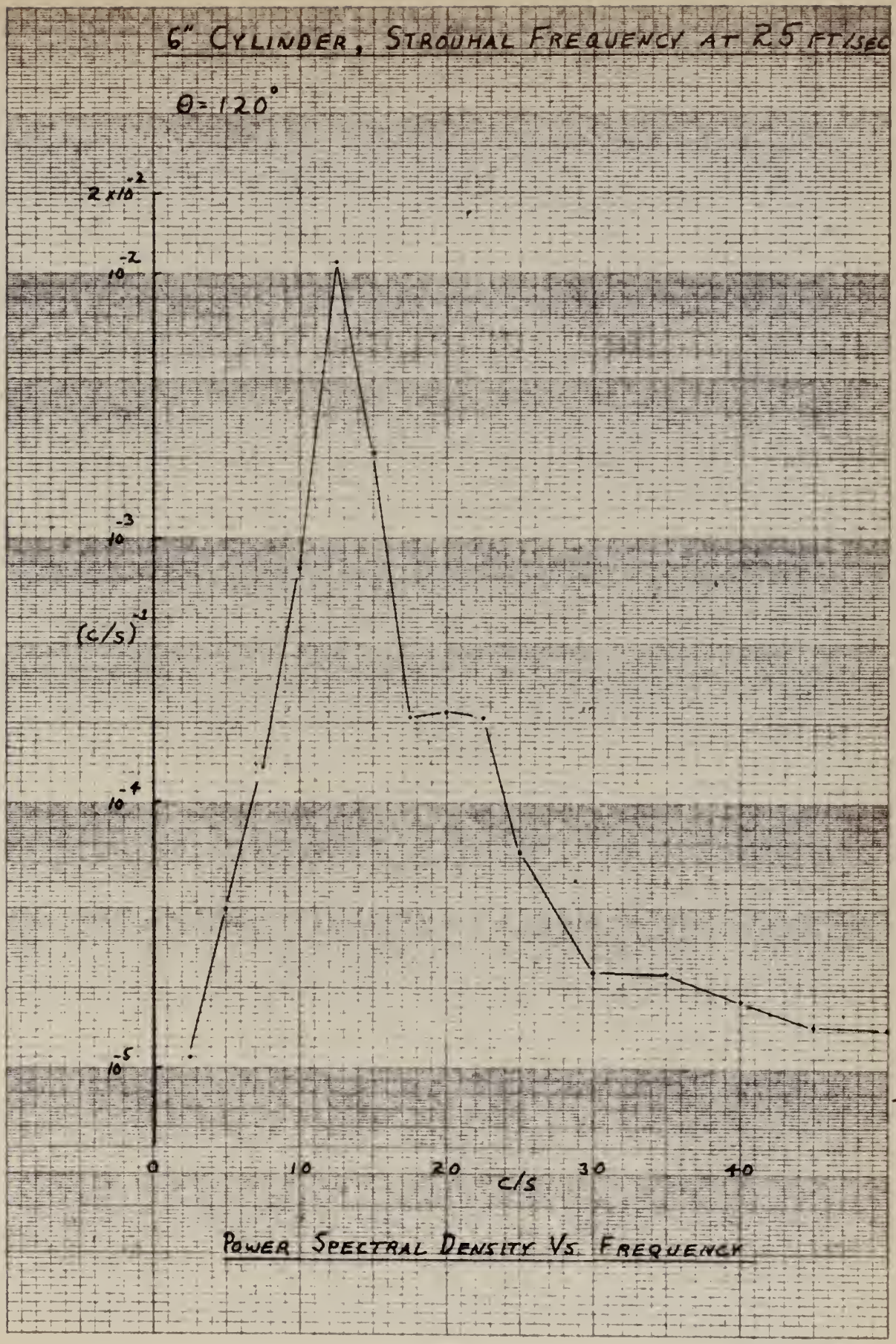
6" CYLINDER, STROUHAL FREQUENCY AT 25 FT/SEC
θ = 120°
2 x 10^-2
10^-2
10^-3
10^-4
10^-5
(c/s)^-1
0
10
20
30
40
c/s
POWER SPECTRAL DENSITY VS. FREQUENCY

FIG. 27

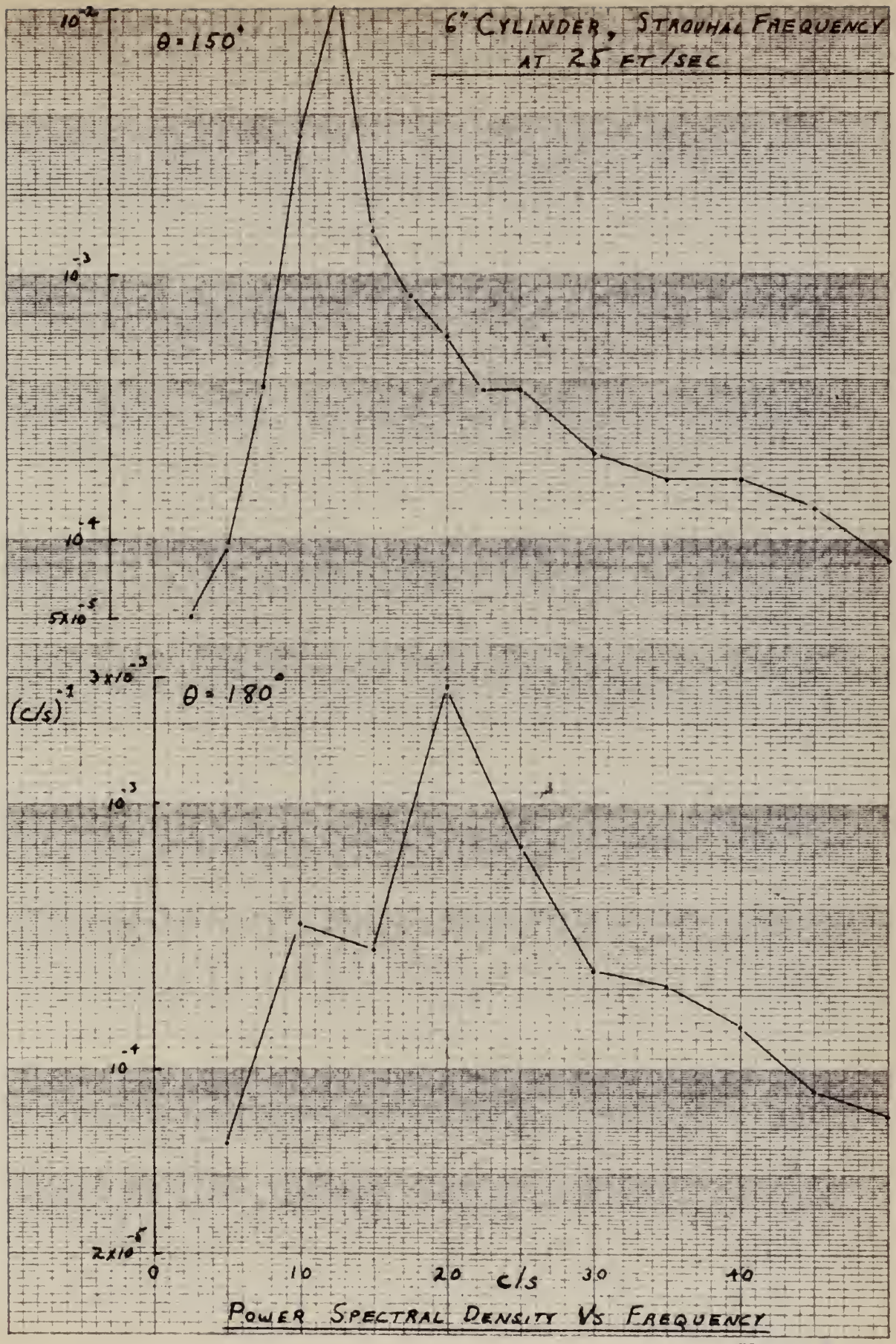
6" CYLINDER, STROUHAL FREQUENCY AT 25 FT/SEC
θ = 150°
θ = 180°
(c/s)
c/s
0
10
20
30
40
POWER SPECTRAL DENSITY VS FREQUENCY

FIG. 28

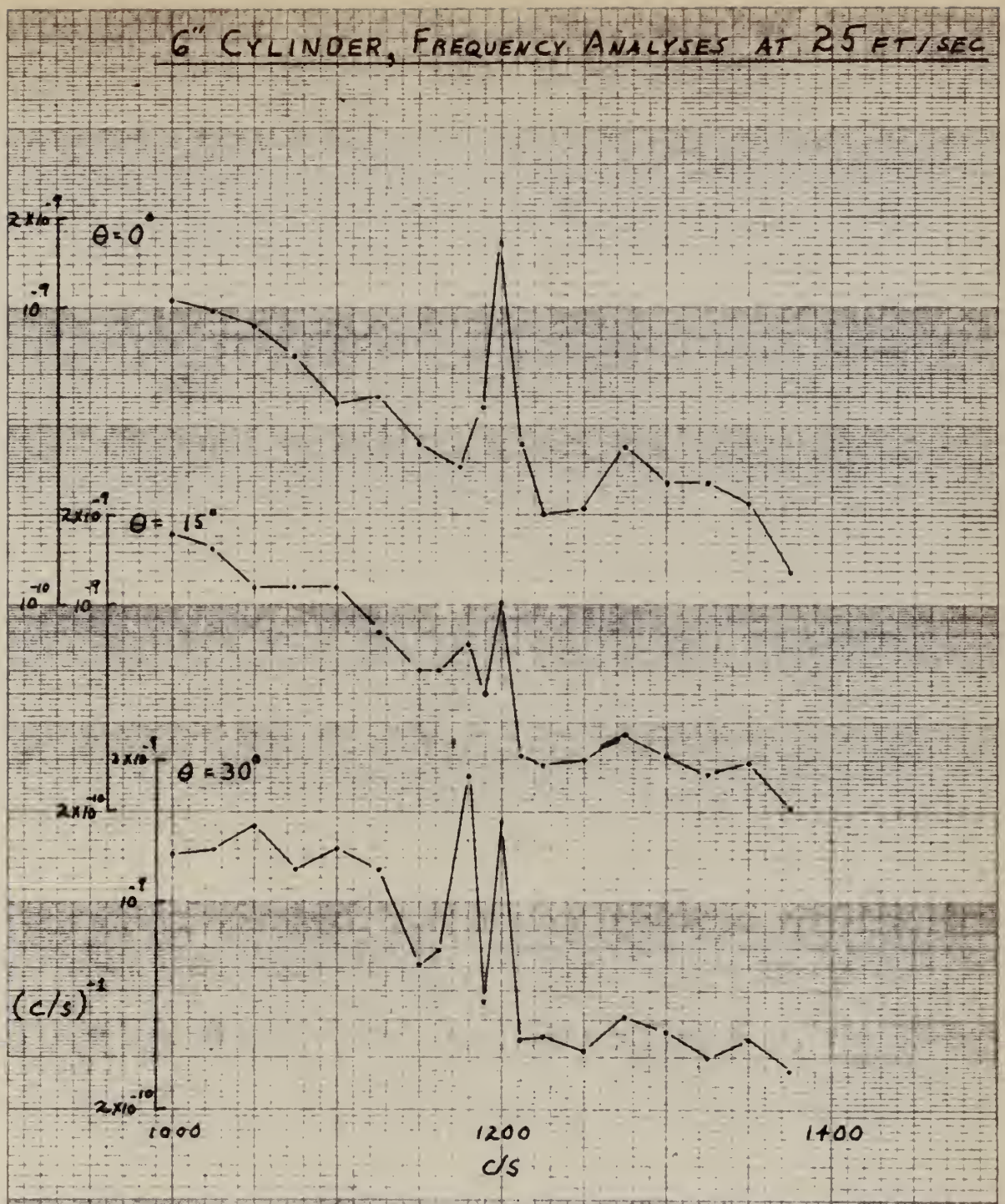
6" CYLINDER, FREQUENCY ANALYSES AT 25 FT/SEC
θ = 0°
θ = 15°
θ = 30°
(c/s)
1000
1200
1400
c/s
POWER SPECTRAL DENSITY VS FREQUENCY

FIG. 29

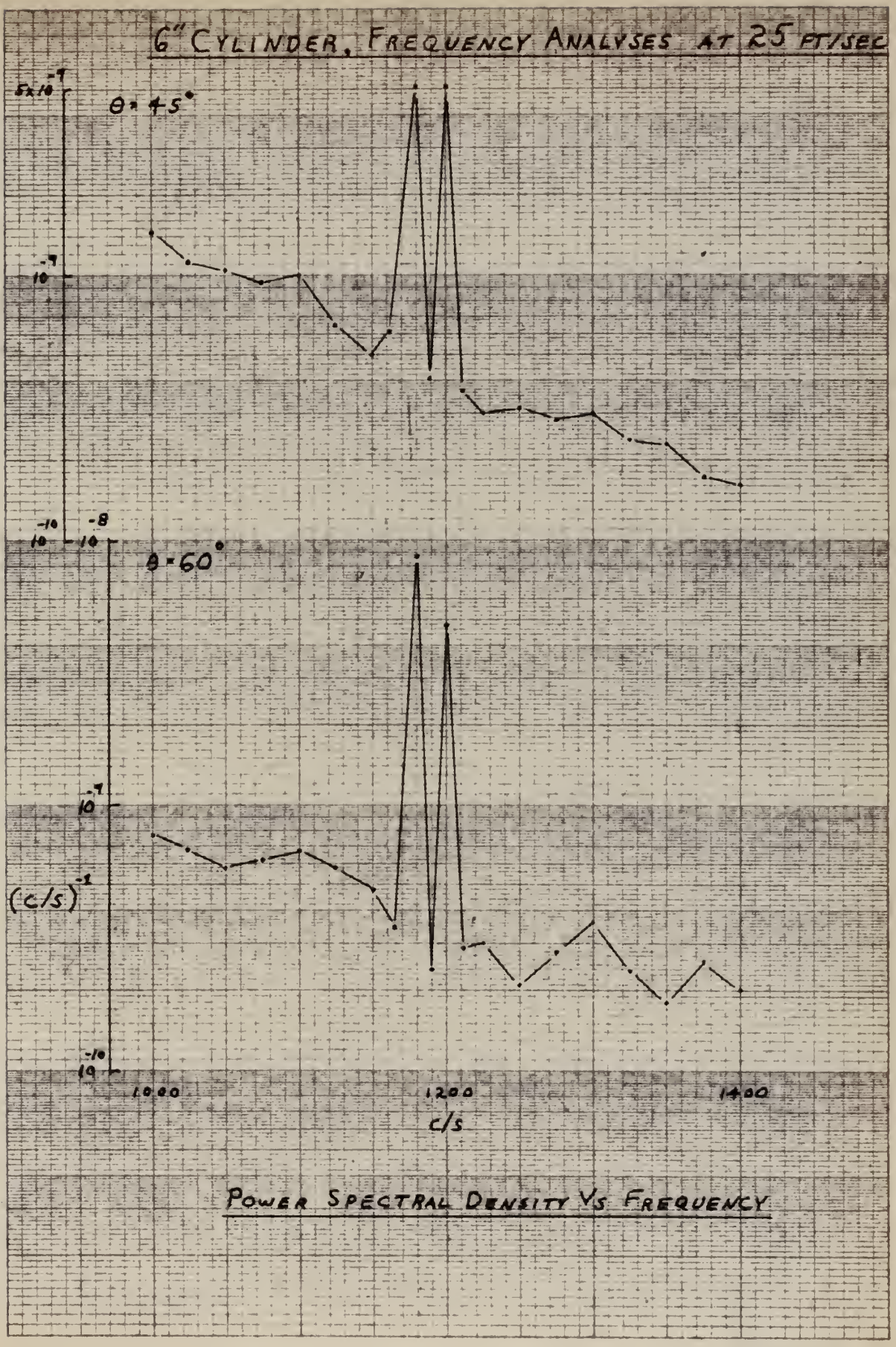
6" CYLINDER, FREQUENCY ANALYSES AT 25 FT/SEC
θ = 45°
θ = 60°
(c/s)
1000
1200
1400
c/s
POWER SPECTRAL DENSITY Vs FREQUENCY

FIG. 30

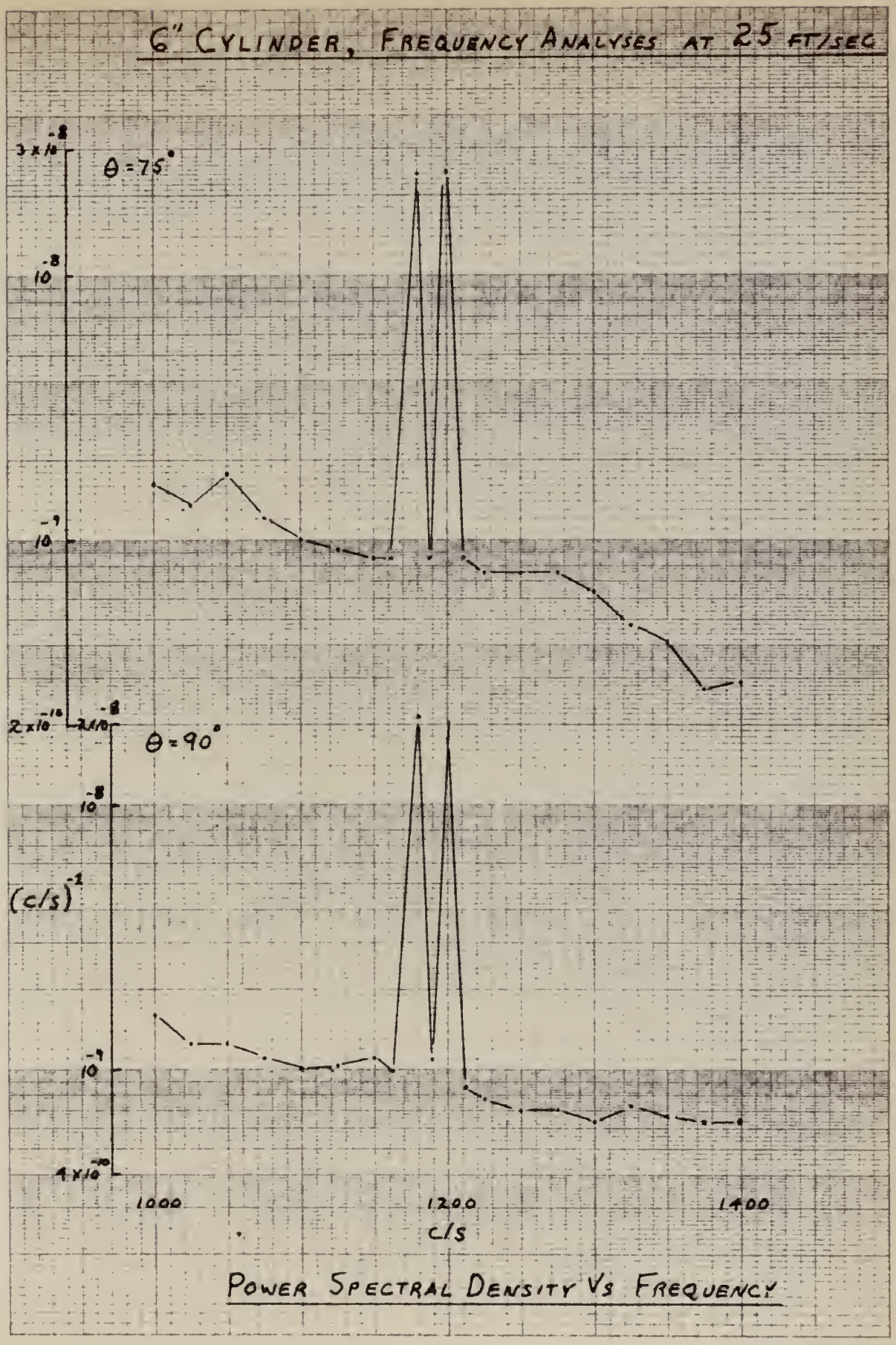
6" CYLINDER, FREQUENCY ANALYSES AT 25 FT/SEC
θ = 75°
θ = 90°
(c/s)⁻²
1000
1200
1400
c/s
POWER SPECTRAL DENSITY Vs FREQUENCY

FIG. 31

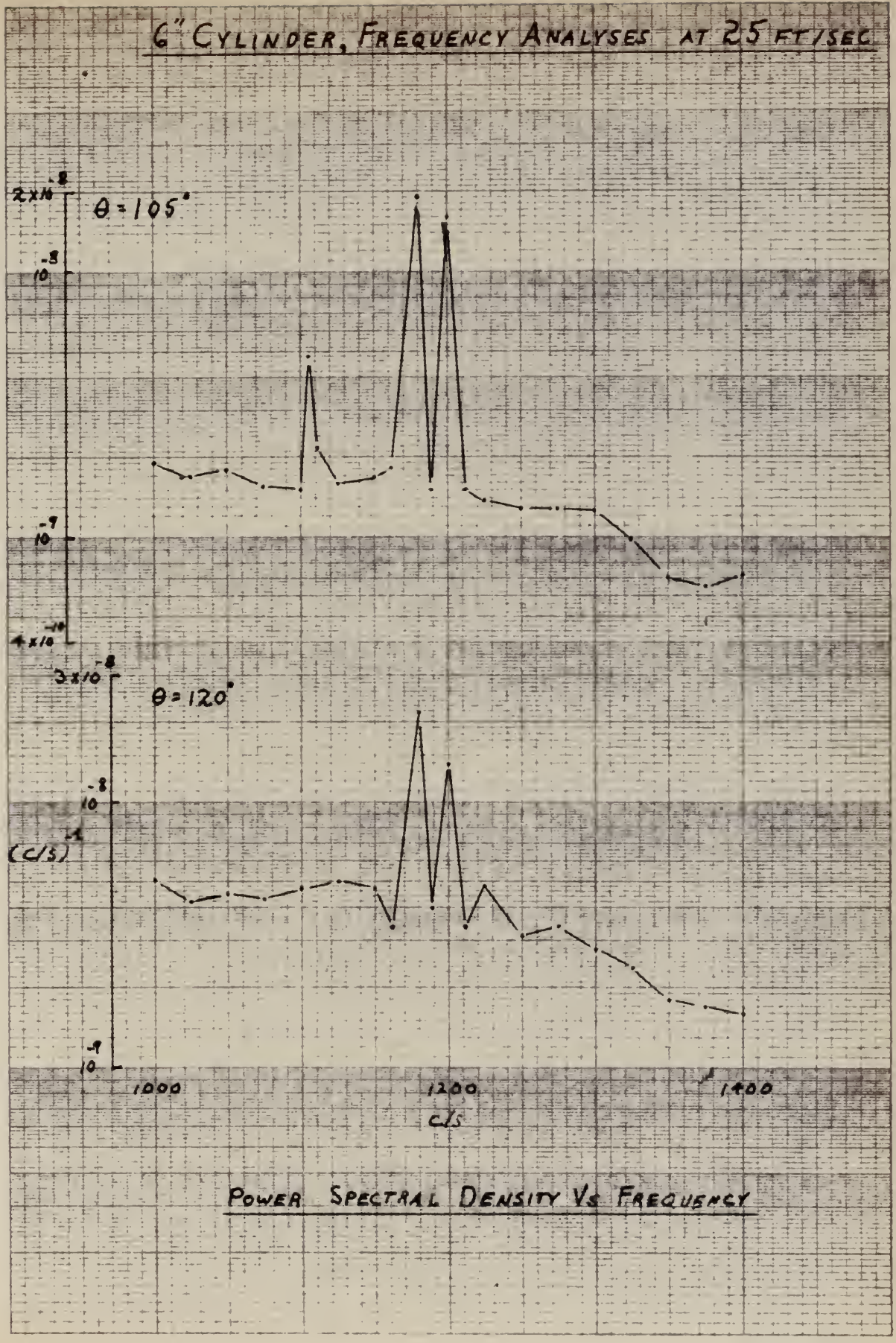
6" CYLINDER, FREQUENCY ANALYSES AT 25 FT/SEC
θ = 105°
θ = 120°
(C/S)
1000
1200
1400
C/S
POWER SPECTRAL DENSITY Vs FREQUENCY

FIG. 32

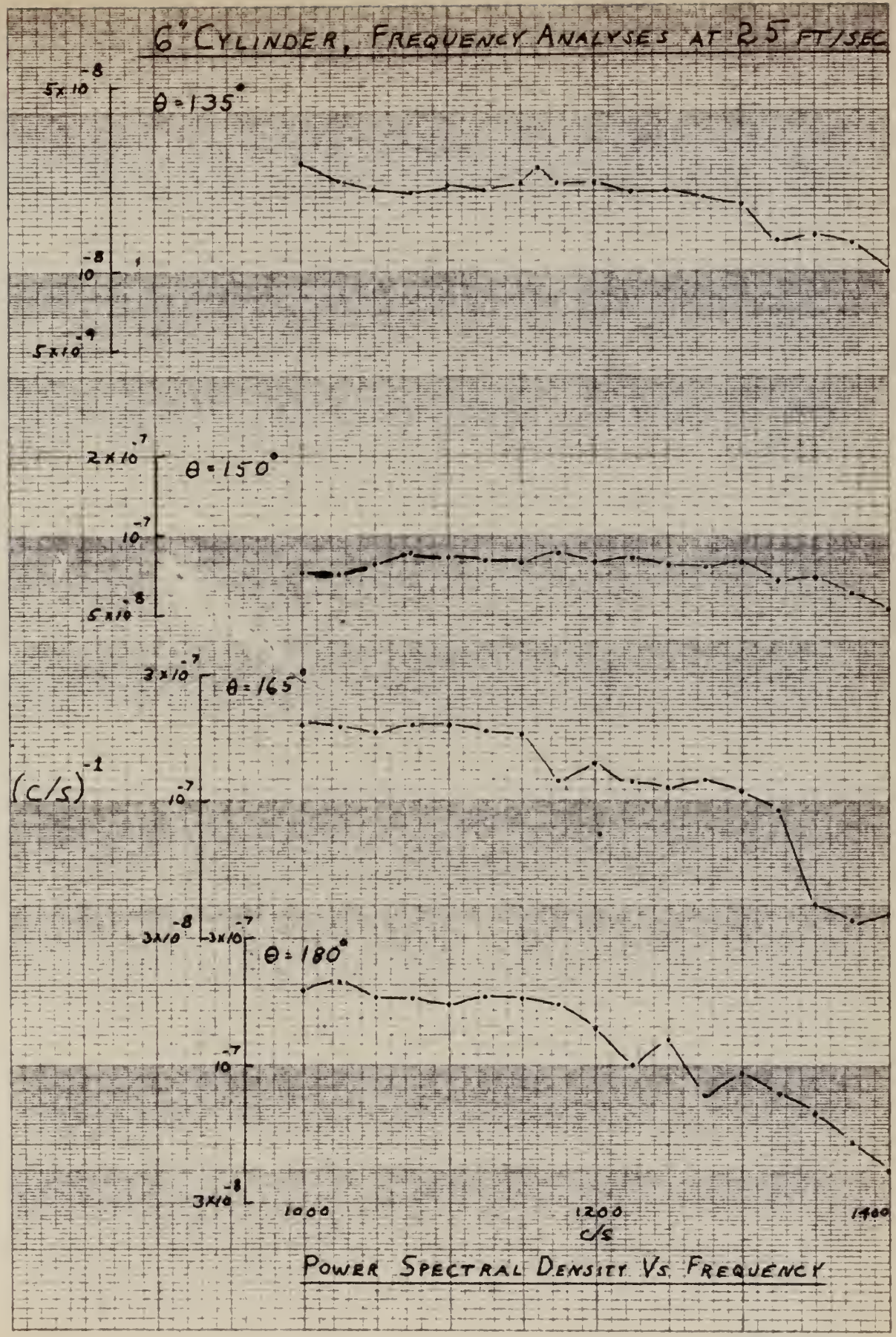
6" CYLINDER, FREQUENCY ANALYSES AT 2.5 FT/SEC
θ = 135°
θ = 150°
θ = 165°
θ = 180°
(c/s)⁻¹
1000
1200
1400
c/s
POWER SPECTRAL DENSITY VS. FREQUENCY

FIG. 33

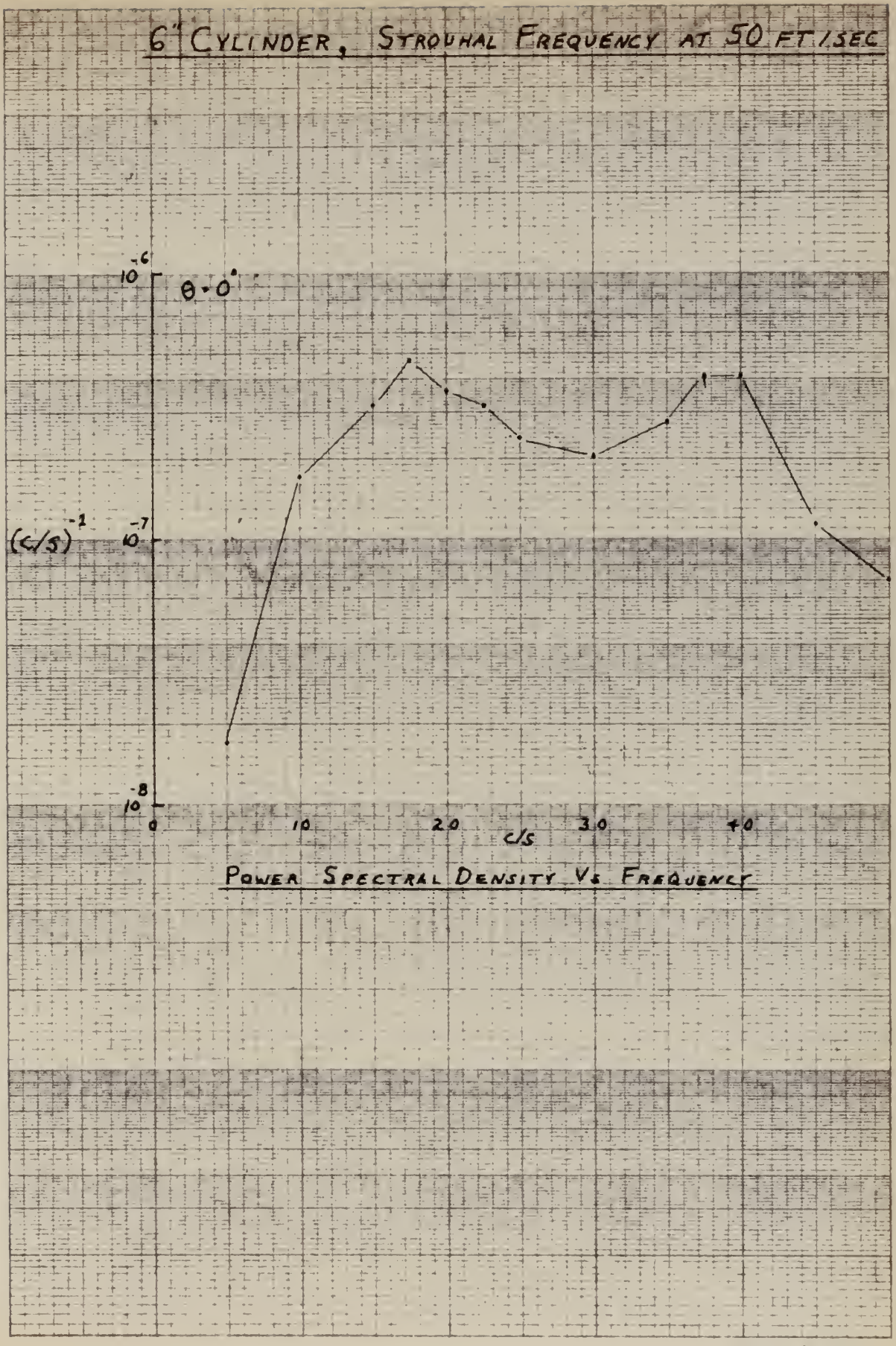
6" CYLINDER, STROUHAL FREQUENCY AT 50 FT/SEC
θ = 0°
10^{-6}
10^{-7}
10^{-8}
$(C/S)^{-1}$
0
10
20
30
40
C/S
POWER SPECTRAL DENSITY VS FREQUENCY

FIG. 34

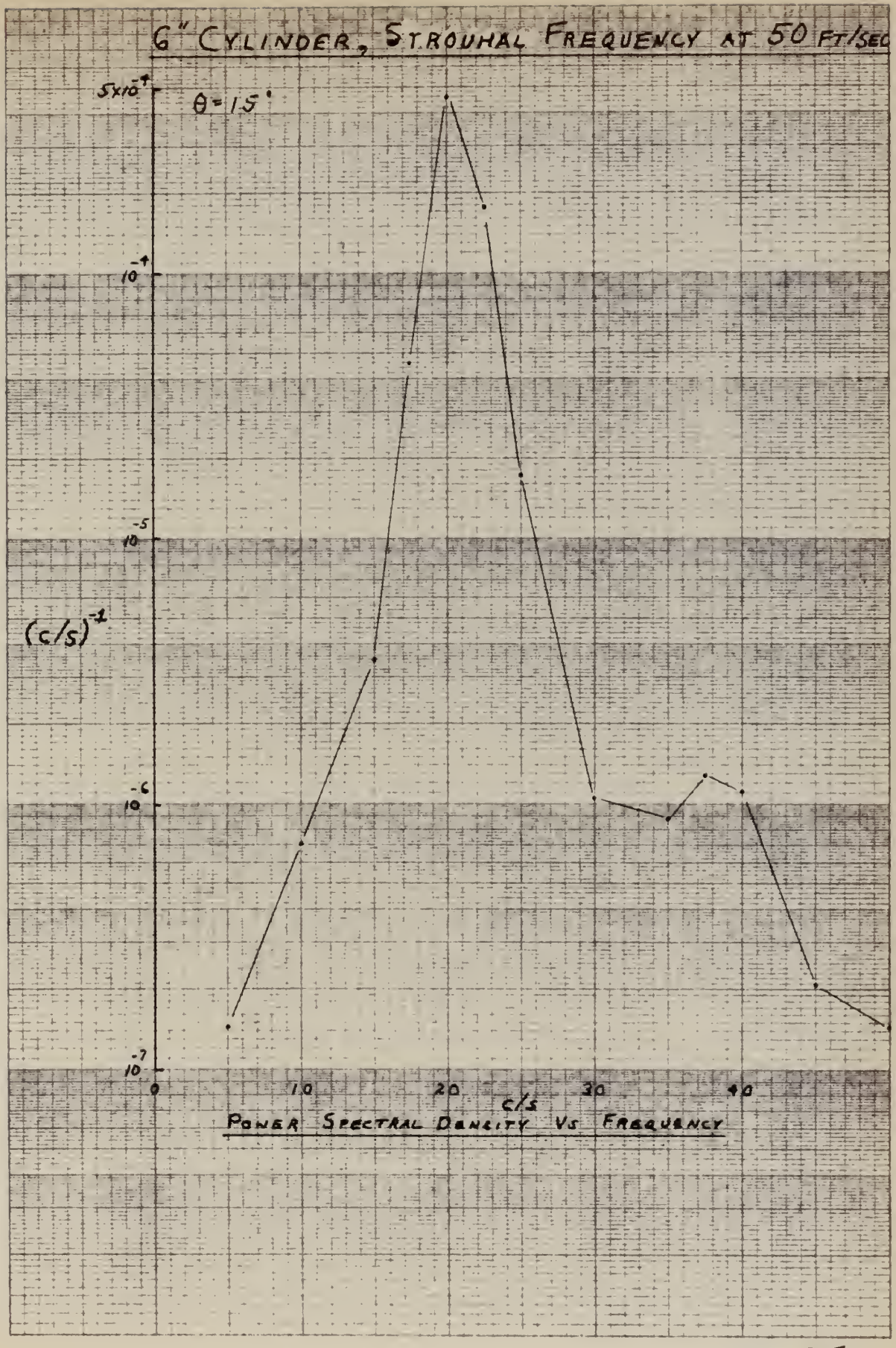
6" CYLINDER, STROUHAL FREQUENCY AT 50 FT/SEC
θ = 15°
5x10⁻⁴
10⁻⁴
10⁻⁵
10⁻⁶
10⁻⁷
(c/s)⁻¹
0
10
20
30
40
c/s
POWER SPECTRAL DENSITY VS FREQUENCY

FIG. 35

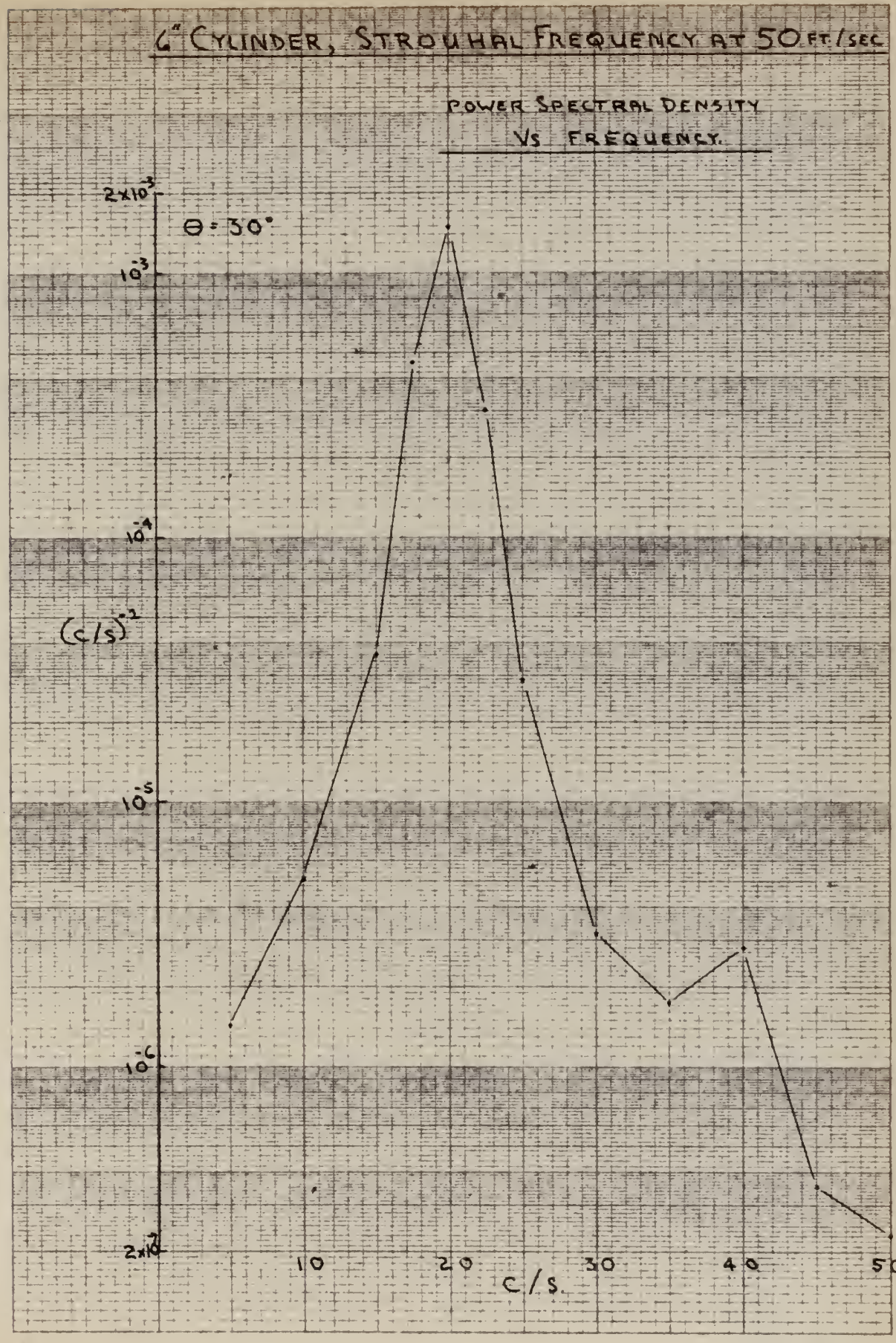
6" CYLINDER, STROUHAL FREQUENCY AT 50 FT/SEC
POWER SPECTRAL DENSITY
VS FREQUENCY
θ = 30°
2x10⁻³
10⁻³
10⁻⁴
(c/s)⁻¹
10⁻⁵
10⁻⁶
2x10⁻⁷
10
20
30
40
50
c/s

FIG. 36

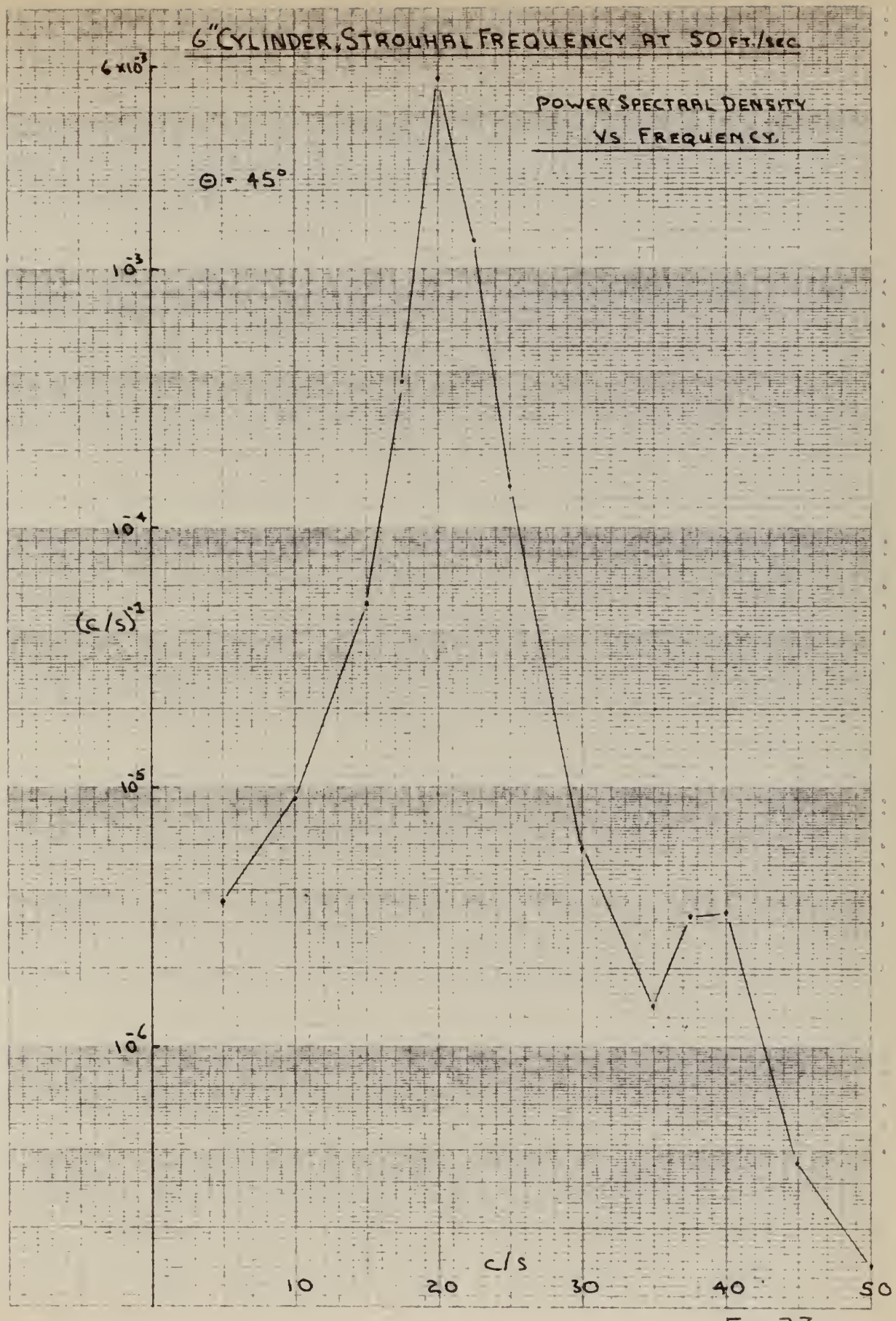
6"CYLINDER, STROUHAL FREQUENCY AT 50 FT./SEC.
POWER SPECTRAL DENSITY
VS FREQUENCY.
Θ = 45°
6 x 10⁻³
10⁻³
10⁻⁴
(c/s)⁻¹
10⁻⁵
10⁻⁶
c/s
10
20
30
40
50

FIG. 37

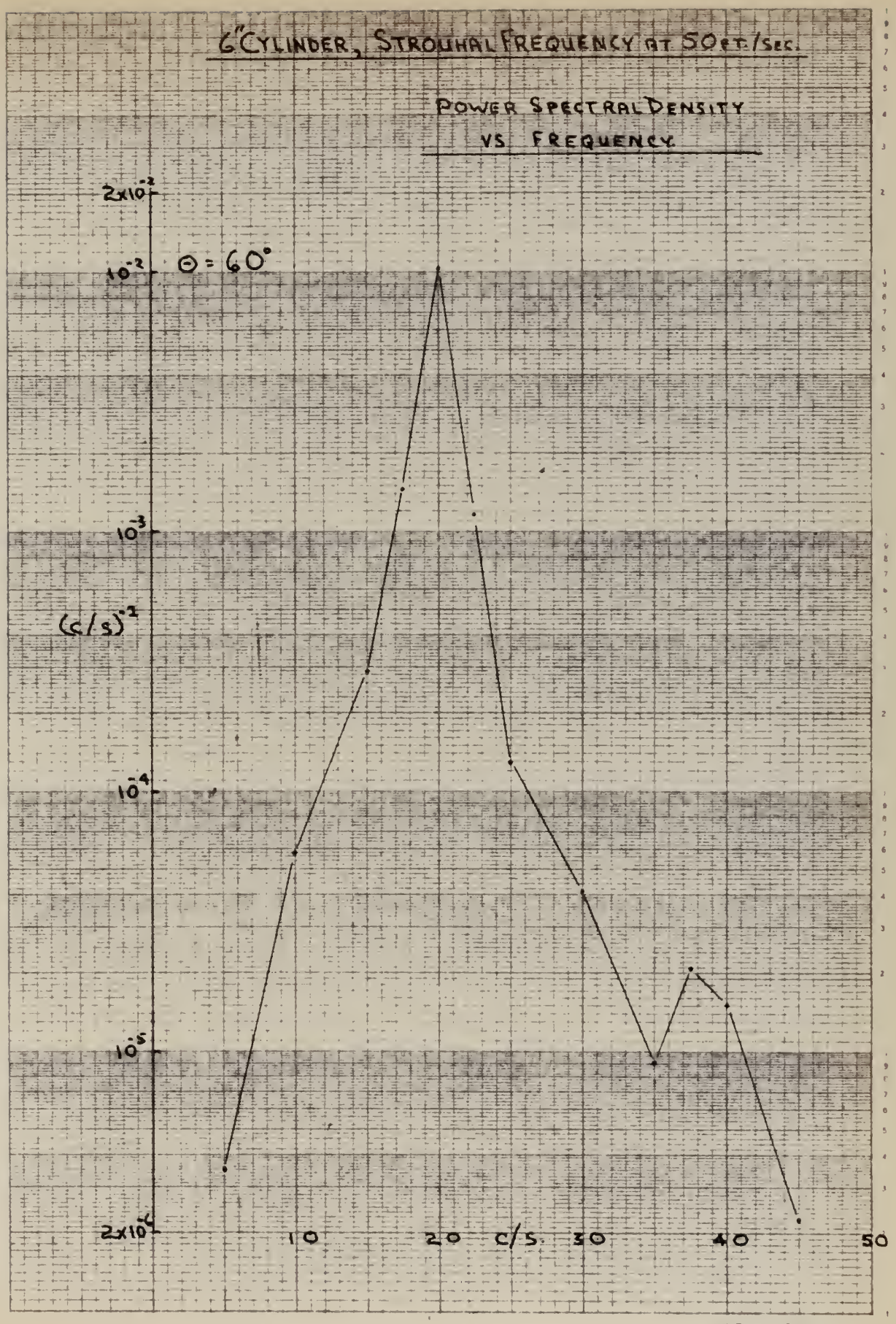
6" CYLINDER, STROUHAL FREQUENCY AT 50 FT./SEC.
POWER SPECTRAL DENSITY
VS FREQUENCY
2×10^{-2}
10^{-2}
$\Theta = 60°$
10^{-3}
$(c/s)^{-2}$
10^{-4}
10^{-5}
2×10^{-6}
10
20
c/s.
30
40
50

FIG. 38

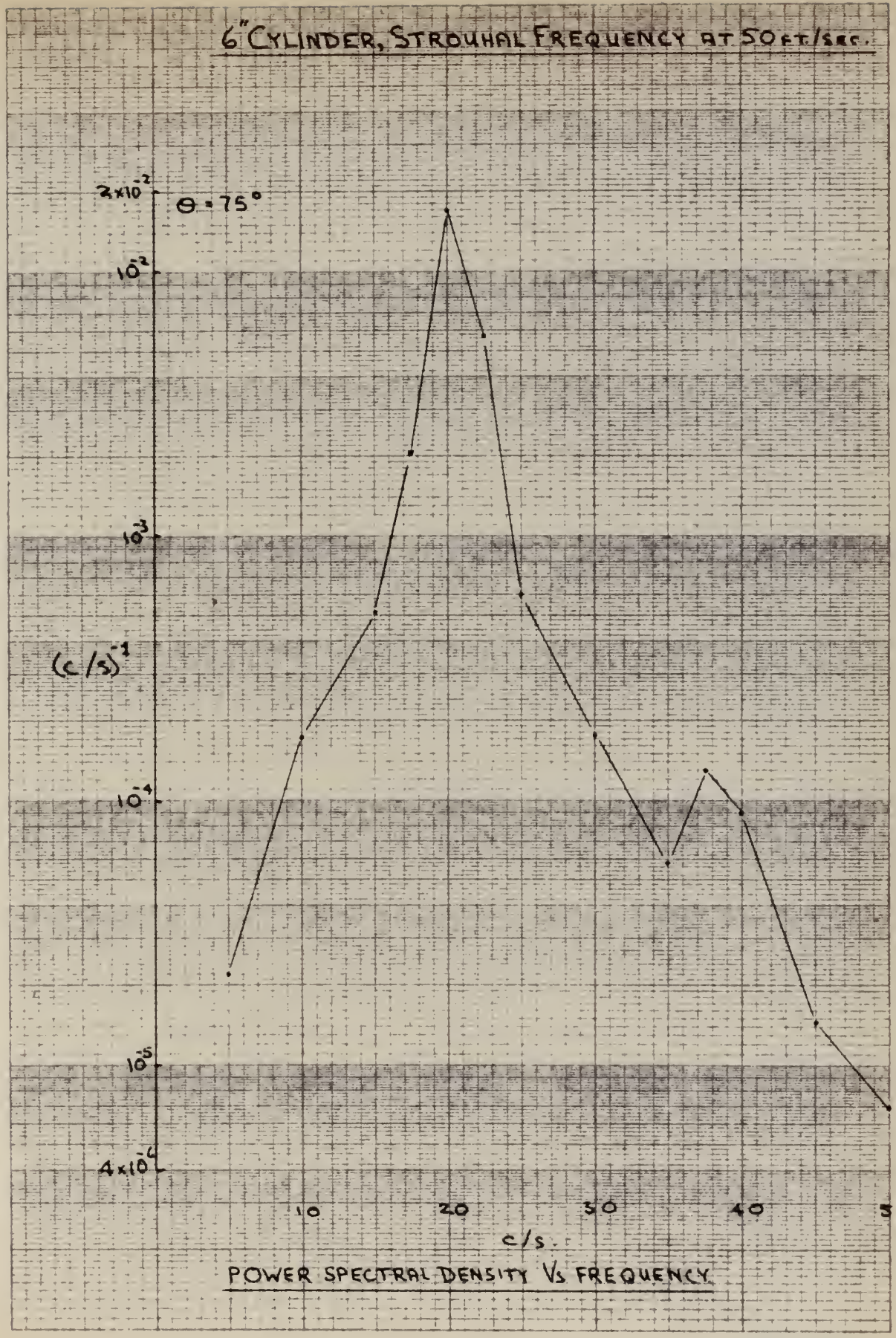
6" CYLINDER, STROUHAL FREQUENCY AT 50 FT/SEC.
θ = 75°
2×10⁻²
10⁻²
10⁻³
(c/s)⁻¹
10⁻⁴
10⁻⁵
4×10⁻⁶
10
20
30
40
50
c/s.
POWER SPECTRAL DENSITY Vs FREQUENCY

FIG. 39

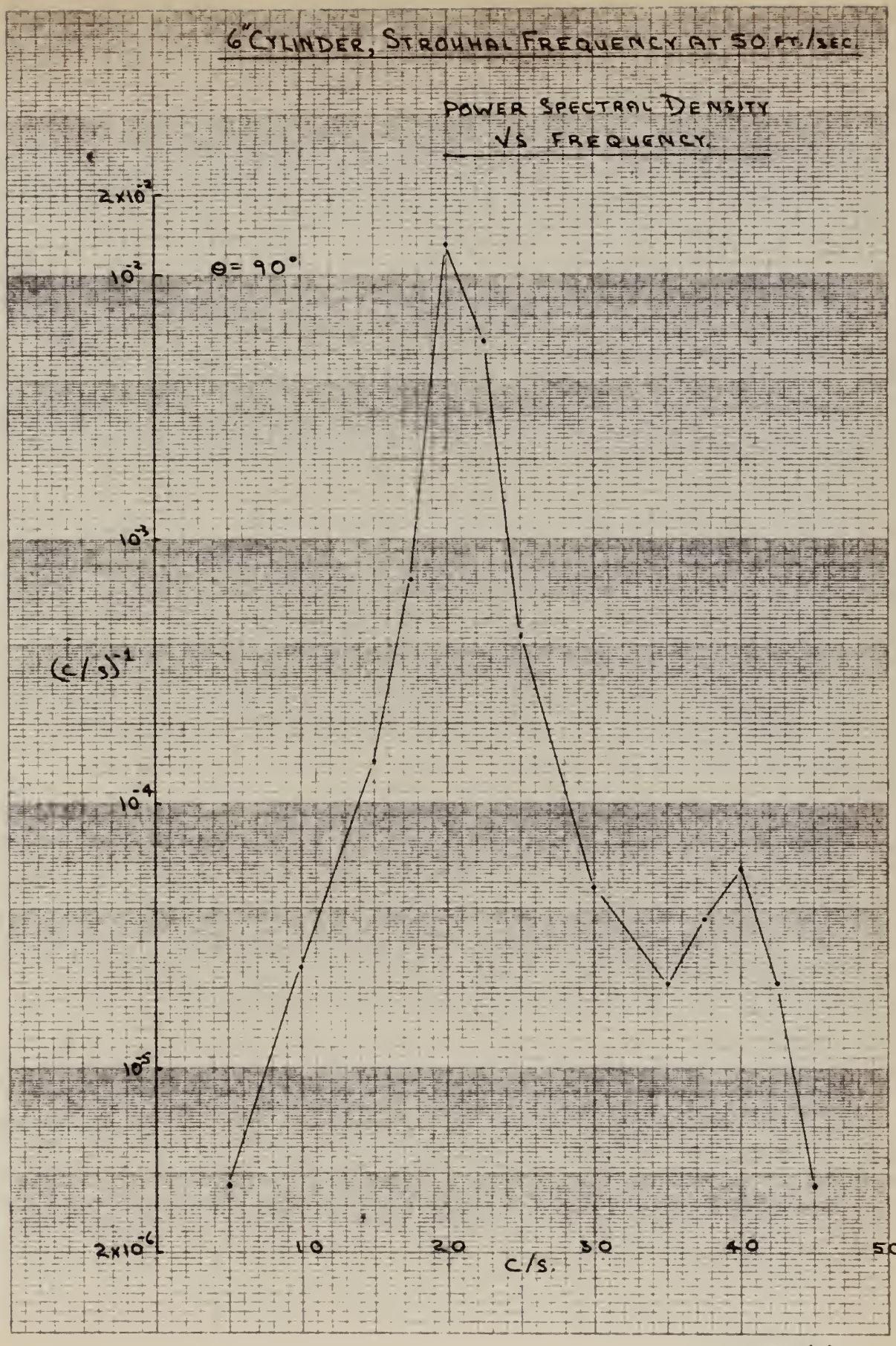
6" CYLINDER, STROUHAL FREQUENCY AT 50 FT./SEC.
POWER SPECTRAL DENSITY
VS FREQUENCY.
θ = 90°
2x10⁻²
10⁻²
10⁻³
(c/s)⁻¹
10⁻⁴
10⁻⁵
2x10⁻⁶
10
20
30
40
50
c/s.

FIG. 40

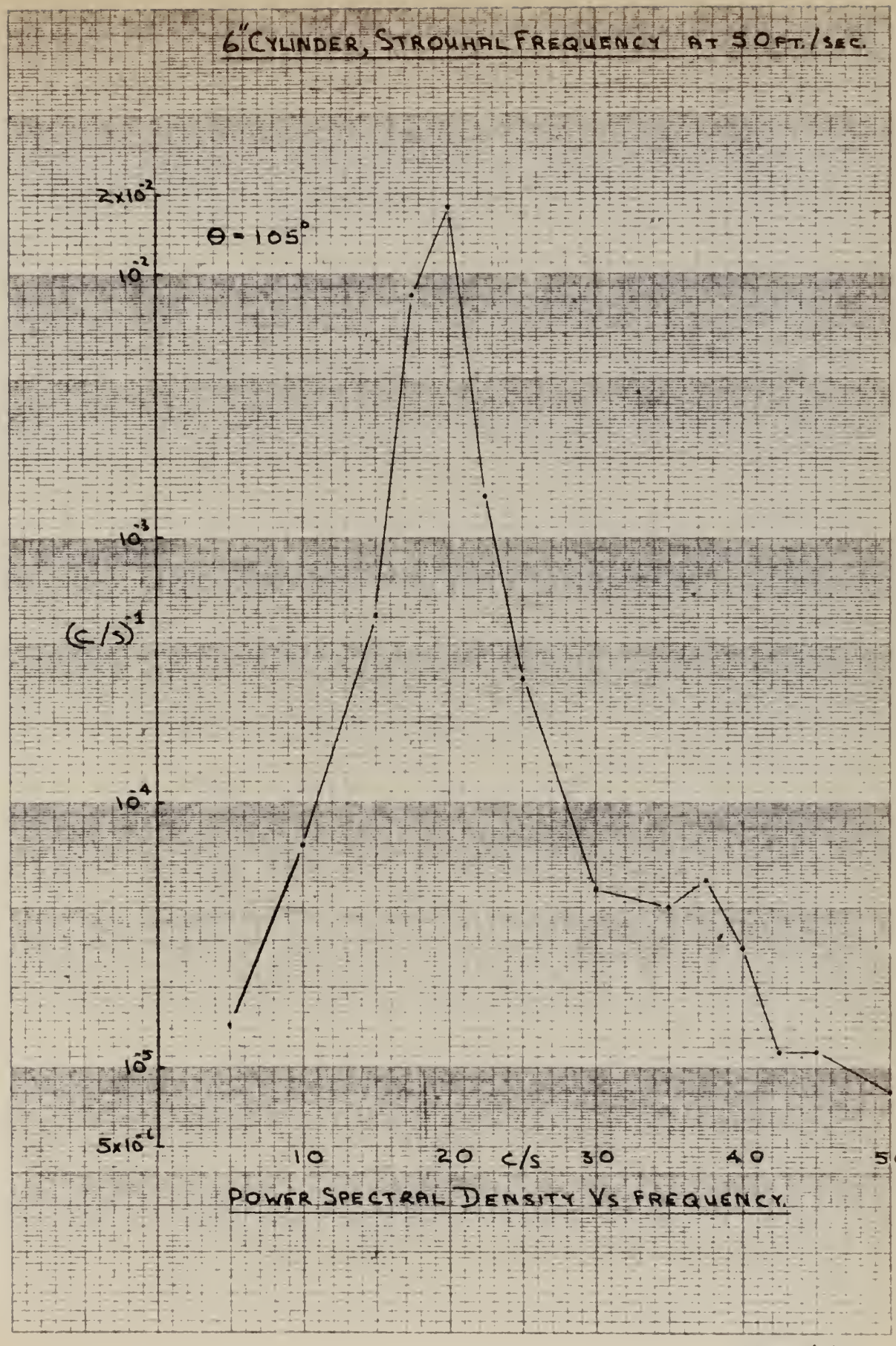
6" CYLINDER, STROUHAL FREQUENCY AT 50 FT./SEC.
θ = 105°
2x10⁻²
10⁻²
10⁻³
(c/s)⁻¹
10⁻⁴
10⁻⁵
5x10⁻⁶
10
20 c/s
30
40
50
POWER SPECTRAL DENSITY VS FREQUENCY.

FIG. 41

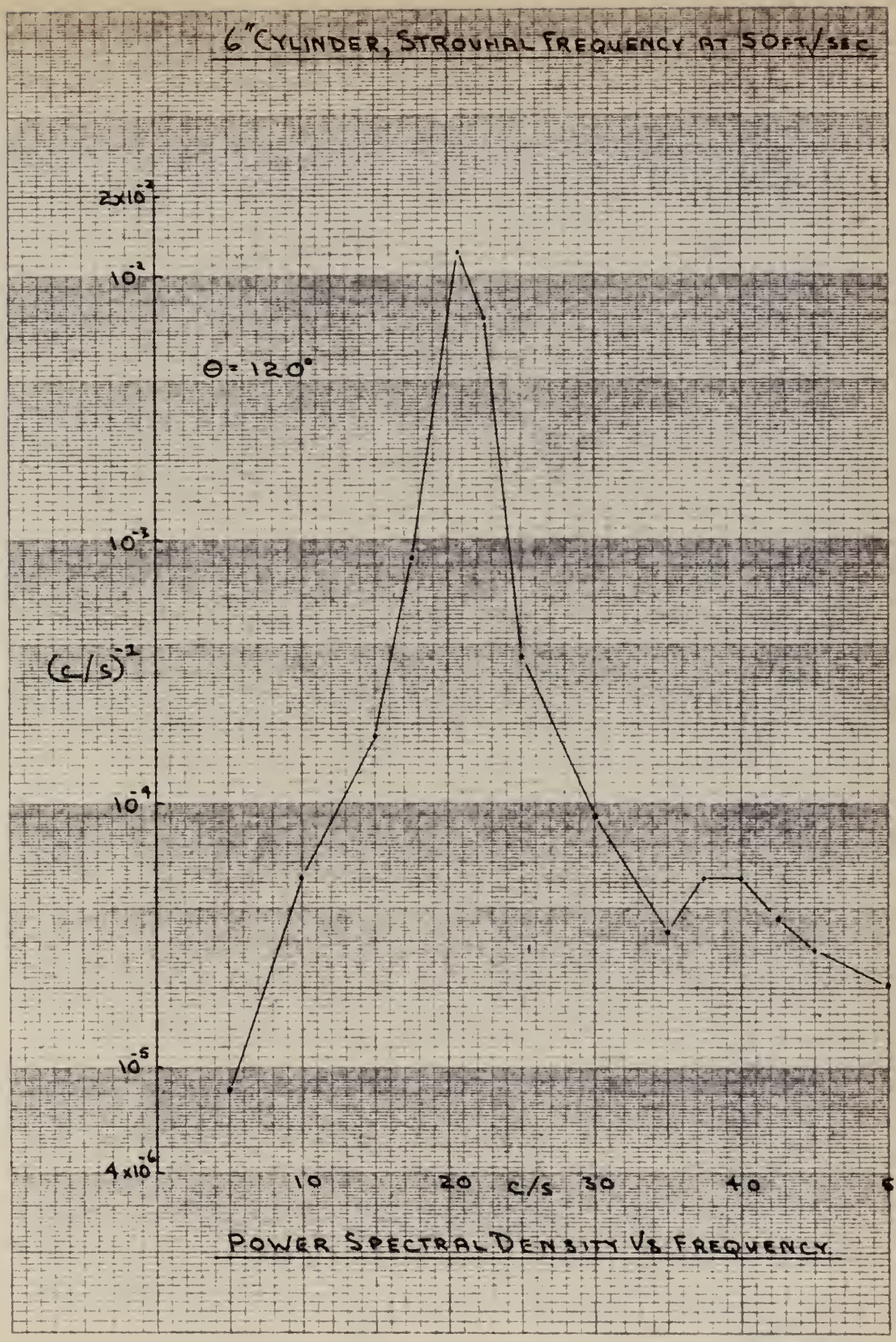
6" CYLINDER, STROUHAL FREQUENCY AT 50FT/SEC
2×10^{-2}
10^{-2}
$\theta = 120°$
10^{-3}
$(c/s)^{-2}$
10^{-4}
10^{-5}
4×10^{-6}
10
20
c/s
30
40
50
POWER SPECTRAL DENSITY VS FREQUENCY

FIG. 42

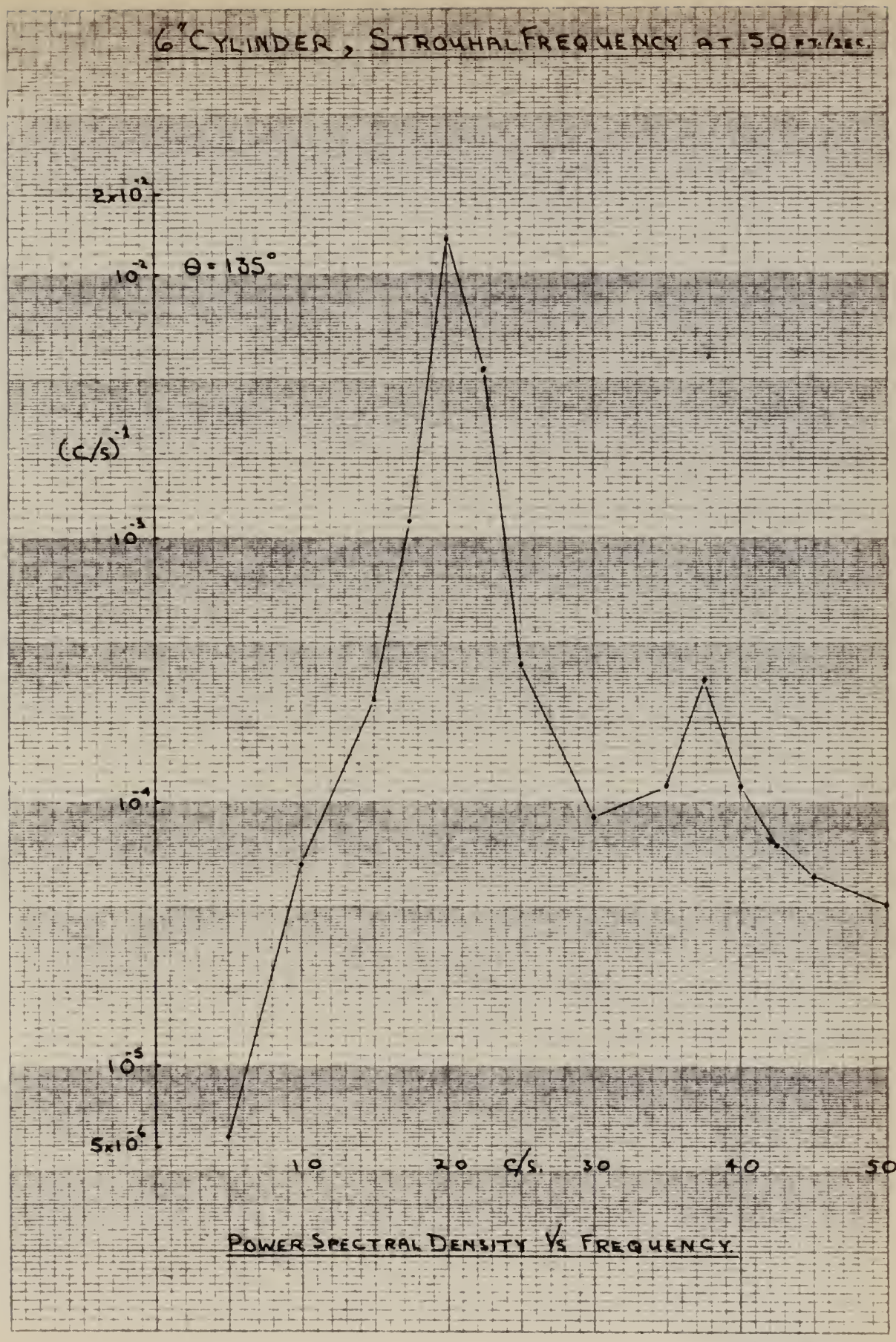
6" CYLINDER, STROUHAL FREQUENCY AT 50 FT/SEC.
2×10^{-2}
10^{-2}
$\theta = 135°$
$(C/S)^{-1}$
10^{-3}
10^{-4}
10^{-5}
5×10^{-6}
10
20
C/S.
30
40
50
POWER SPECTRAL DENSITY VS FREQUENCY

FIG. 43

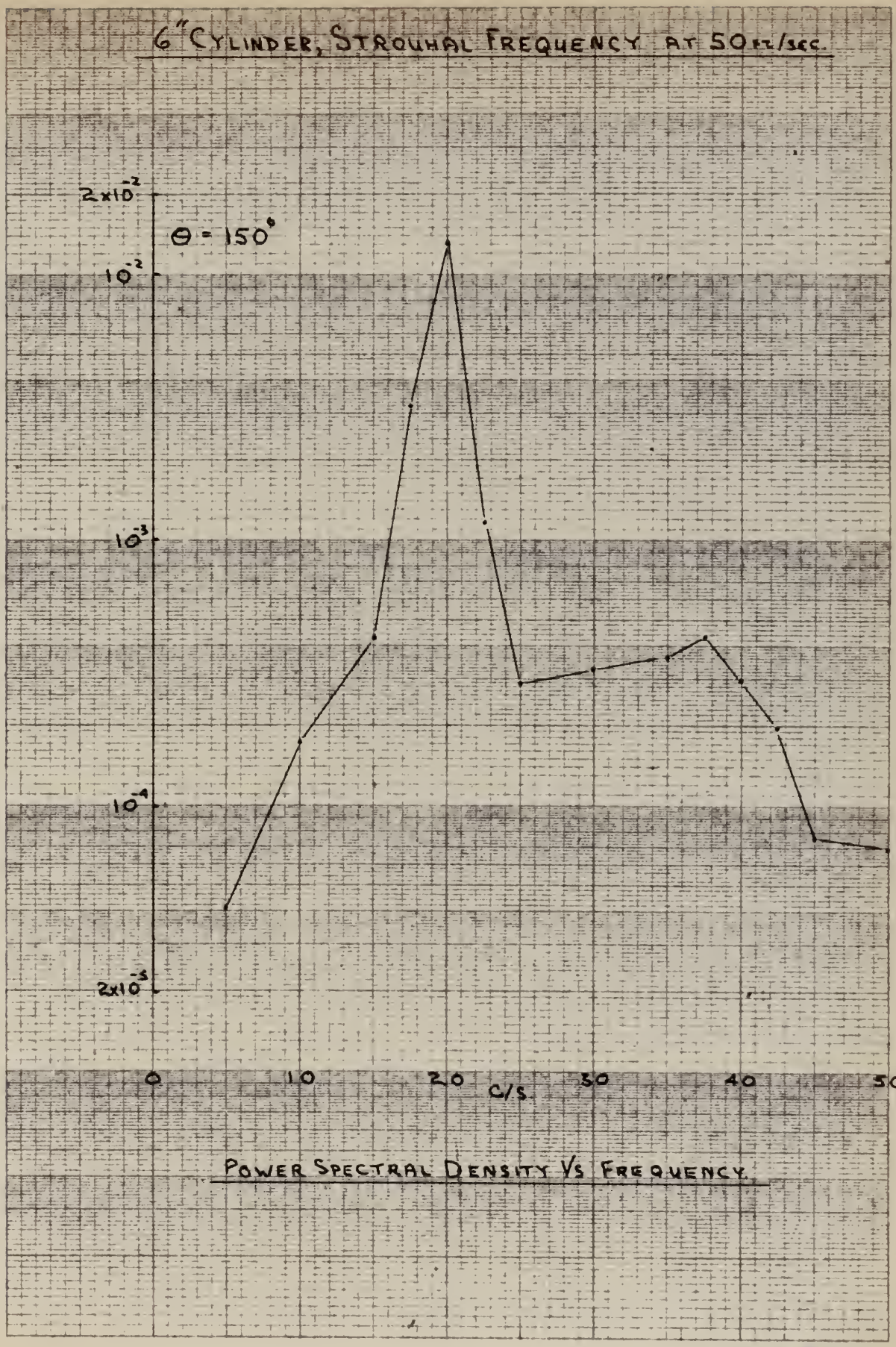
6" CYLINDER, STROUHAL FREQUENCY AT 50 FT/SEC.
2×10^{-2}
$\theta = 150^{\circ}$
10^{-2}
10^{-3}
10^{-4}
2×10^{-5}
0
10
20
C/S
30
40
50
POWER SPECTRAL DENSITY VS FREQUENCY

FIG. 44

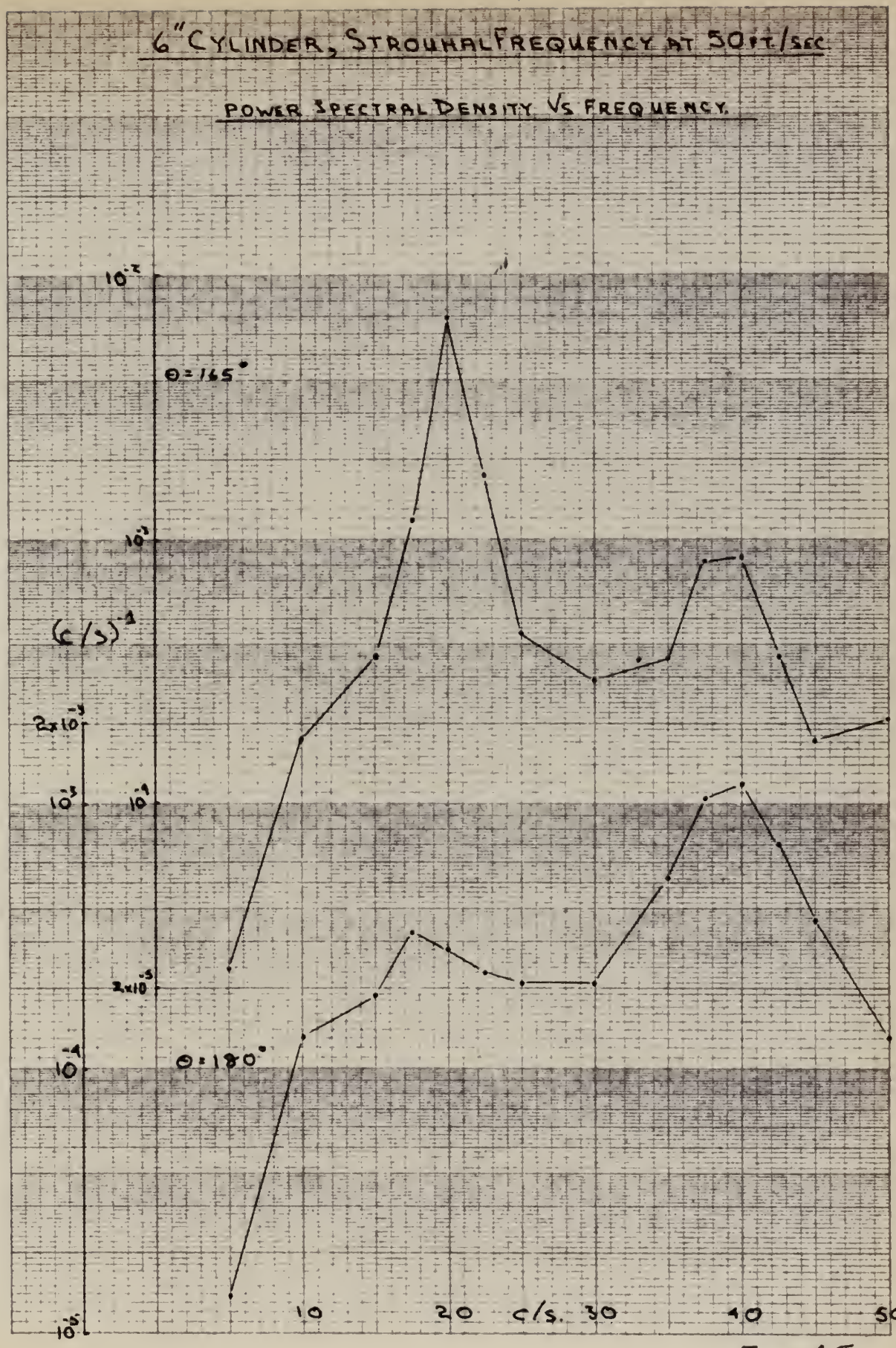
6" CYLINDER, STROUHAL FREQUENCY AT 50 FT/SEC.
POWER SPECTRAL DENSITY VS FREQUENCY.
θ = 165°
θ = 180°
(c/s)⁻¹
10⁻²
10⁻³
2×10⁻³
10⁻³
10⁻⁴
2×10⁻⁵
10⁻⁴
10⁻⁵
10
20
c/s.
30
40
50

FIG. 45

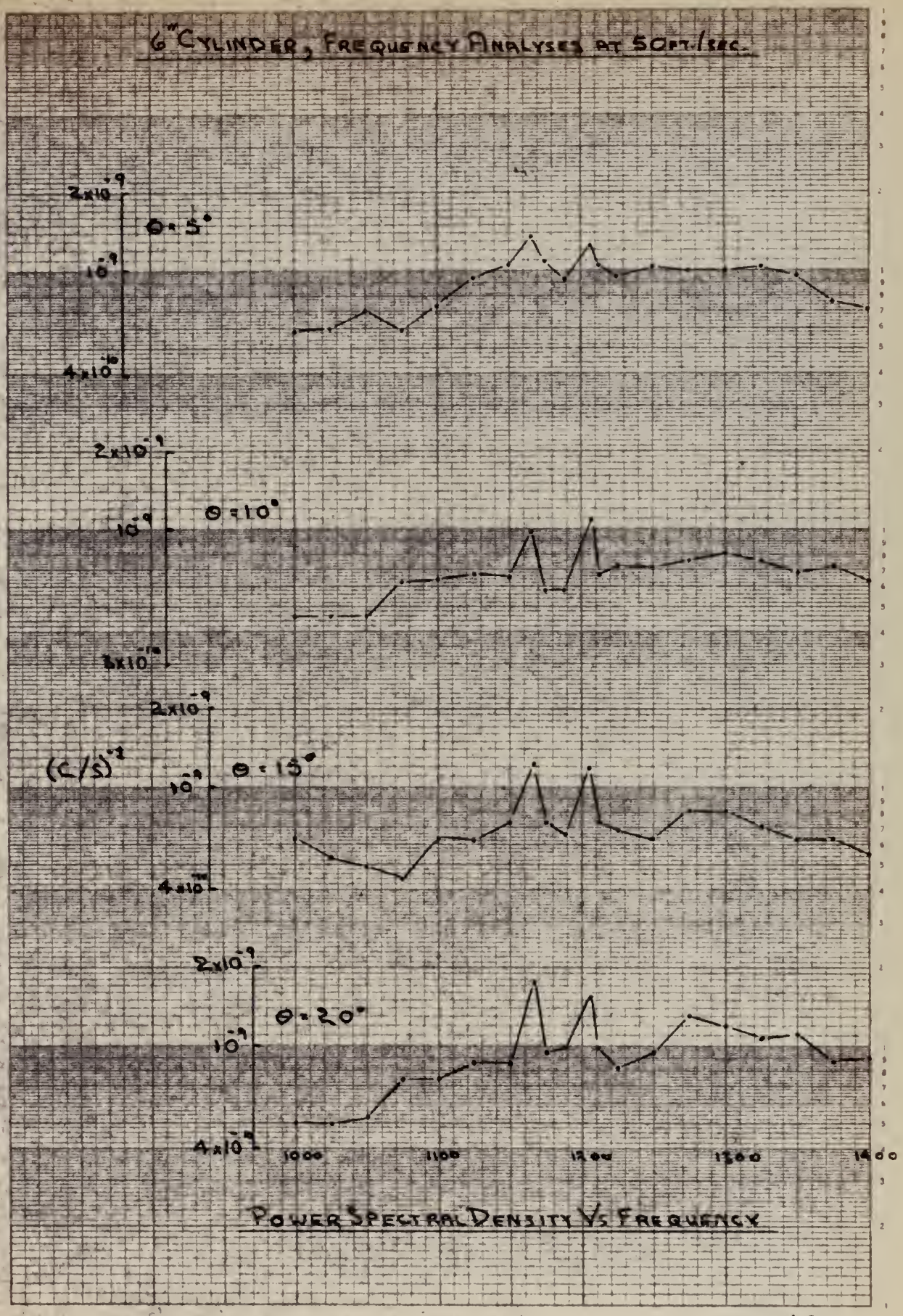
6" CYLINDER, FREQUENCY ANALYSES AT 50 FT./SEC.
2x10⁻⁹
θ = 5°
10⁻⁹
4x10⁻¹⁰
2x10⁻⁹
θ = 10°
10⁻⁹
3x10⁻¹⁰
2x10⁻⁹
(C/S)⁻²
θ = 15°
10⁻⁹
4x10⁻¹⁰
2x10⁻⁹
θ = 20°
10⁻⁹
4x10⁻¹⁰
1000
1100
1200
1300
1400
POWER SPECTRAL DENSITY VS FREQUENCY

FIG. 16

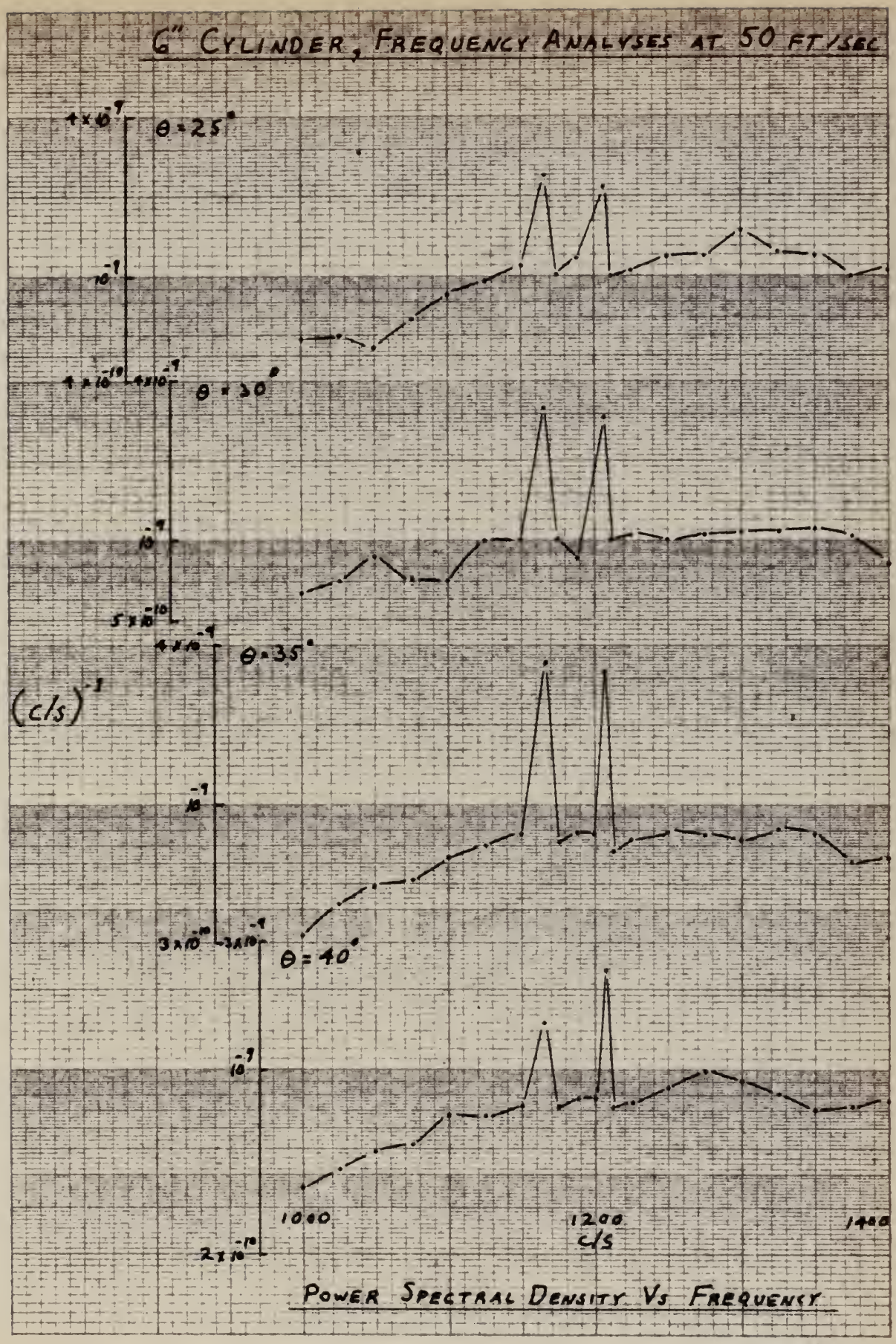
6" CYLINDER, FREQUENCY ANALYSES AT 50 FT/SEC
θ = 25°
θ = 30°
θ = 35°
θ = 40°
(c/s)⁻¹
1000
1200
1400
c/s
POWER SPECTRAL DENSITY VS FREQUENCY

FIG. 47

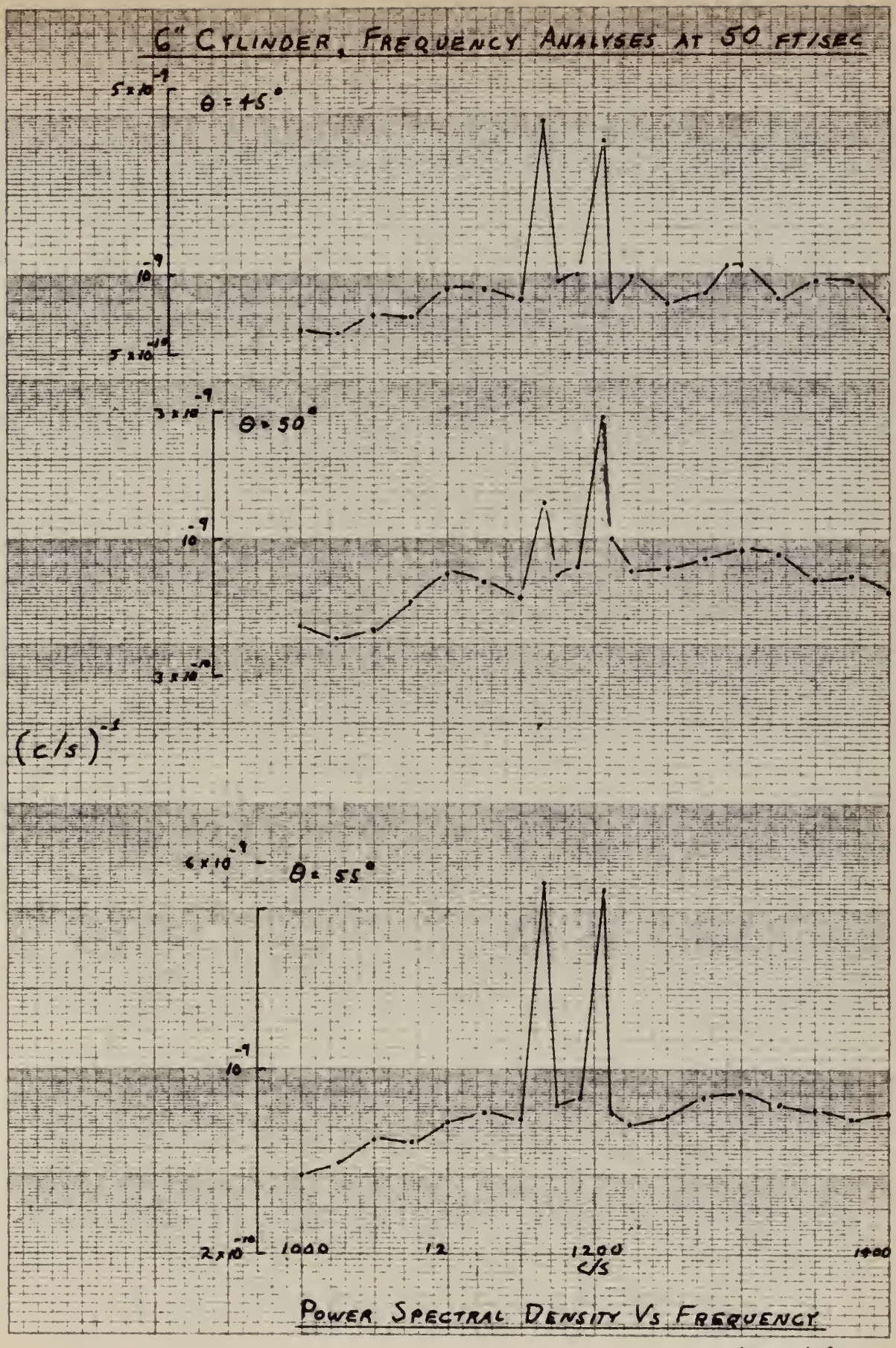
6" CYLINDER, FREQUENCY ANALYSES AT 50 FT/SEC
θ = 45°
θ = 50°
θ = 55°
(c/s)⁻¹
1000
1200
1400
c/s
POWER SPECTRAL DENSITY VS FREQUENCY

FIG. 48

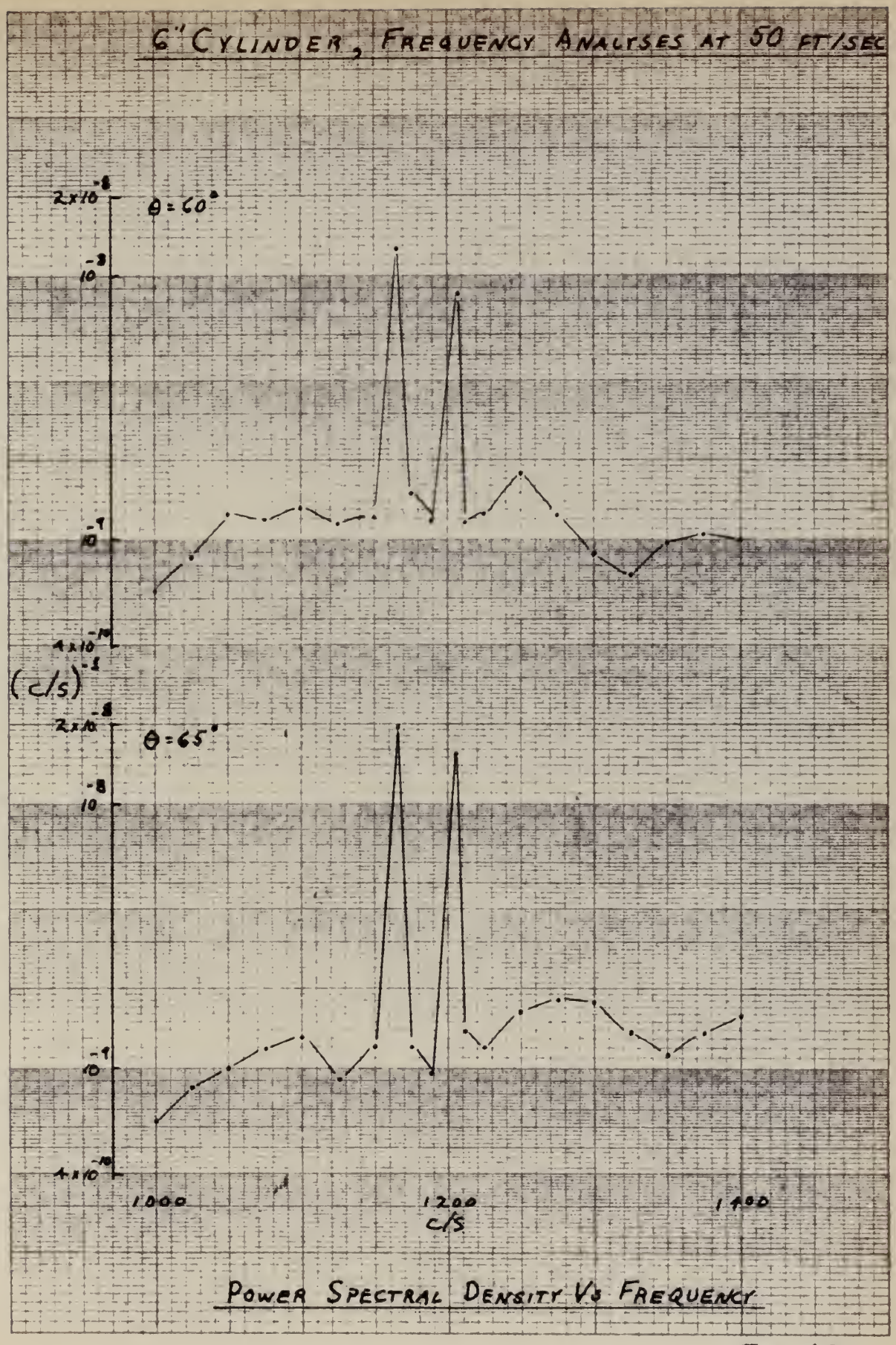
6" CYLINDER, FREQUENCY ANALYSES AT 50 FT/SEC
θ = 60°
θ = 65°
(c/s)
1000
1200
1400
c/s
POWER SPECTRAL DENSITY Vs FREQUENCY

FIG. 49

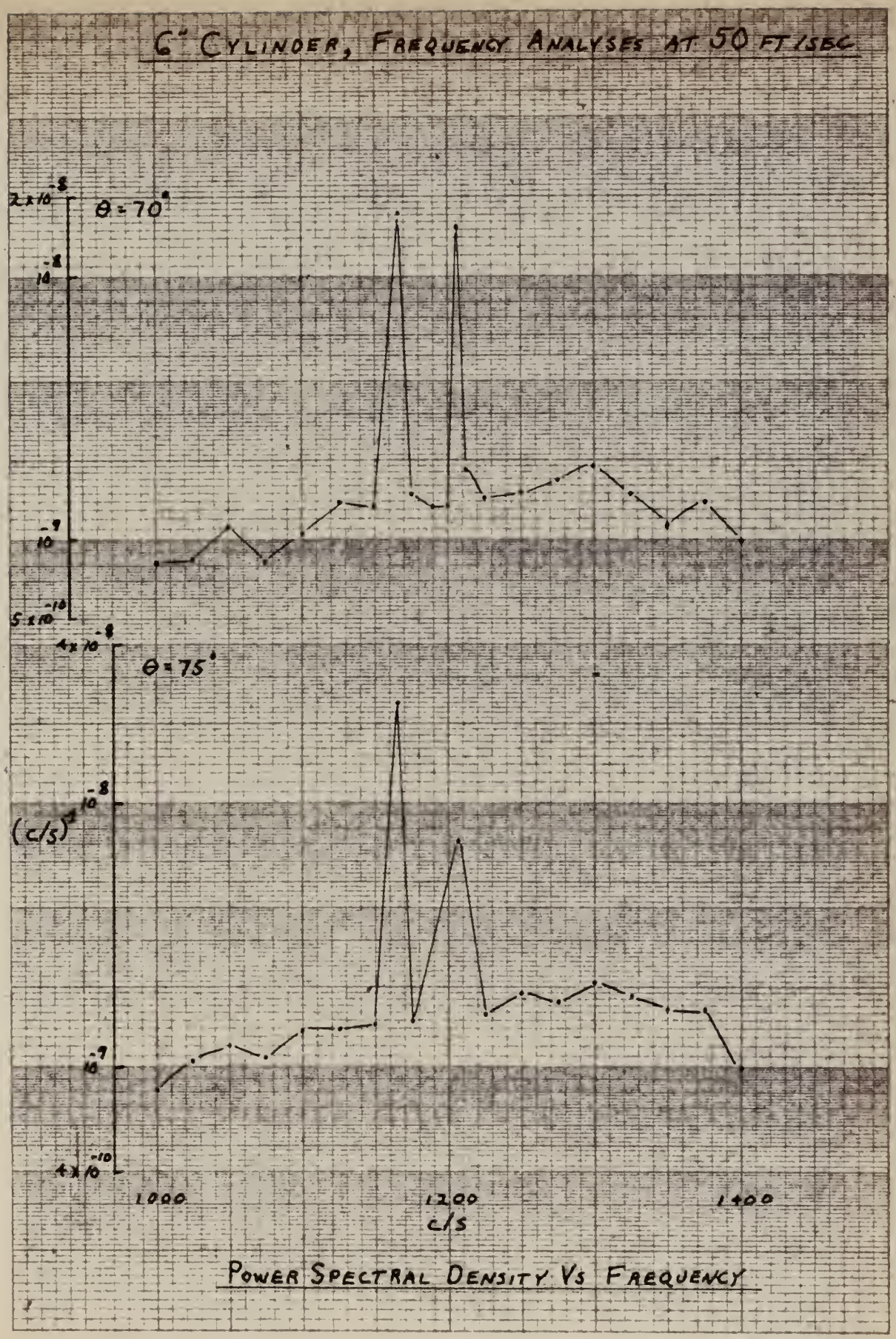
6" Cylinder, Frequency Analyses at 50 ft/sec
θ = 70°
θ = 75°
(c/s)
1000
1200
1400
c/s
Power Spectral Density Vs Frequency

Fig. 50

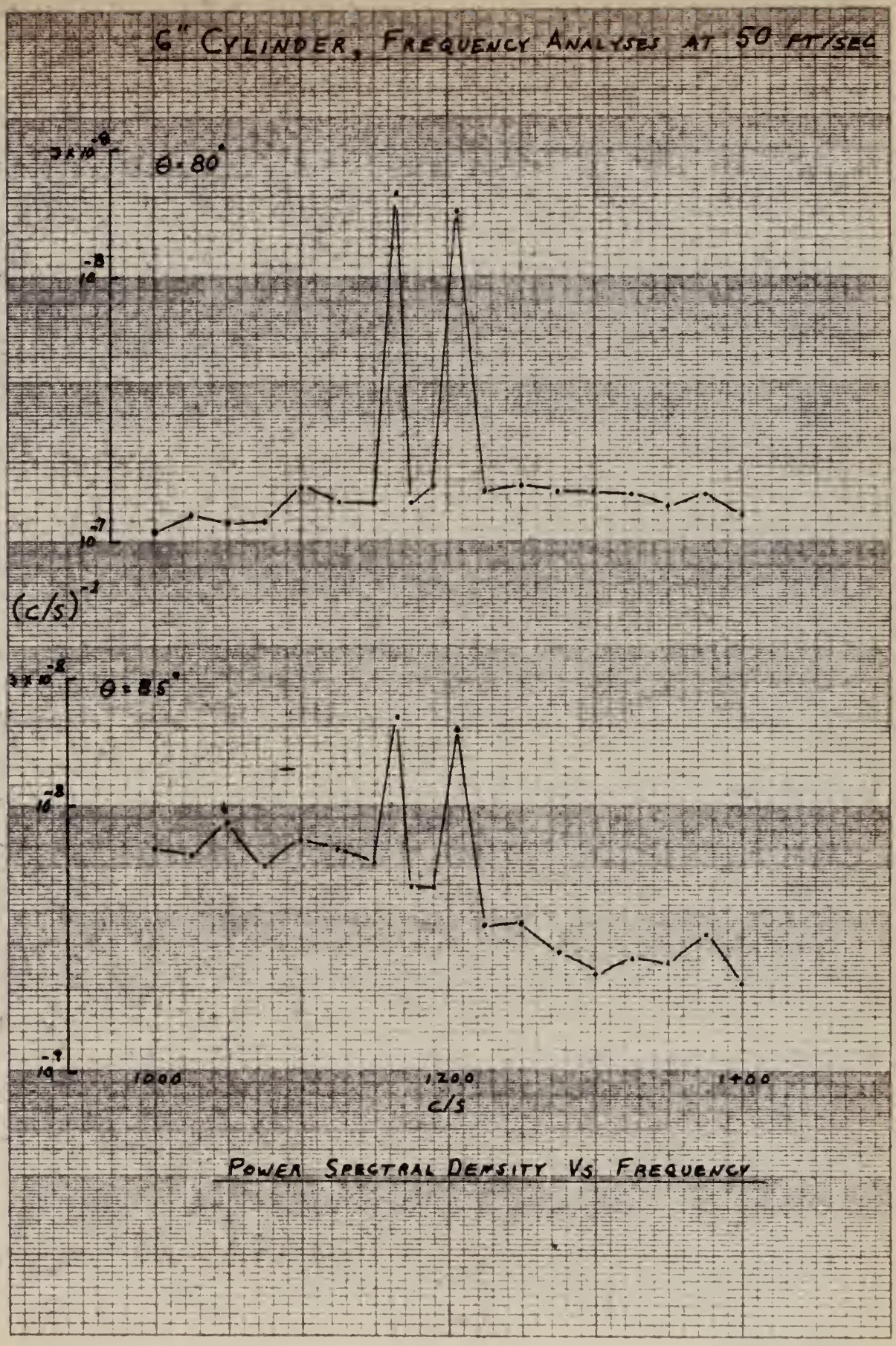
6" CYLINDER, FREQUENCY ANALYSES AT 50 FT/SEC
θ = 80°
θ = 85°
(c/s)⁻¹
1000
1200
1400
c/s
POWER SPECTRAL DENSITY VS FREQUENCY

FIG. 51

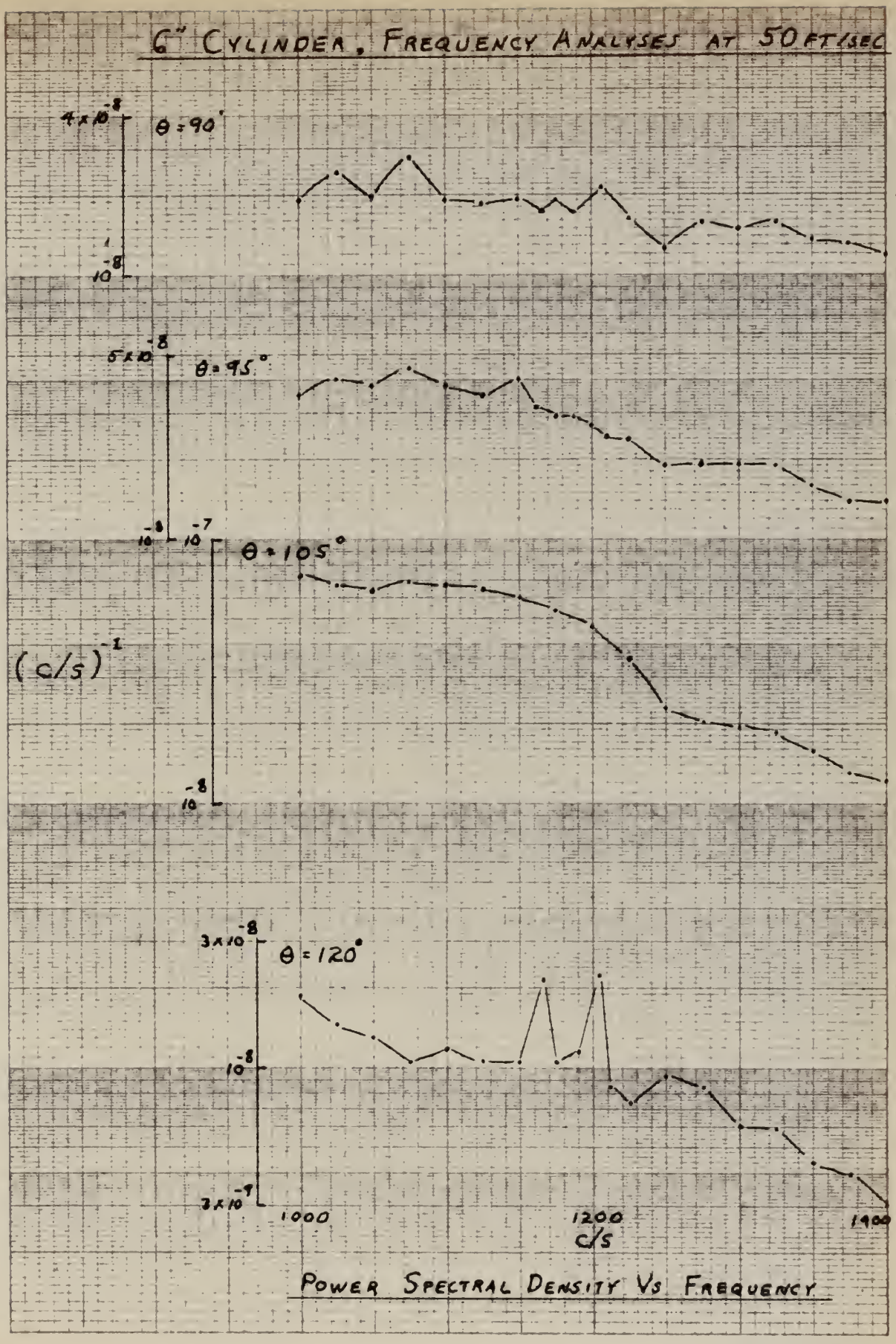
6" CYLINDER, FREQUENCY ANALYSES AT 50 FT/SEC
θ = 90°
θ = 95°
θ = 105°
θ = 120°
(c/s)⁻¹
1000
1200
1900
c/s
POWER SPECTRAL DENSITY VS FREQUENCY

FIG. 52

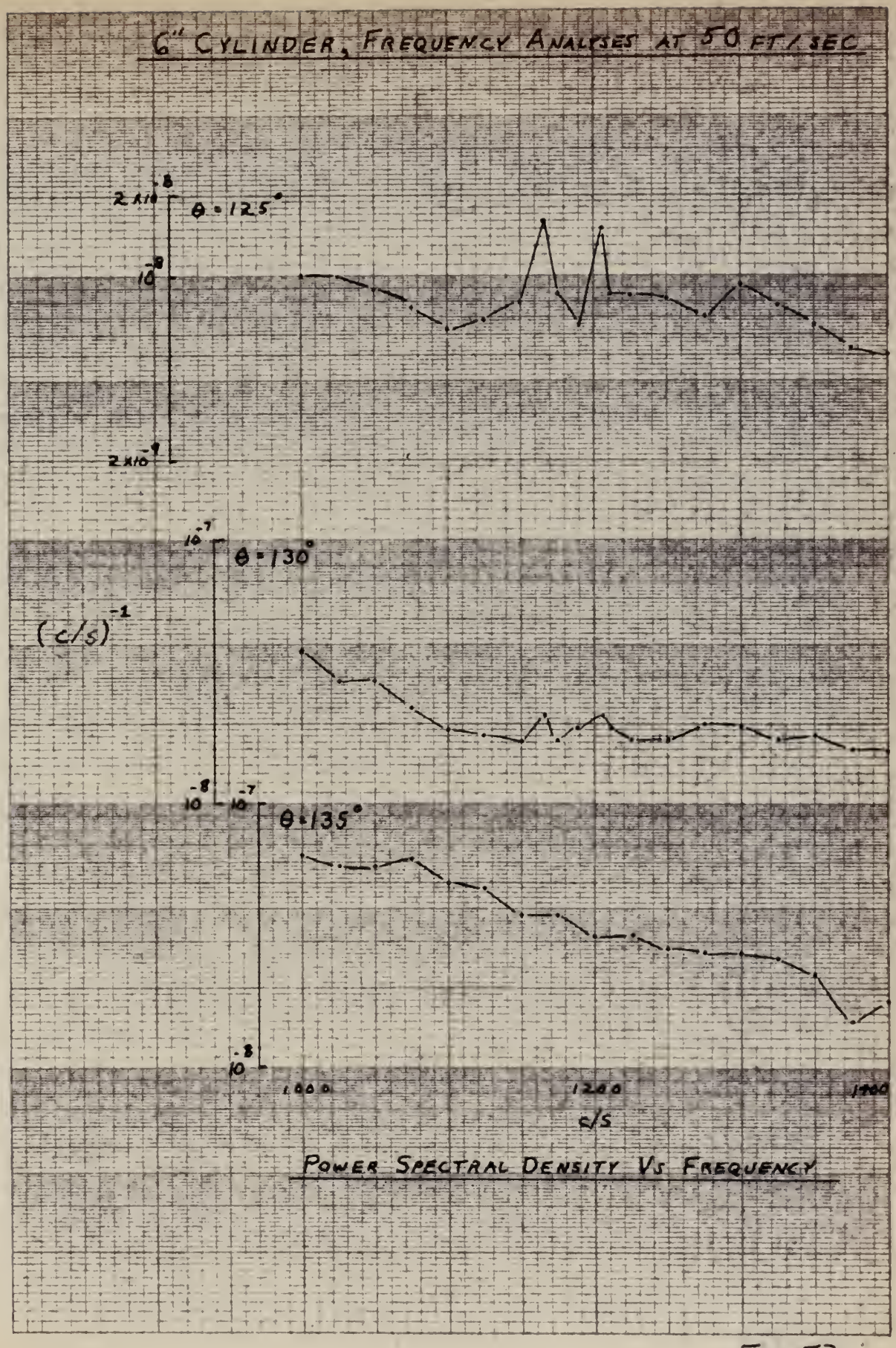
6" CYLINDER, FREQUENCY ANALYSES AT 50 FT/SEC
θ = 125°
θ = 130°
θ = 135°
(c/s)⁻¹
1000
1200
1400
c/s
POWER SPECTRAL DENSITY VS FREQUENCY

FIG. 53

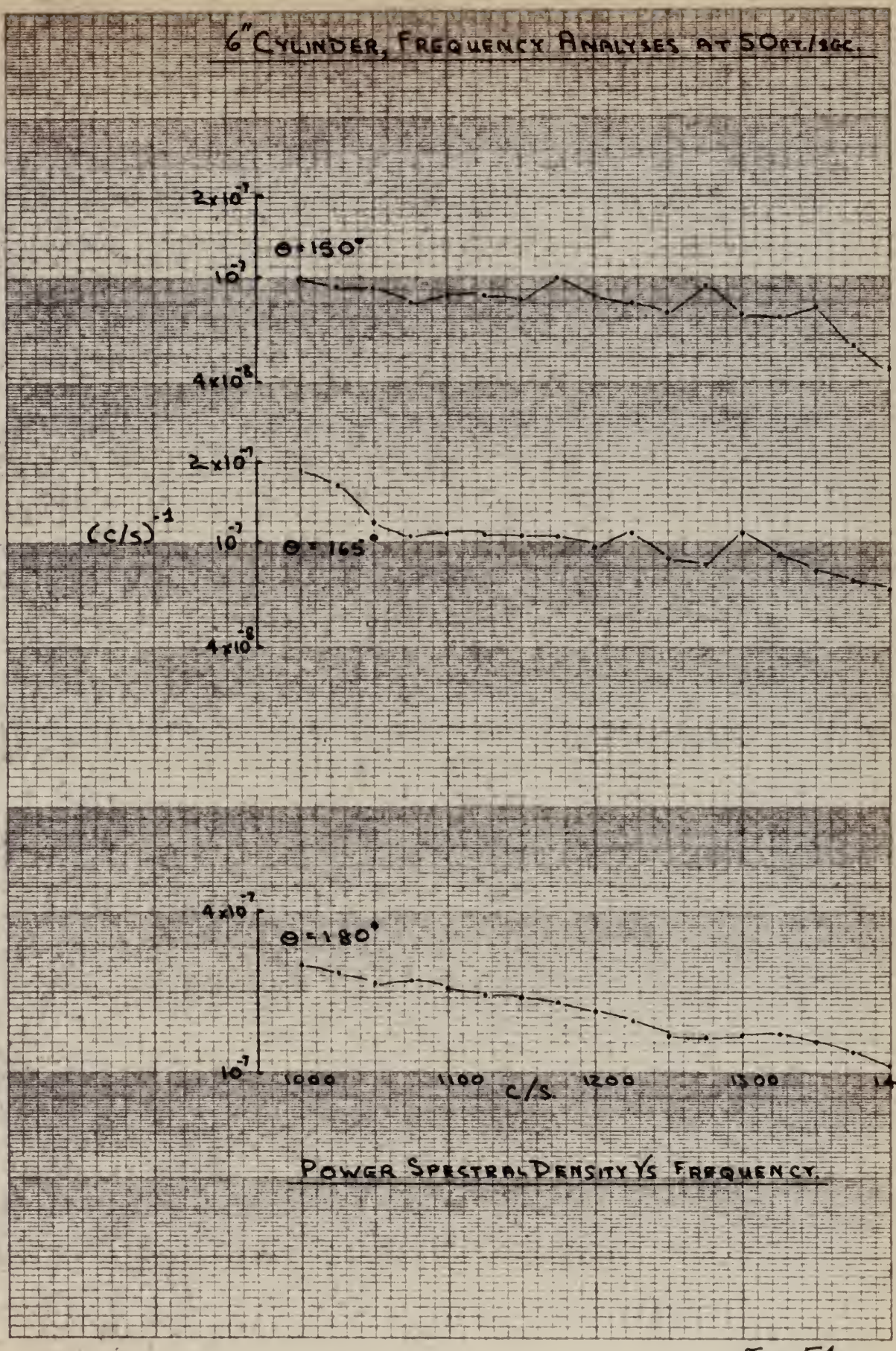
6" CYLINDER, FREQUENCY ANALYSES AT 50 PT./SEC.
2x10⁻⁷
θ=150°
10⁻⁷
4x10⁻⁸
2x10⁻⁷
(c/s)⁻¹
10⁻⁷
θ=165°
4x10⁻⁸
4x10⁻⁷
θ=180°
10⁻⁷
1000
1100
c/s.
1200
1300
1400
POWER SPECTRAL DENSITY Vs FREQUENCY.

FIG. 54

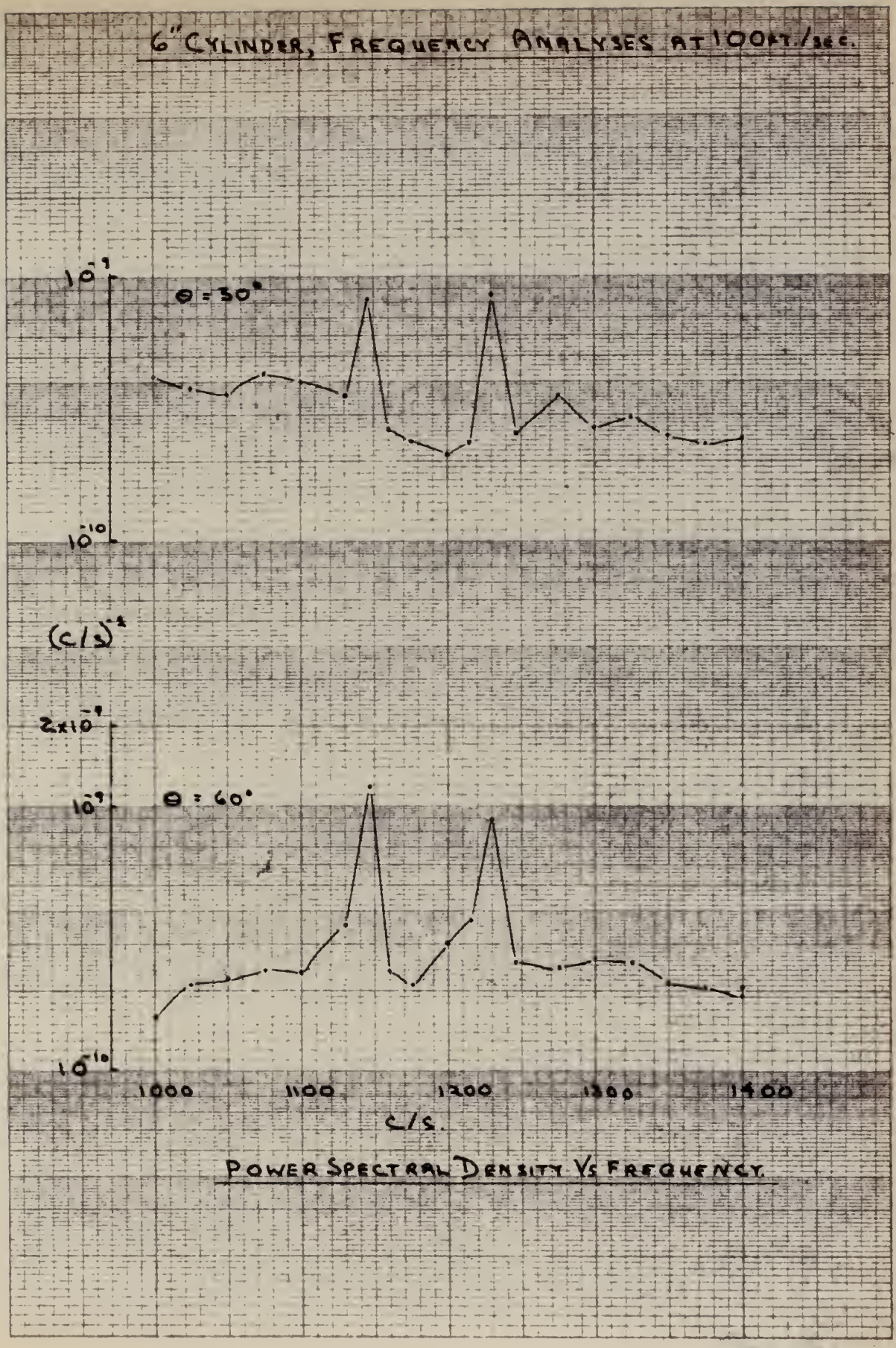
6" CYLINDER, FREQUENCY ANALYSES AT 100 FT./SEC.
10^{-9}
$\theta = 30°$
10^{-10}
$(c/s)^{-1}$
2×10^{-9}
10^{-9}
$\theta = 60°$
10^{-10}
1000
1100
1200
1300
1400
c/s.
POWER SPECTRAL DENSITY VS FREQUENCY.

FIG. 55

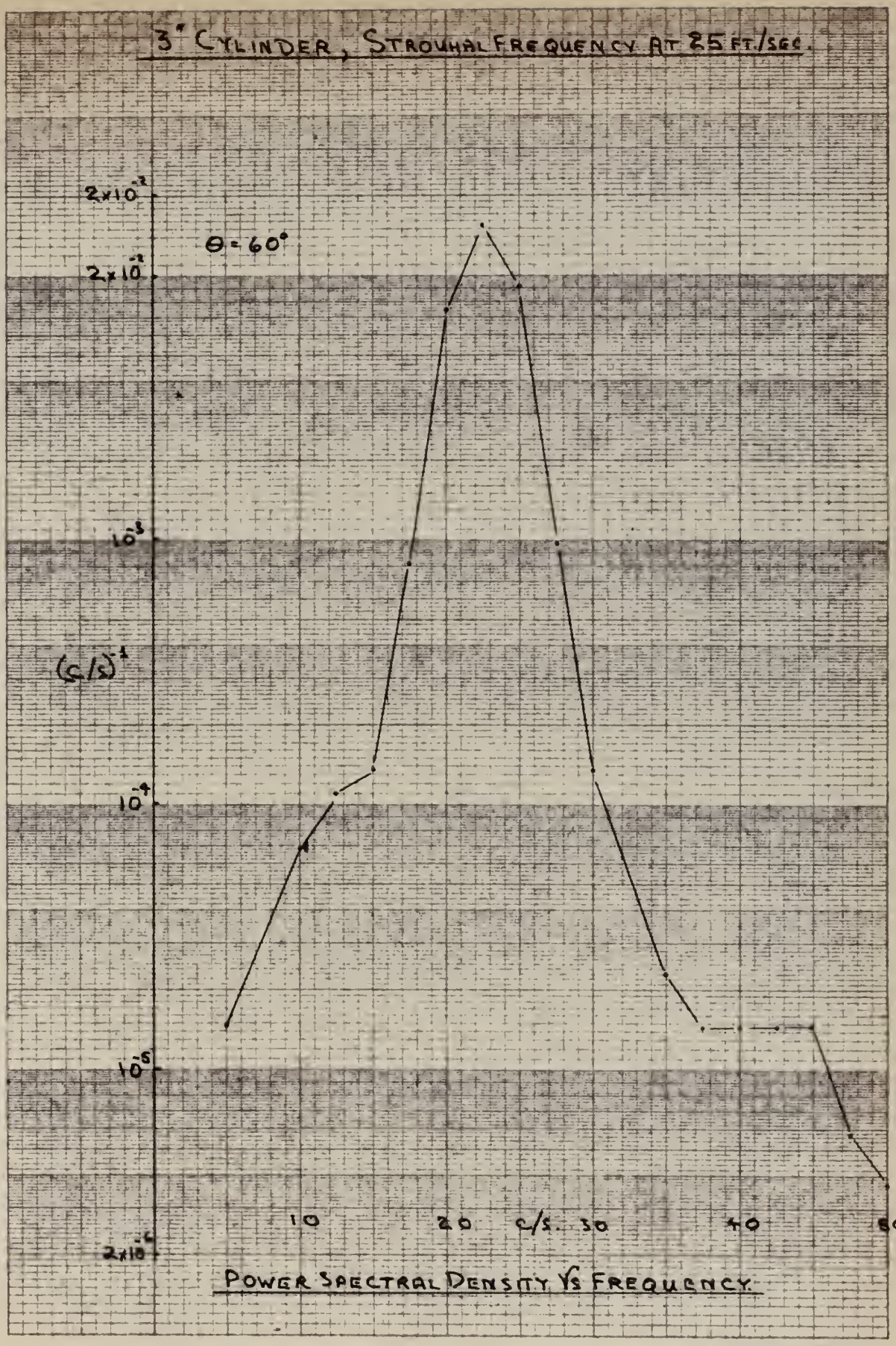
3" CYLINDER, STROUHAL FREQUENCY AT 25 FT./SEC.
θ = 60°
2×10^{-3}
2×10^{-2}
10^{-3}
10^{-4}
10^{-5}
2×10^{-6}
$(\text{ft}/\text{s})^{-1}$
10
20
c/s.
30
40
50
POWER SPECTRAL DENSITY Vs FREQUENCY.

FIG. 56

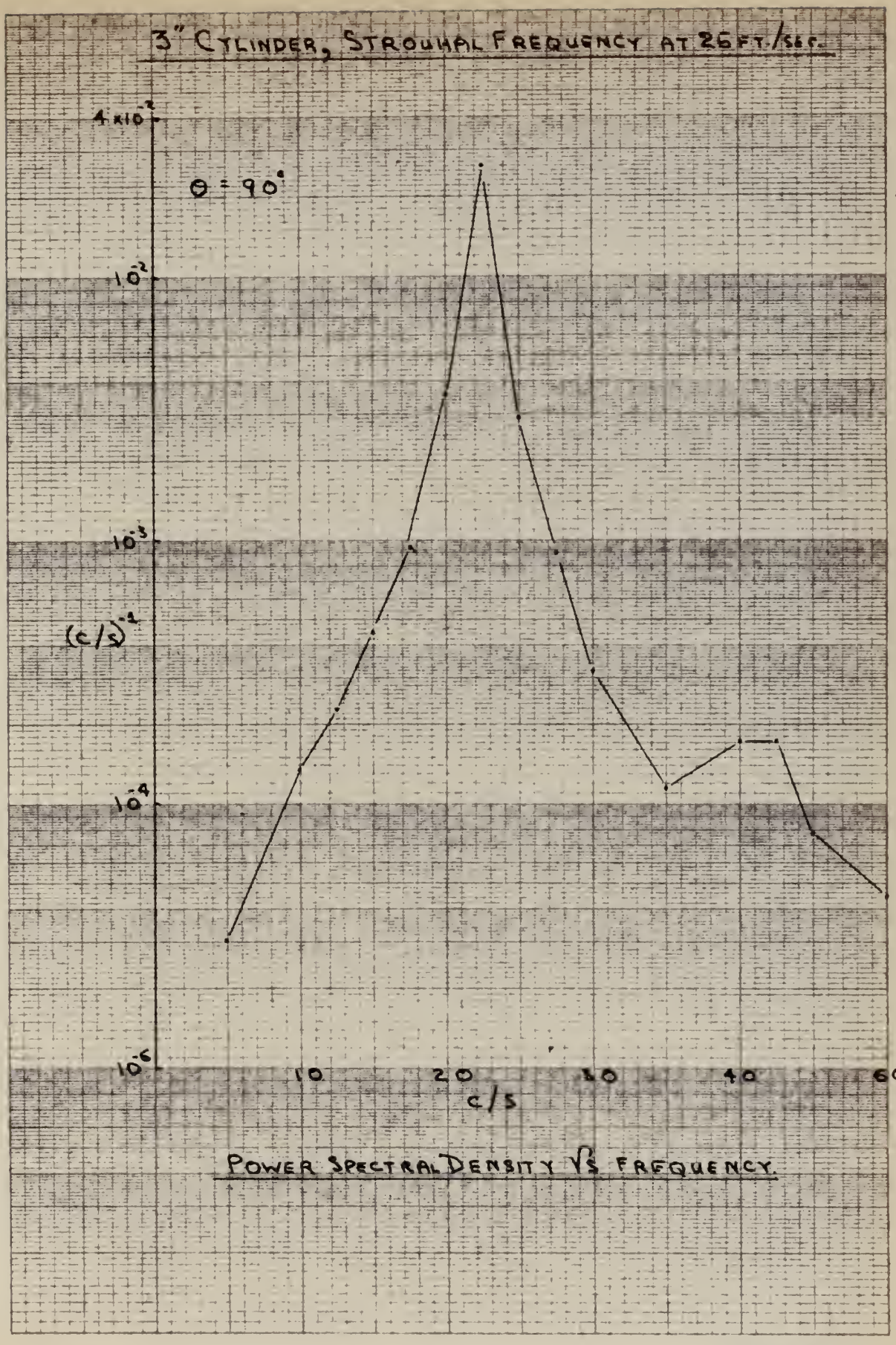
3" CYLINDER, STROUHAL FREQUENCY AT 25 FT./SEC.
4 x 10⁻²
θ = 90°
10⁻²
10⁻³
(c/s)⁻²
10⁻⁴
10⁻⁵
10
20
30
40
60
c/s
POWER SPECTRAL DENSITY VS FREQUENCY.

FIG. 57

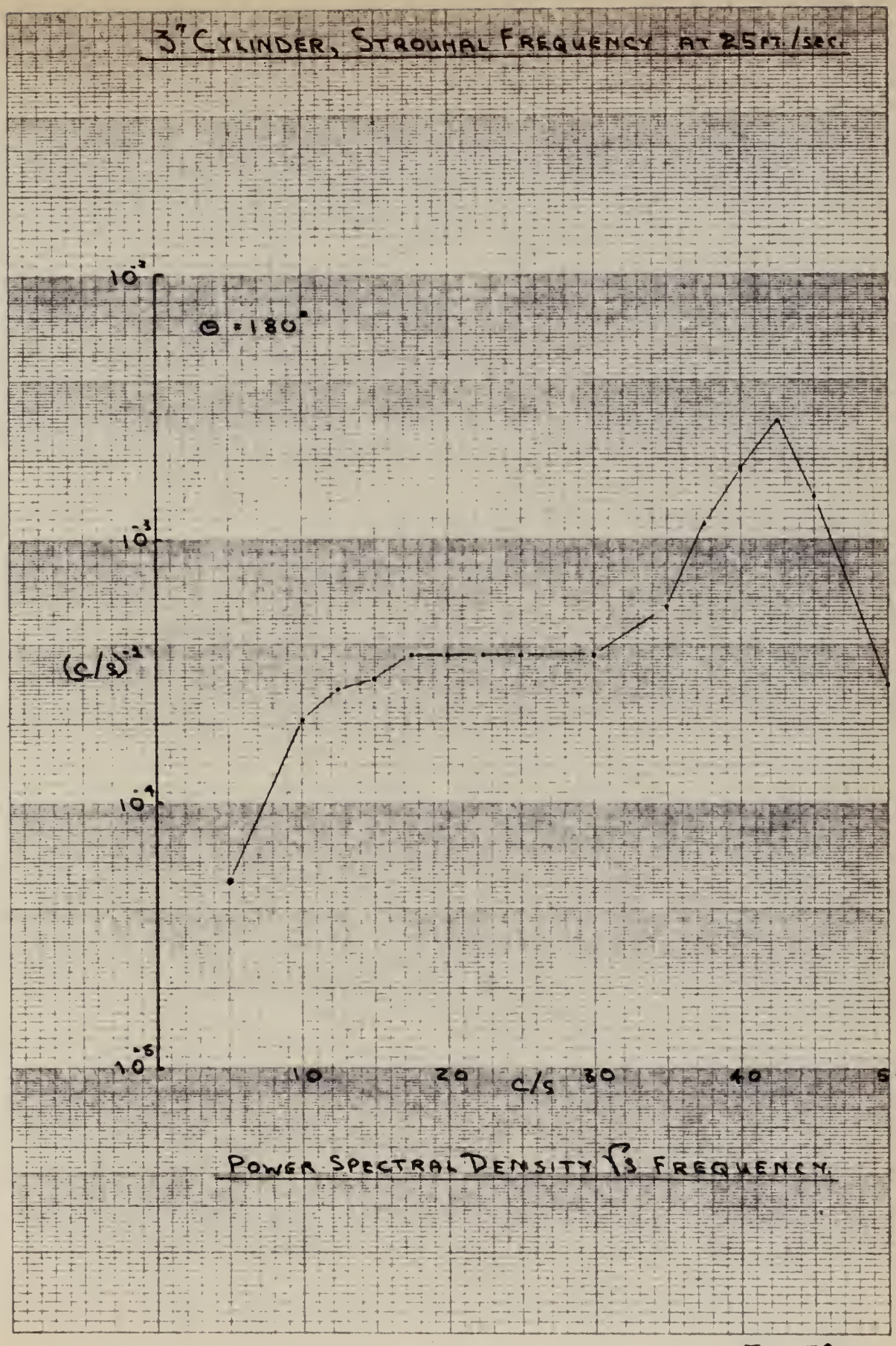
3" CYLINDER, STROUHAL FREQUENCY AT 25 FT./SEC.
10^{-2}
$\Theta = 180°$
10^{-3}
$(c/s)^{-1}$
10^{-4}
10^{-5}
10
20
c/s
30
40
50
POWER SPECTRAL DENSITY $\int$s FREQUENCY.

FIG. 58

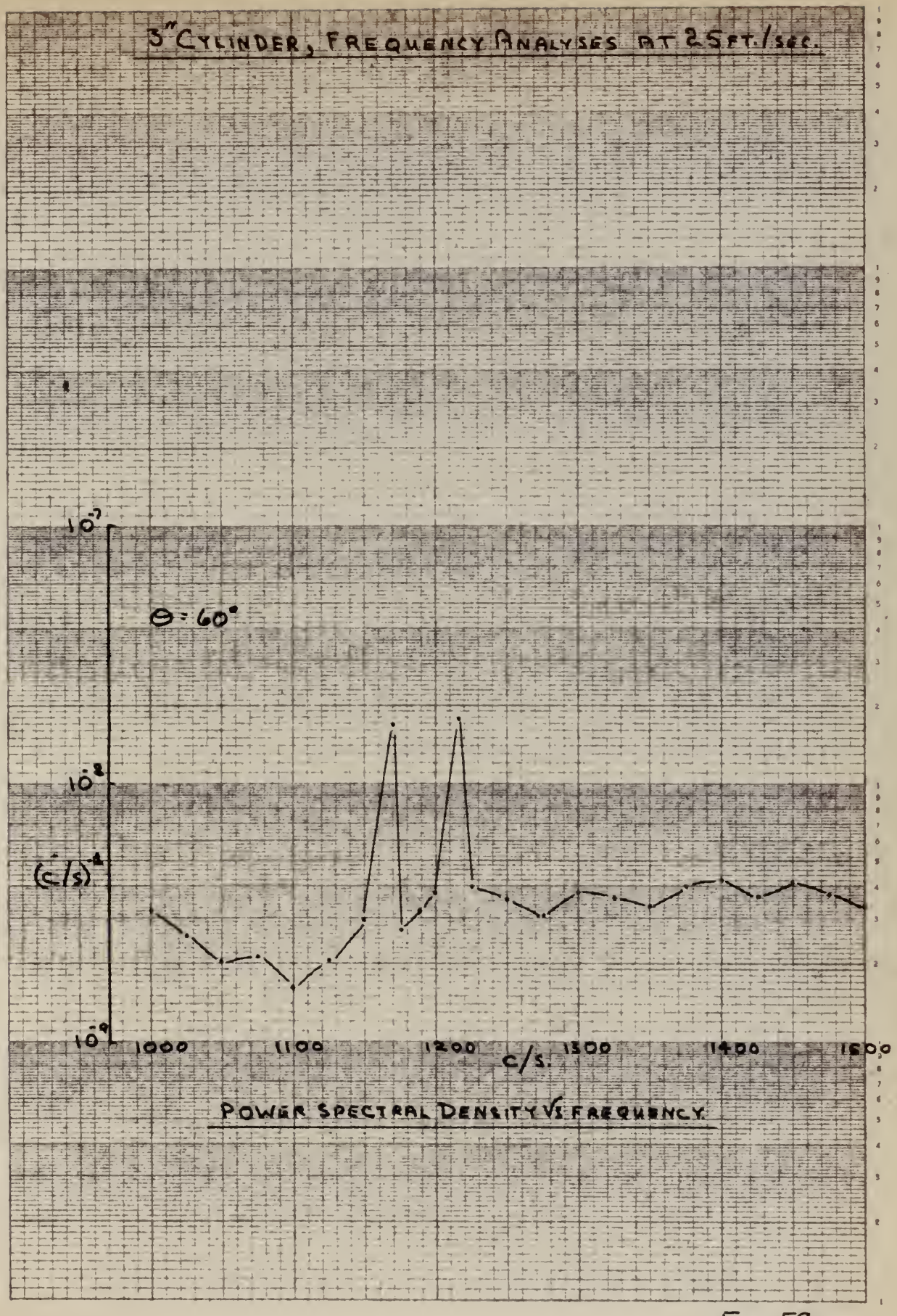
3" CYLINDER, FREQUENCY ANALYSES AT 25FT./SEC.
10^{-7}
$\theta = 60°$
10^{-8}
$(\bar{c}/s)^{-2}$
10^{-9}
1000
1100
1200
c/s.
1300
1400
1500
POWER SPECTRAL DENSITY VS FREQUENCY.

FIG. 59

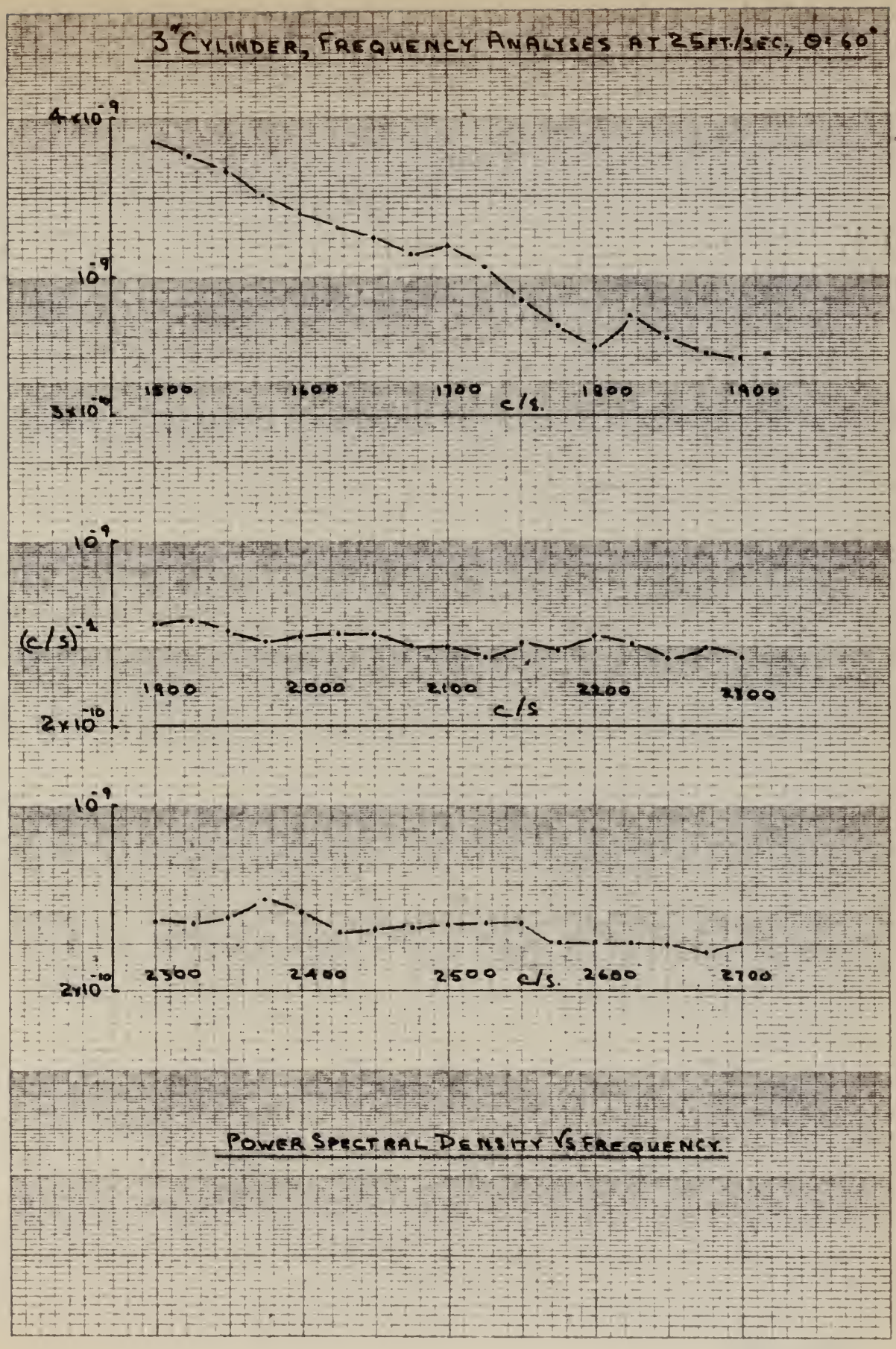
3" Cylinder, Frequency Analyses at 25 ft./sec, Θ = 60°
4×10⁻⁹
10⁻⁹
3×10⁻¹⁰
1500
1600
1700
c/s.
1800
1900
10⁻⁹
(c/s)⁻¹
2×10⁻¹⁰
1900
2000
2100
c/s
2200
2300
10⁻⁹
2×10⁻¹⁰
2300
2400
2500
c/s.
2600
2700
Power Spectral Density vs Frequency.

Fig. 60

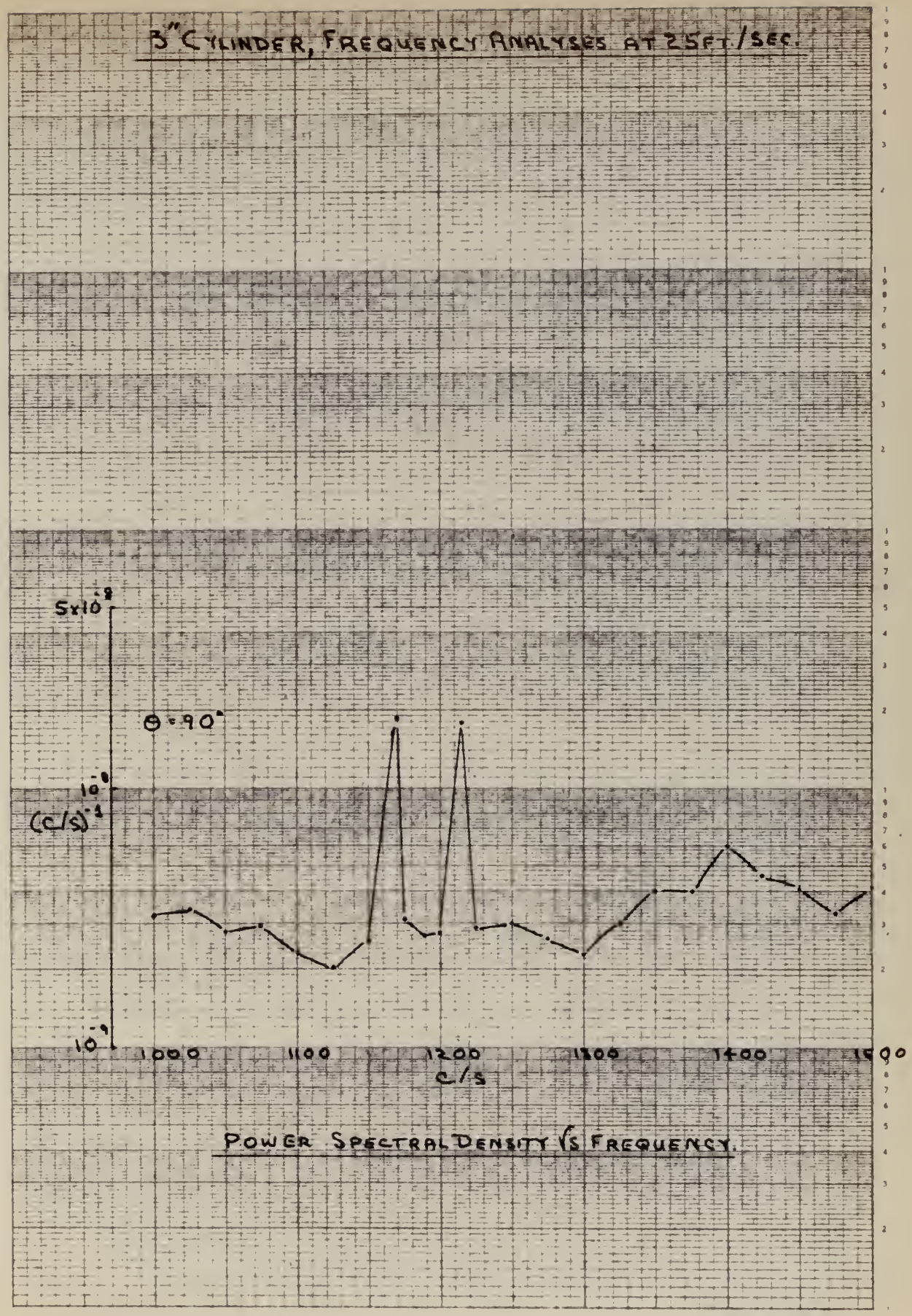
3" CYLINDER, FREQUENCY ANALYSES AT 25FT./SEC.
5x10⁻⁸
θ=90°
10⁻⁸
(c/s)⁻¹
10⁻⁹
1000
1100
1200
1300
1400
1500
c/s
POWER SPECTRAL DENSITY VS FREQUENCY.

FIG. 61

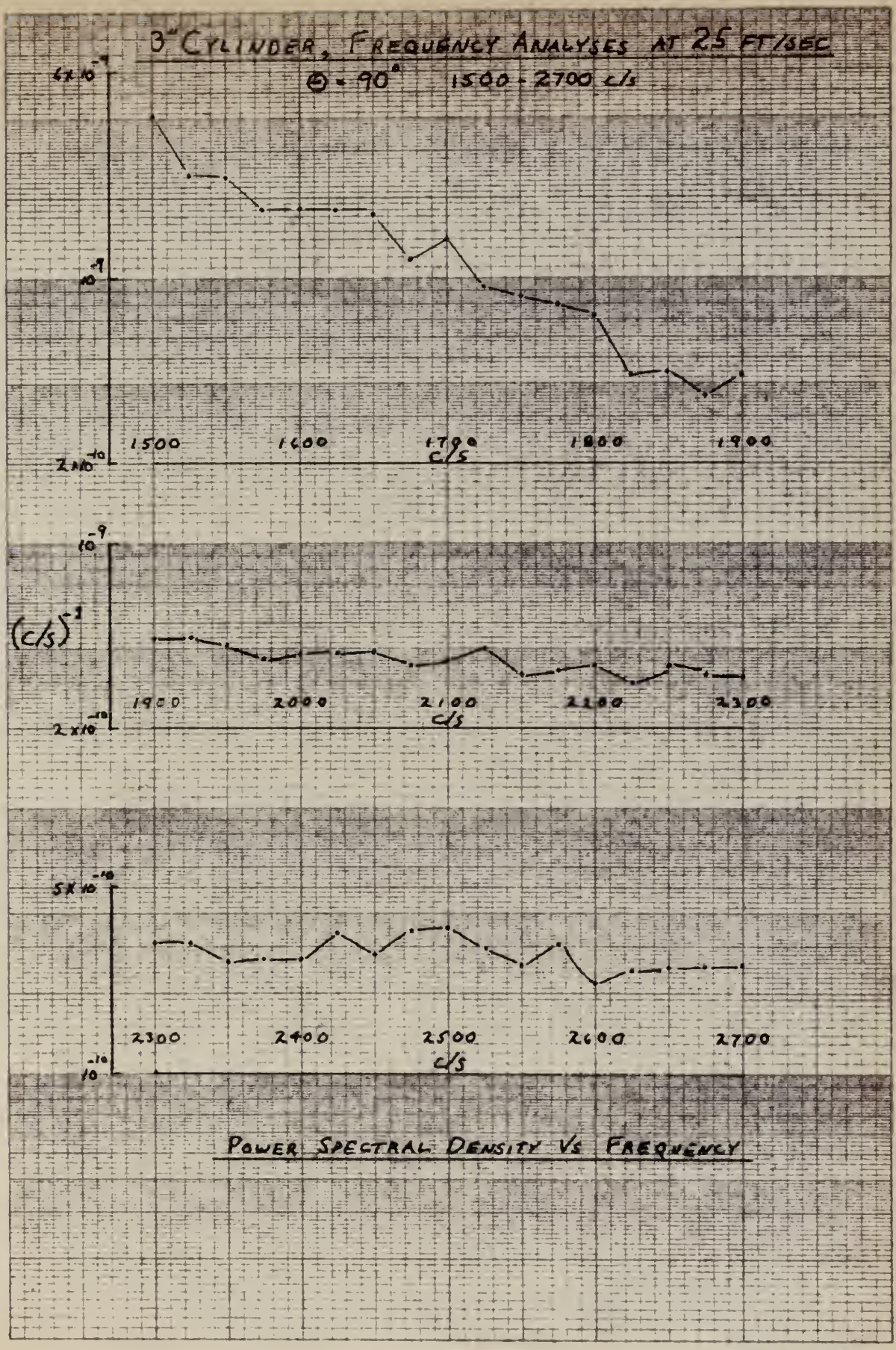
3" CYLINDER, FREQUENCY ANALYSES AT 25 FT/SEC
Θ = 90°
1500 - 2700 c/s
4x10
-9
10
2x10
-10
1500
1600
1700
1800
1900
c/s
10
-9
(c/s)
-1
2x10
-10
1900
2000
2100
2200
2300
c/s
5x10
-10
10
-10
2300
2400
2500
2600
2700
c/s
POWER SPECTRAL DENSITY VS FREQUENCY

FIG. 62

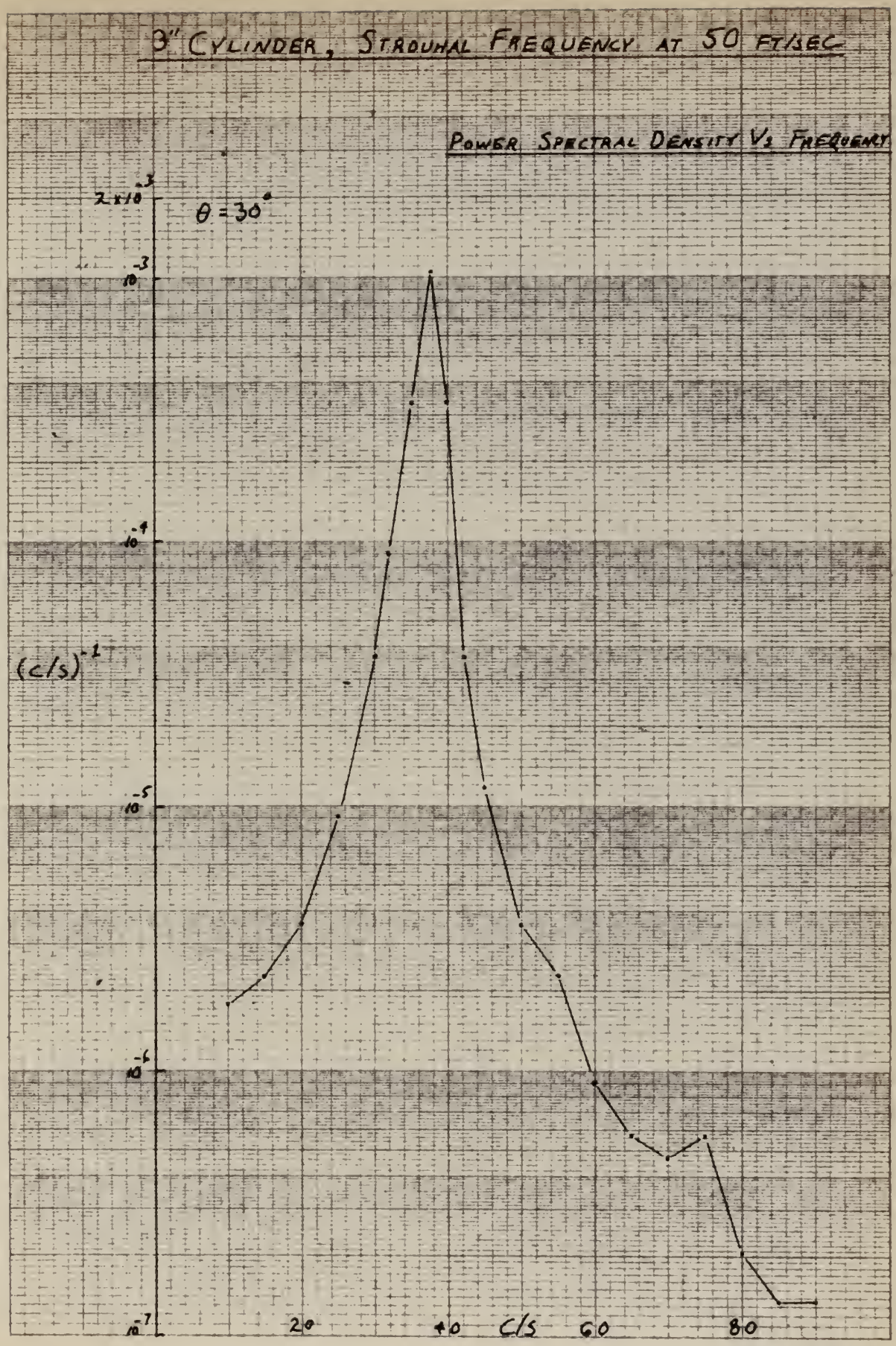
3" CYLINDER, STROUHAL FREQUENCY AT 50 FT/SEC
POWER SPECTRAL DENSITY V₂ FREQUENCY
θ = 30°
2 x 10⁻³
10⁻³
10⁻⁴
10⁻⁵
10⁻⁶
10⁻⁷
(c/s)⁻¹
20
40
C/S
60
80

FIG. 63

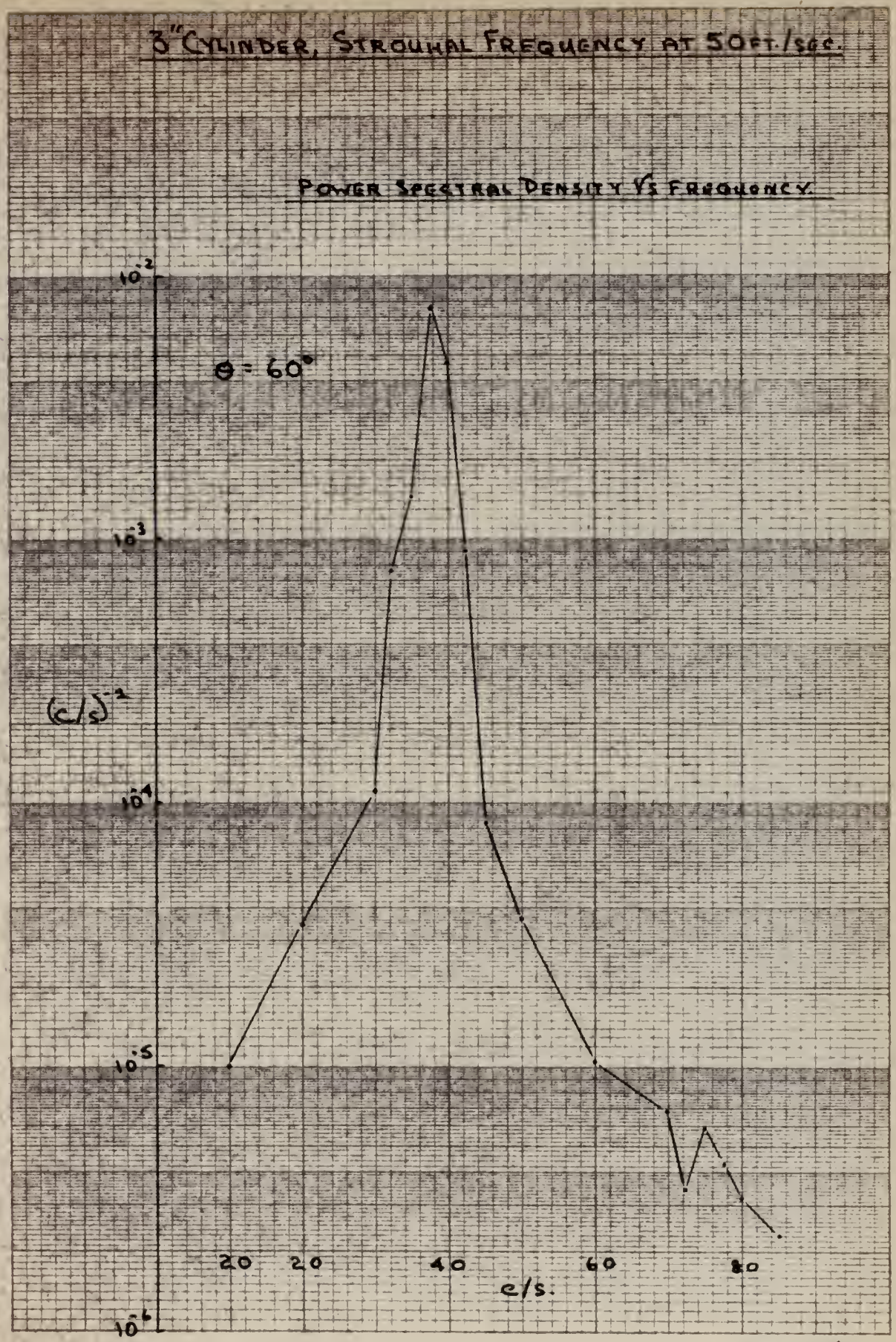
3" CYLINDER, STROUHAL FREQUENCY AT 50 FT./SEC.
POWER SPECTRAL DENSITY VS FREQUENCY.
θ = 60°
10^-2
10^-3
10^-4
10^-5
10^-6
(c/s)^-2
20
20
40
60
80
c/s.

FIG. 64

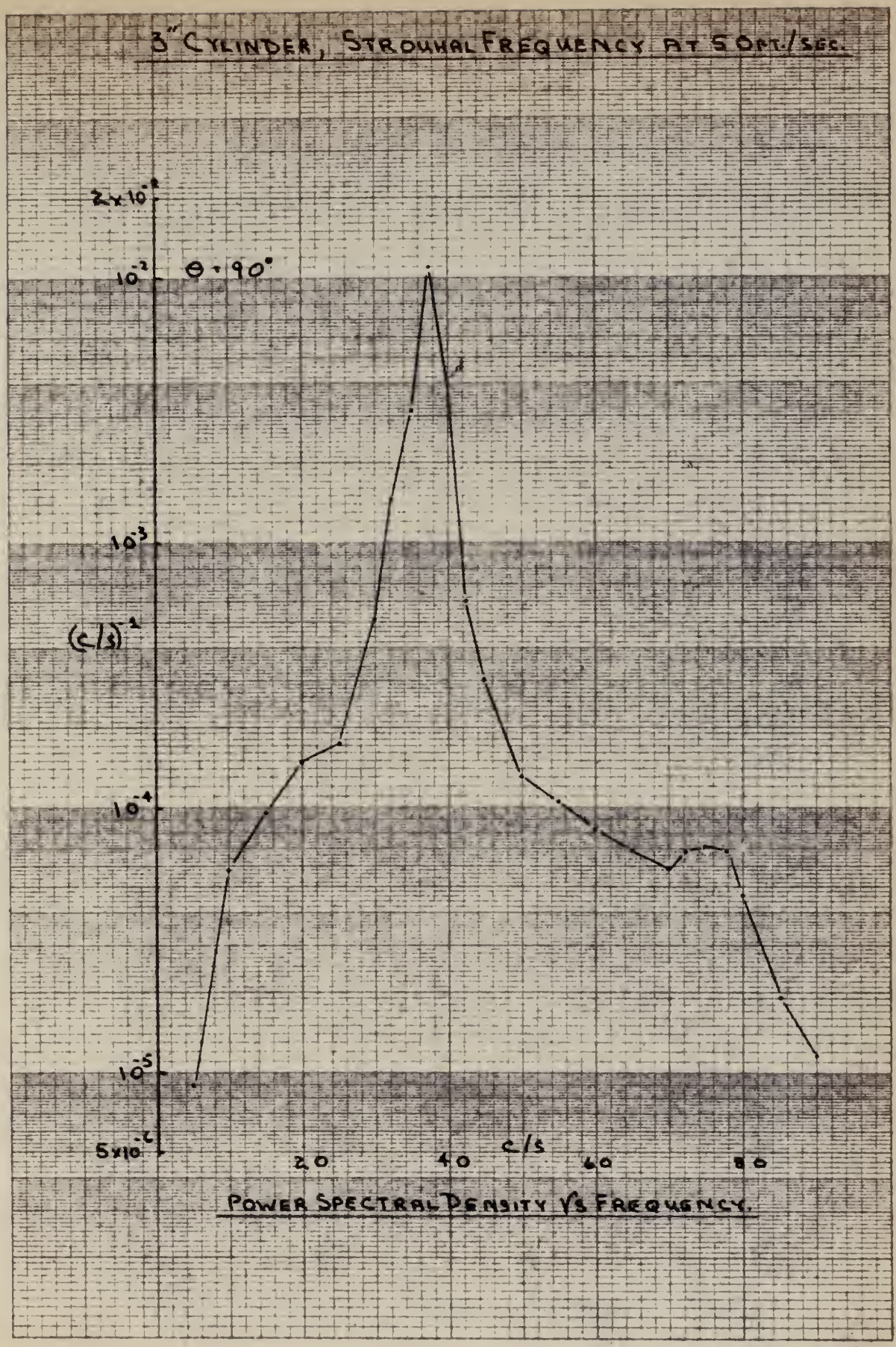
3" CYLINDER, STROUHAL FREQUENCY AT 50 FT./SEC.
2x10⁻²
10⁻²
θ = 90°
10⁻³
(c/s)⁻¹
10⁻⁴
10⁻⁵
5x10⁻⁶
20
40
c/s
60
80
POWER SPECTRAL DENSITY VS FREQUENCY.

FIG. 65

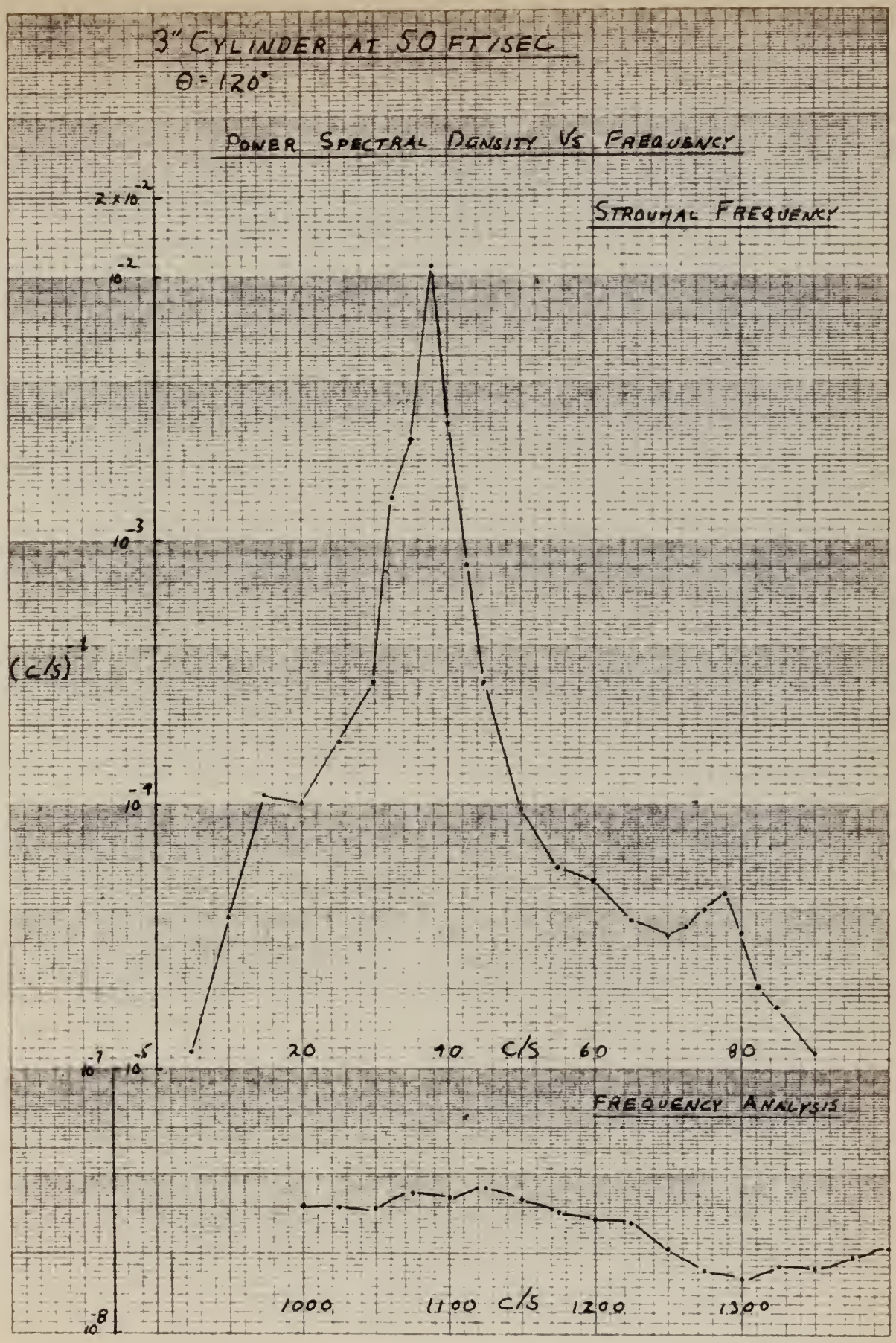
3" CYLINDER AT 50 FT/SEC
θ = 120°
POWER SPECTRAL DENSITY VS FREQUENCY
STROUHAL FREQUENCY
2 x 10^-2
10^-2
10^-3
10^-4
(C/S)^-1
20
40 C/S
60
80
10^-7
10^-5
FREQUENCY ANALYSIS
1000
1100 C/S
1200
1300
10^-8

FIG. 66

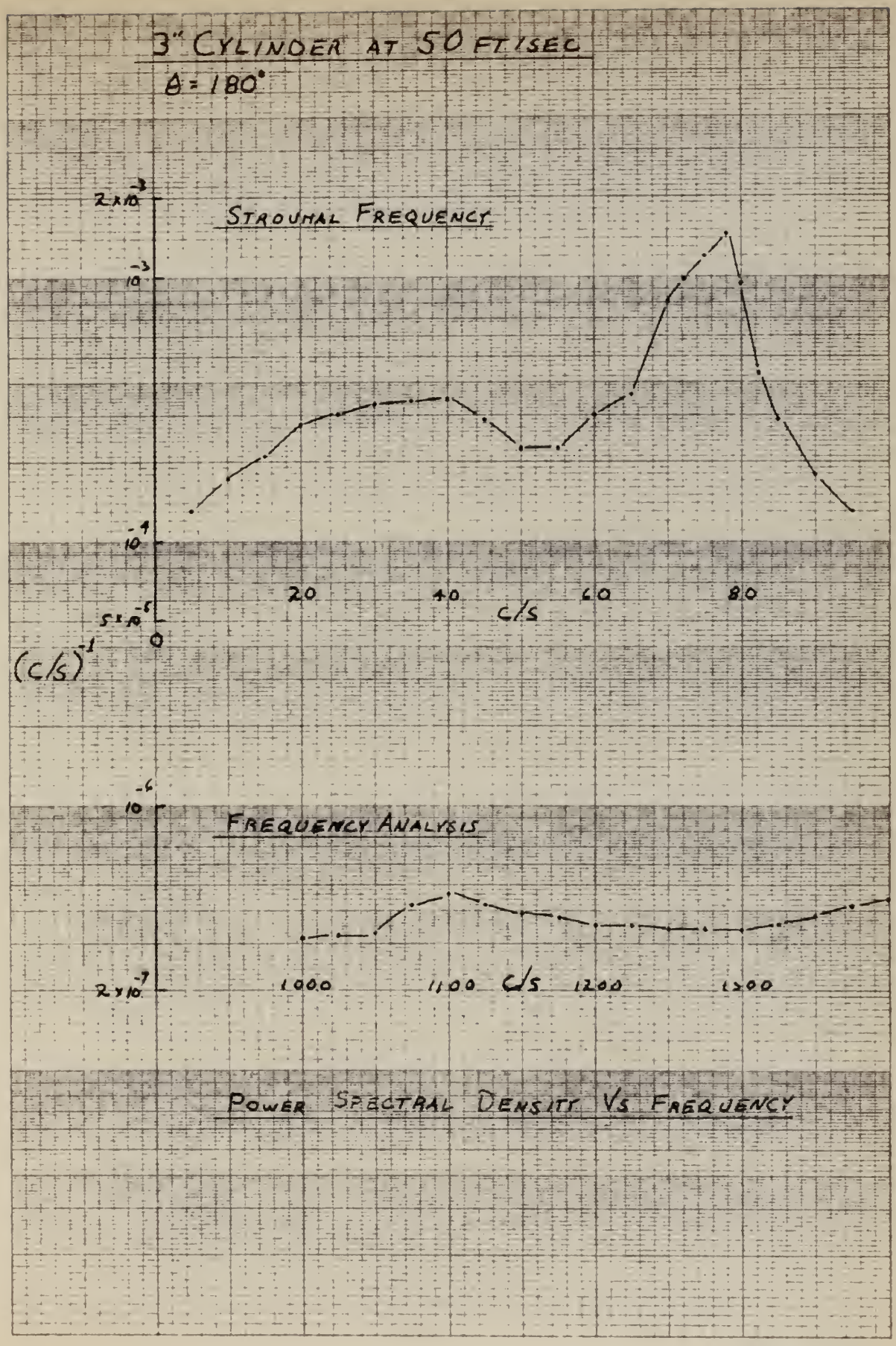
3" CYLINDER AT 50 FT/SEC
θ = 180°
STROUHAL FREQUENCY
2x10^-3
10^-3
10^-4
5x10^-5
0
20
40
60
80
C/S
(C/S)^-1
FREQUENCY ANALYSIS
10^-6
2x10^-7
1000
1100
C/S
1200
1300
POWER SPECTRAL DENSITY VS FREQUENCY

FIG. 67

3" Cylinder, Frequency Analyses at 50 ft/sec

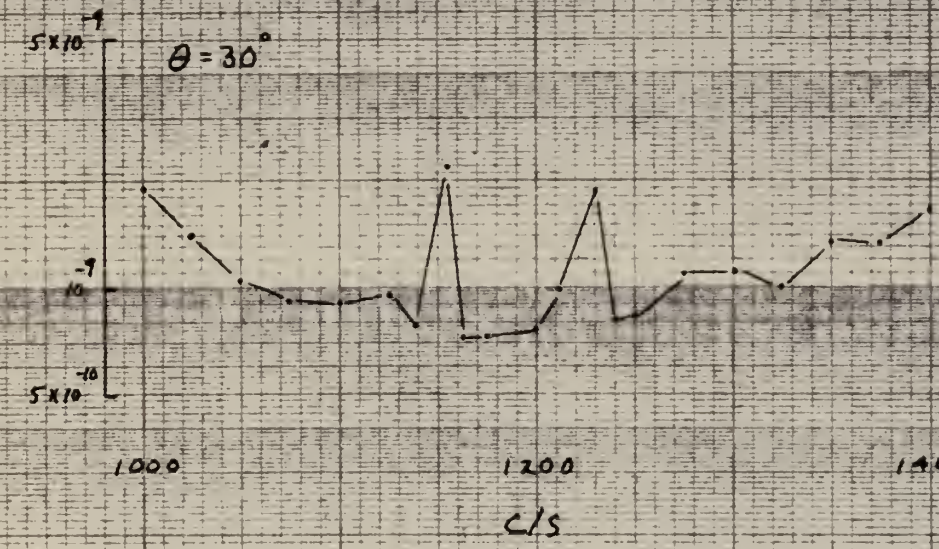

Power Spectral Density Vs Frequency

Fig. 68

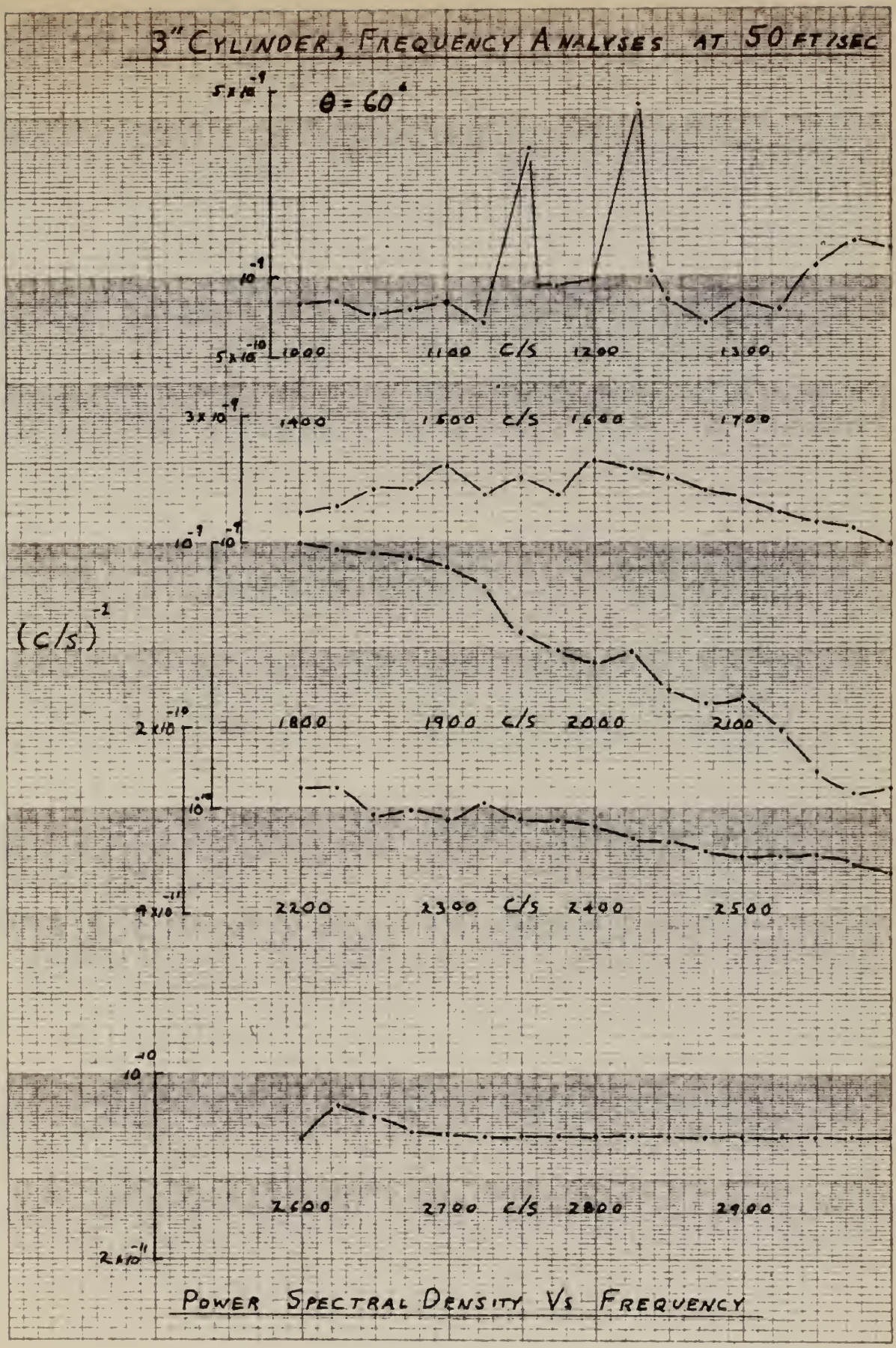
3" CYLINDER, FREQUENCY ANALYSES AT 50 FT/SEC
θ = 60°
5x10^-9
10^-9
5x10^-10
1000
1100 C/S
1200
1300
3x10^-9
1400
1500 C/S
1600
1700
10^-9
10^-10
(C/S)^-1
2x10^-10
10^-9
1800
1900 C/S
2000
2100
9x10^-11
2200
2300 C/S
2400
2500
10^-10
2600
2700 C/S
2800
2900
2x10^-11
POWER SPECTRAL DENSITY VS FREQUENCY

FIG. 69

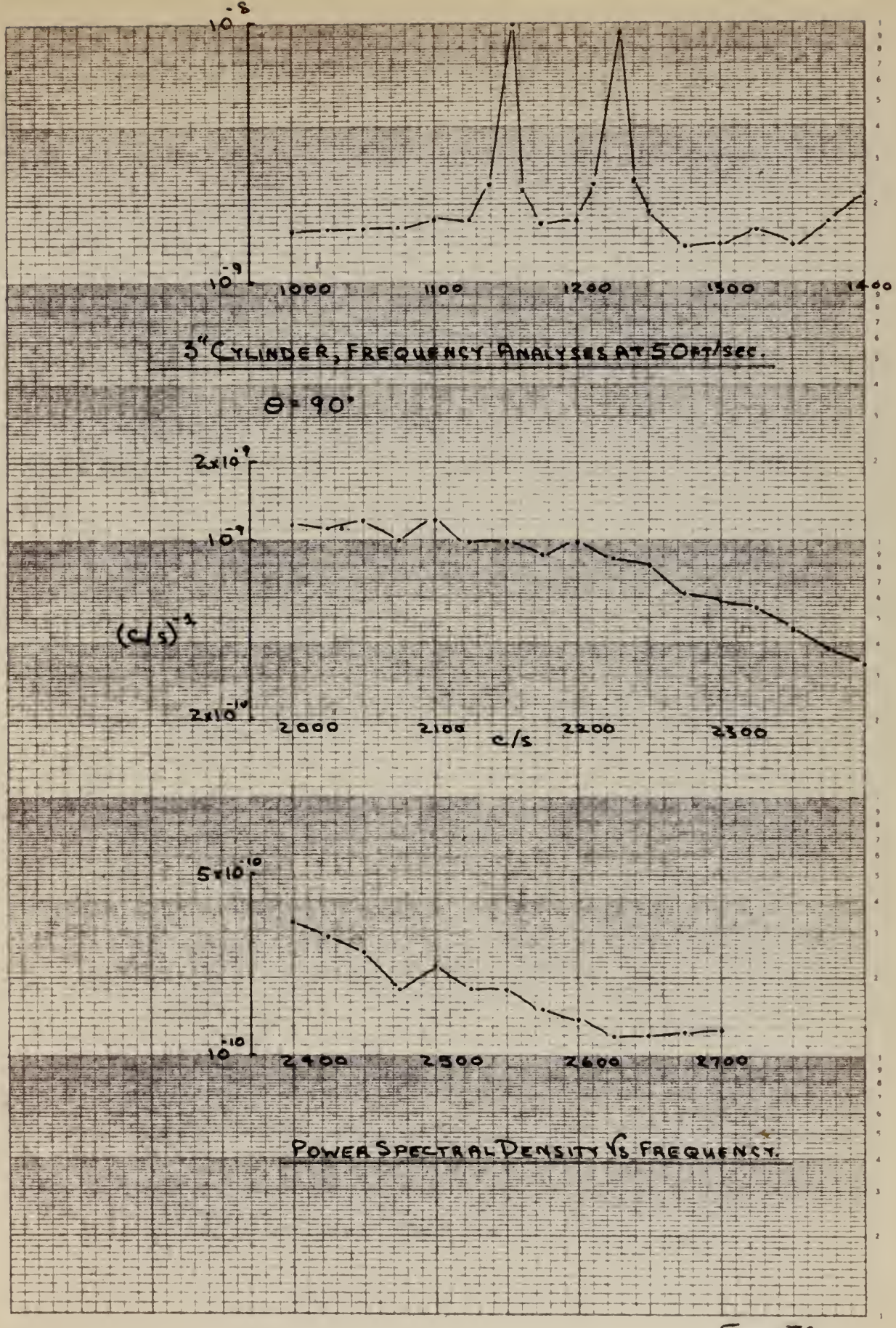
10^-8
10^-9
1000
1100
1200
1300
1400
3" CYLINDER, FREQUENCY ANALYSES AT 50 FT/SEC.
θ = 90°
2x10^-9
10^-9
(c/s)^-2
2x10^-10
2000
2100
c/s
2200
2300
5x10^-10
10^-10
2400
2500
2600
2700
POWER SPECTRAL DENSITY VS FREQUENCY.

FIG. 70

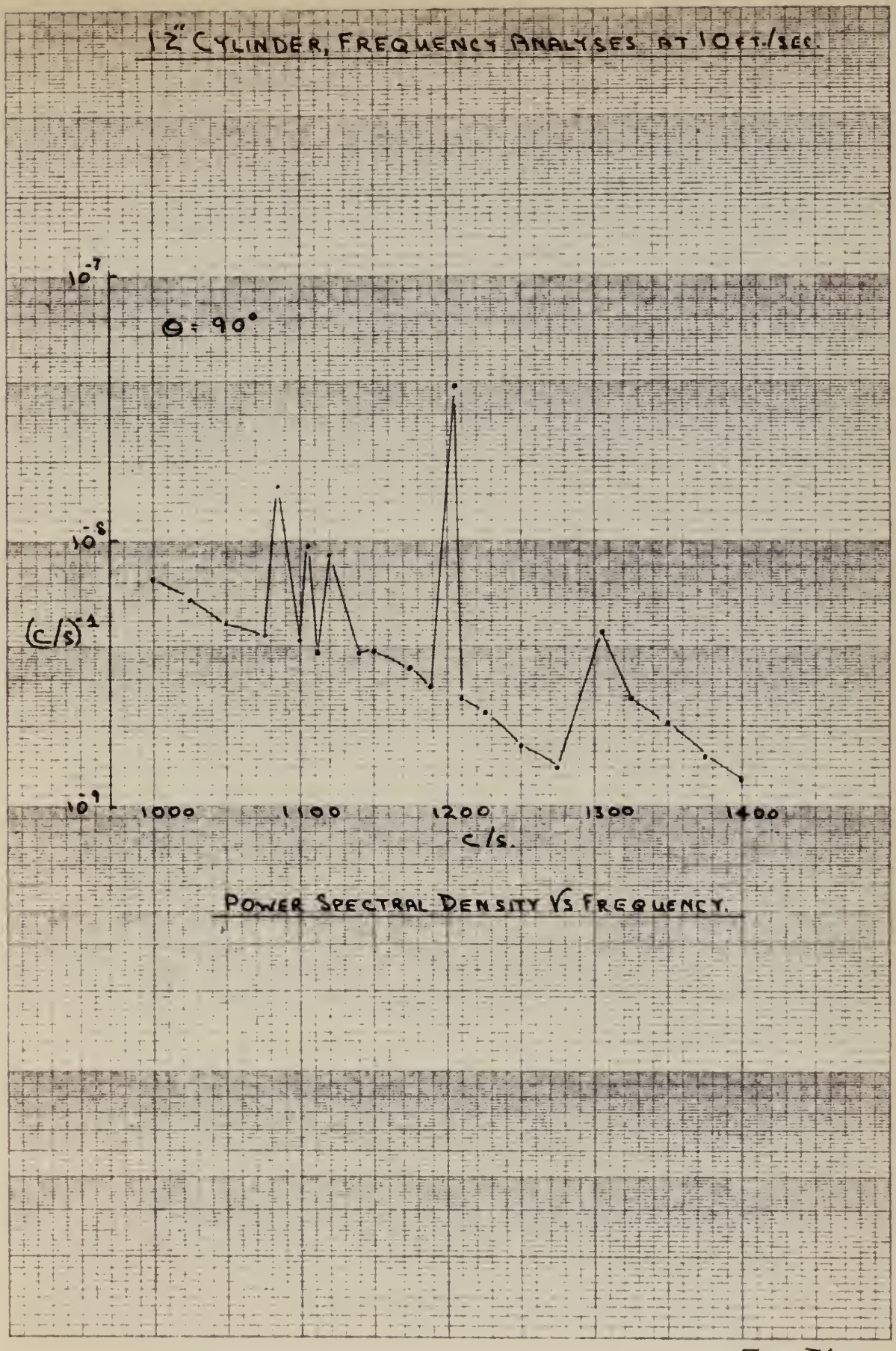
12" CYLINDER, FREQUENCY ANALYSES AT 10 FT./SEC.
10^{-7}
$\theta = 90°$
10^{-8}
$(c/s)^{-1}$
10^{-9}
1000
1100
1200
1300
1400
c/s.
POWER SPECTRAL DENSITY VS FREQUENCY.

FIG. 71

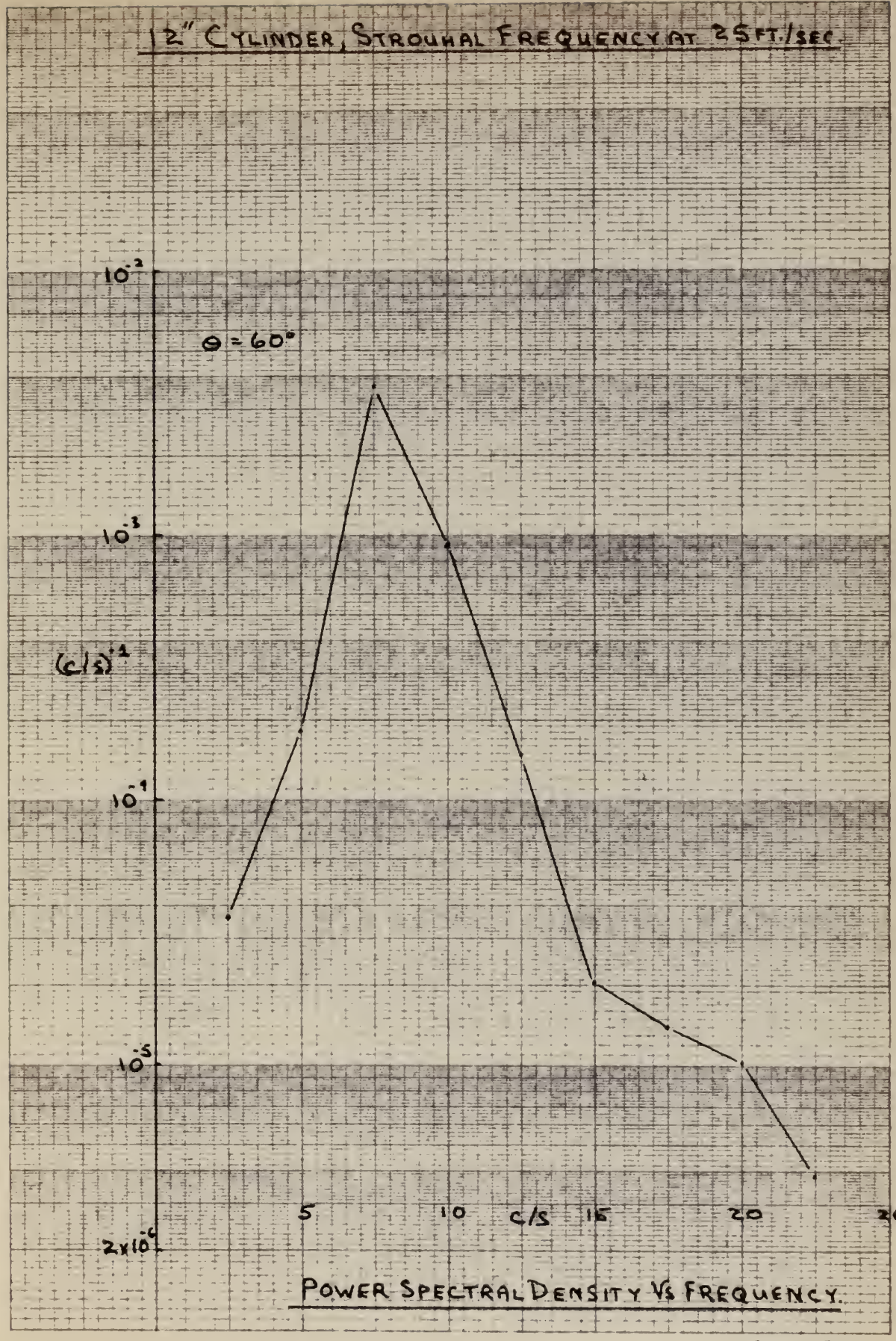
12" CYLINDER, STROUHAL FREQUENCY AT 25 FT./SEC.
10^{-2}
$\theta = 60°$
10^{-3}
$(c/s)^{-1}$
10^{-4}
10^{-5}
2×10^{-6}
5
10
c/s
15
20
25
POWER SPECTRAL DENSITY Vs FREQUENCY.

FIG. 72

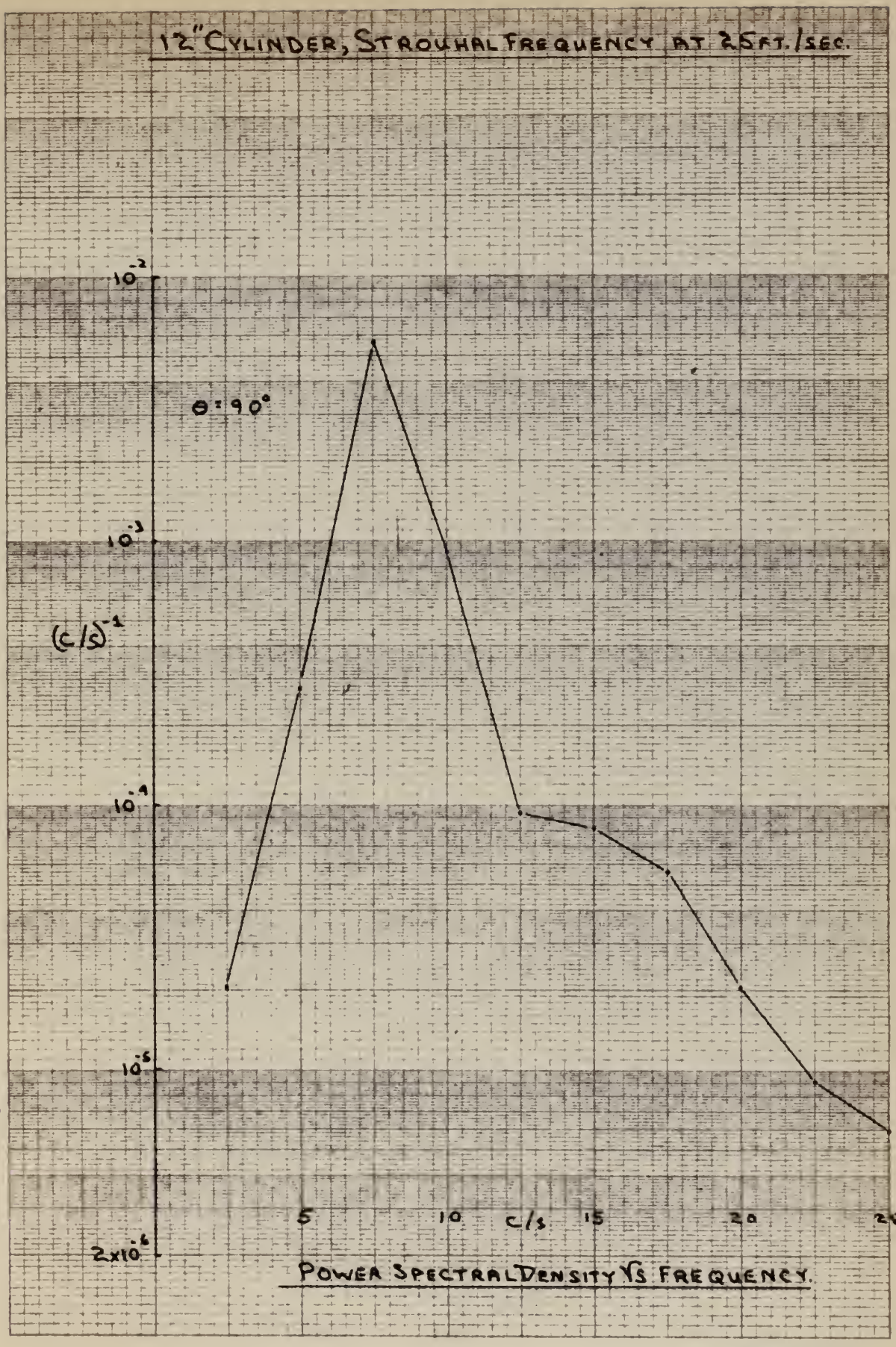
12" CYLINDER, STROUHAL FREQUENCY AT 2.5 FT./SEC.
10^{-2}
$\theta = 90°$
10^{-3}
$(c/s)^{-1}$
10^{-4}
10^{-5}
2×10^{-6}
5
10
c/s
15
20
25
POWER SPECTRAL DENSITY VS FREQUENCY.

FIG. 73

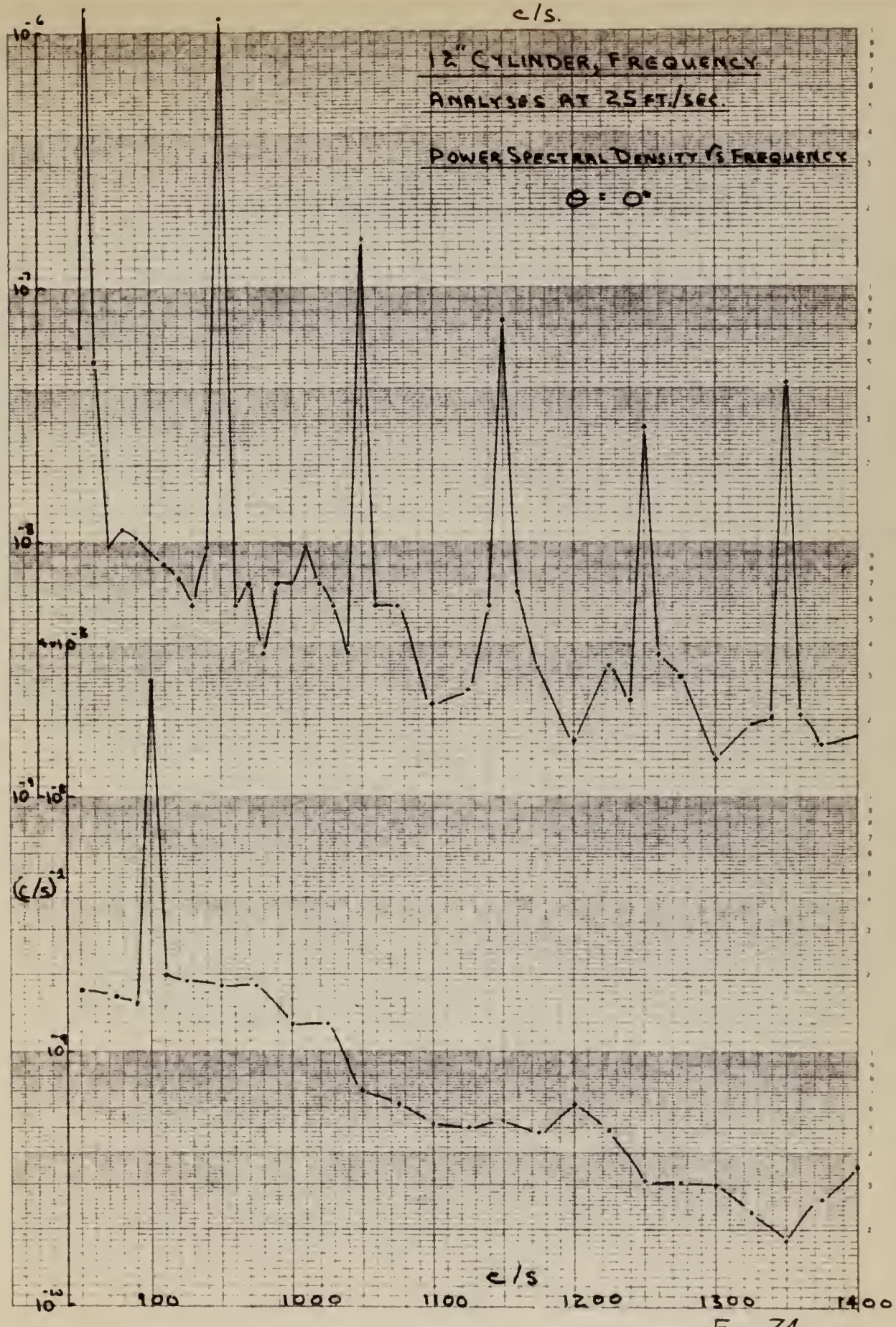
c/s.
12" CYLINDER, FREQUENCY
ANALYSES AT 25 FT./SEC.
POWER SPECTRAL DENSITY VS FREQUENCY
θ = 0°
(c/s)⁻¹
c/s
100
1000
1100
1200
1300
1400

FIG. 74

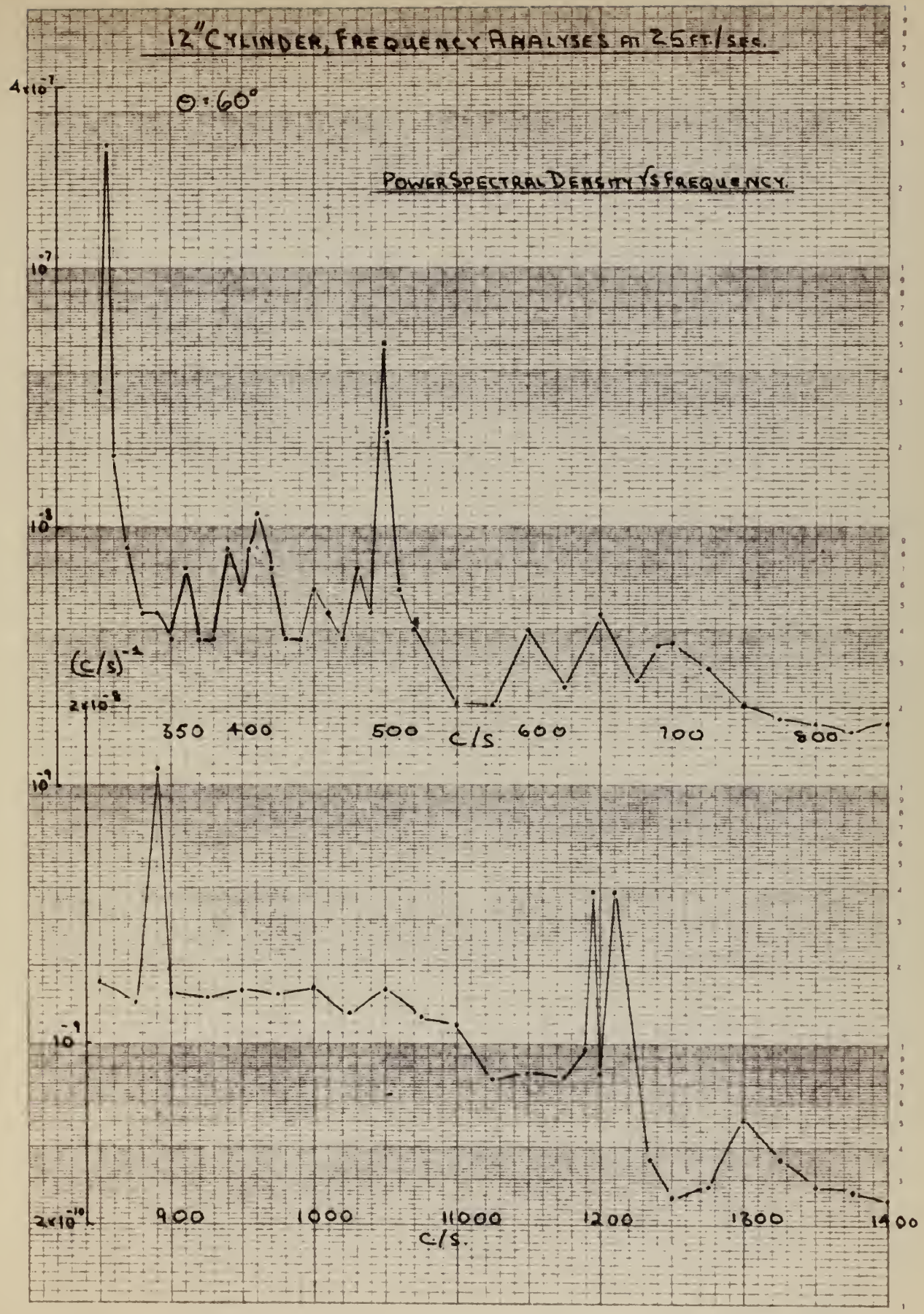
12" CYLINDER, FREQUENCY ANALYSES AT 25 FT/SEC.
Θ = 60°
POWER SPECTRAL DENSITY VS FREQUENCY.
4×10⁻⁷
10⁻⁷
10⁻⁸
(c/s)⁻¹
2×10⁻⁸
10⁻⁹
350
400
500
c/s
600
700
800
10⁻⁹
2×10⁻¹⁰
900
1000
1100
1200
1300
1400
c/s.

Fig. 75

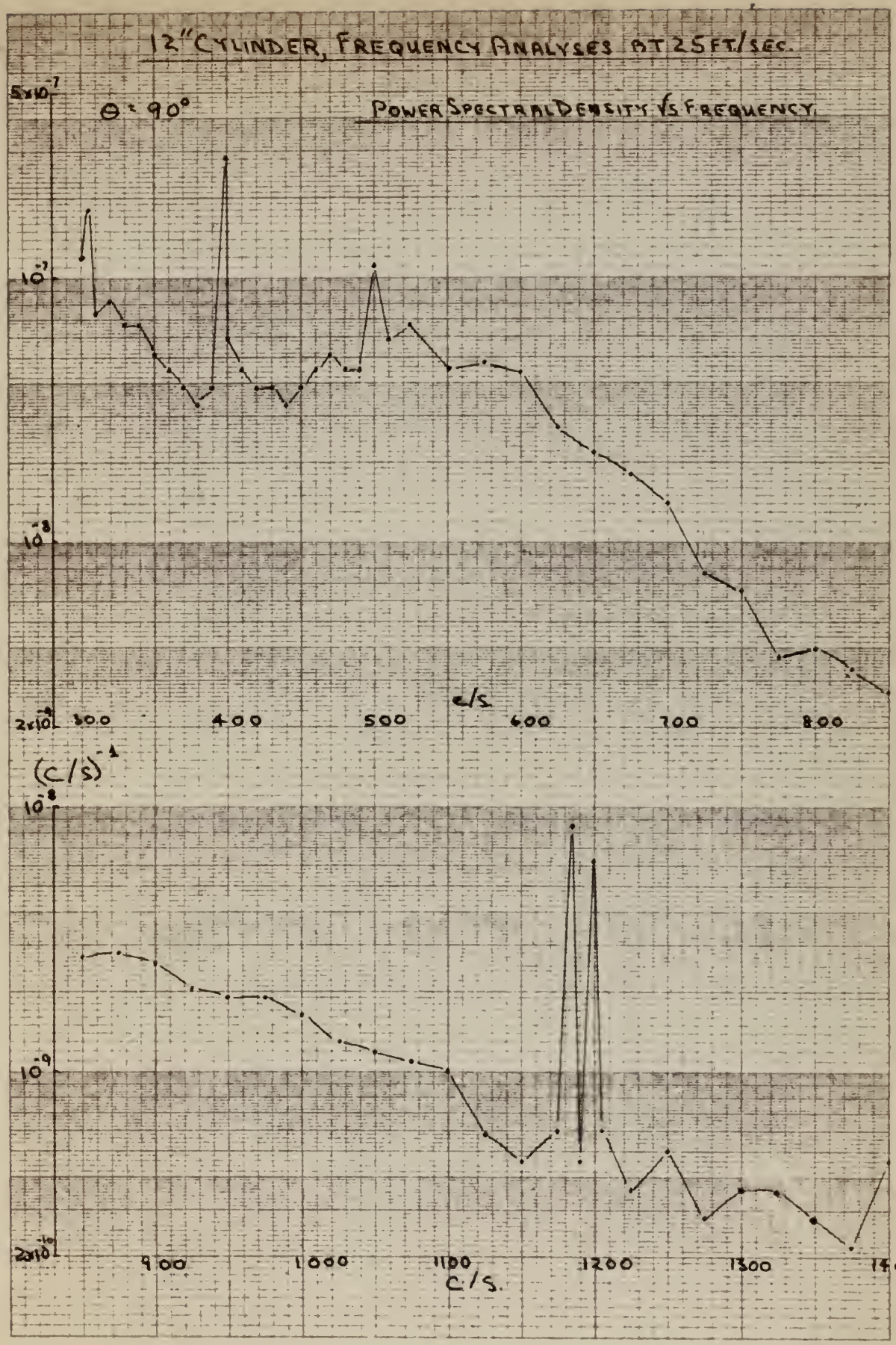
12" CYLINDER, FREQUENCY ANALYSES AT 25 FT/SEC.
POWER SPECTRAL DENSITY VS FREQUENCY.
θ = 90°
5x10⁻⁷
10⁻⁷
10⁻⁸
2x10⁻⁹
300
400
500
600
700
800
c/s
(c/s)⁻¹
10⁻⁸
10⁻⁹
2x10⁻¹⁰
900
1000
1100
1200
1300
1400
c/s.

FIG. 76

thesR666
An investigation of pressure fluctuation
3 2768 001 94934 0
DUDLEY KNOX LIBRARY